RICE UNIVERSITY

SELF-ASSEMBLING PEPTIDE HYDROGELS
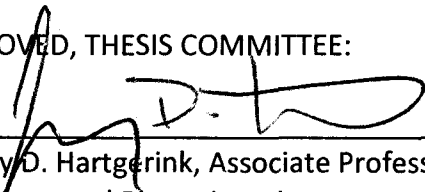# TARGETED FOR DENTAL TISSUE REGENERATION

by

Kerstin Martina Galler
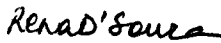
A THESIS SUBMITTED
IN PARTIAL FULFILLMENT OF THE
REQUIREMENTS FOR THE DEGREE

Doctor of Philosophy

APPROVED, THESIS COMMITTEE:

_____
Jeffrey D. Hartgerink, Associate Professor
Chemistry and Bioengineering
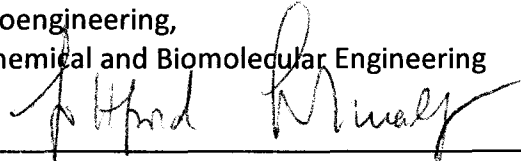
_____
Rena N. D'Souza, Professor, Chair
Biomedical Sciences,
Baylor College of Dentistry, Dallas

_____
K. Jane Grande-Allen, Associate Professor
Bioengineering

_____
Antonios G. Mikos, Professor
Bioengineering,
Chemical and Biomolecular Engineering

_____
Gottfried Schmalz, Professor, Chair
Department of Operative Dentistry,
University or Regensburg, Germany

HOUSTON, TEXAS
AUGUST 2009

UMI Number: 3421416

UMI®

Dissertation Publishing

ProQuest®

ABSTRACT

Self-Assembling Peptide Hydrogels Targeted For Dental Tissue Regeneration

by

Kerstin Martina Galler

Dental caries and traumatic impact are two major causes of destruction of dental soft and mineralized tissues that affect a large segment of the population and pose major public health concerns. Conventional treatment strategies rely on mere replacement with bioinert filling materials. Hence, a critical need exists for biology-based therapeutic approaches to restore damaged dental tissues to their original form and function. Recent developments in tissue engineering, material sciences and stem cell research offer considerable potential to impact dental therapies. A customized scaffolding system laden with bioactive factors could deliver dental stem cells to the site of injury. An applicable scaffold should be biocompatible and biodegradable, accommodate cells, incorporate growth and differentiation factors, and allow for injection into small defects. Synthetic peptide hydrogels are particularly interesting in all these aspects. Our pilot study demonstrated their compatibility with two dental stem cell lines. In Specific Aim 1, peptide sequences were developed to further optimize the system for cell proliferation and spreading. In Specific Aim 2, the gels were modified to incorporate bioactive molecules and growth factors for cell differentiation and vasculogenesis. Release profiles were established, and cell culture studies demonstrated the induction of cellular differentiation. For Specific Aim 3, the generated material was utilized in an animal model, where constructs of cell- and growth-factor-laden gels in standardized dentin cylinders were transplanted into immunocompromised mice. Soft connective tissue formation and new blood vessel formation could be observed, along with localized collagen deposits, indicating beginning dentin formation. In summary, the objective of this research was to modify and optimize peptide-based hydrogels in order to develop a novel tissue engineering approach for the regeneration of dental tissues.

ACKNOWLEDGMENTS

TABLE OF CONTENTS

FIGURES AND TABLES

CHAPTER I: INTRODUCTION

1.   Teeth: Development, Structure and Function, Pathology

Teeth serve important functions of mastication, phonation and speech; dentition shapes our smiles and facial expressions and imparts uniqueness to individuals. This might be reason enough to strive for novel treatment strategies and advance from replacement to true regeneration of damaged or missing teeth. However, beyond the obvious, teeth exhibit several features well worth a closer look. Although small, they come in different shapes and sizes. Humans have a succedaneous dentition and a complex eruption pattern that determines the order in which permanent teeth follow their deciduous predecessors. Each tooth is a complex structure composed of several distinct soft and mineralized tissues of unique architectural characteristics and different functions. The hard tissues enclosing the pulp are classic composite materials. Ordinarily brittle, inorganic hydroxyapatite is re-enforced by organic components, which determine the respective material properties.
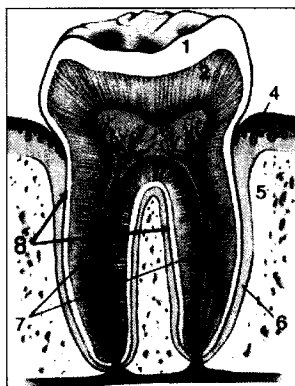
Figure 1: Anatomy of the tooth.
1: enamel; 2: dentin; 3: dental pulp; 4: gingiva; 5: alveolar bone;
6: periodontal ligament; 7: root dentin; 8: cementum.
Adapted from [1].

Enamel covers the tooth crown that is visible in the oral cavity and consists almost exclusively of inorganic hydroxyapatite. It is a ceramic-like material and the hardest substance found in our body due to a high mineral content that is supported by a small percentage of unique non-collagenous proteins. The underlying dentin which makes up the bulk of the tooth has a

composition similar to bone but possesses a different and unique tubular structure. Collagen fibers serve as a template for mineral deposition and provide elasticity, and dentin supports the brittle outer layer of enamel. The dental pulp is enclosed in a chamber in the core of the tooth and is made of fibroblasts, nerves, blood and lymph vessels, and soft connective tissue. Highly specialized dentin-forming odontoblasts line the pulp chamber, and they secrete a collagenous matrix called predentin, which later mineralizes. As the production of dentin progresses, each odontoblast leaves a cellular process behind, embedded in a single dentinal tubule. The intimate association between dentin and the odontoblasts that is established during development continues through the life of a tooth. Hence the structure of dentin maintains tooth vitality by communicating various pathologic and biomechanical signals to the underlying pulp.
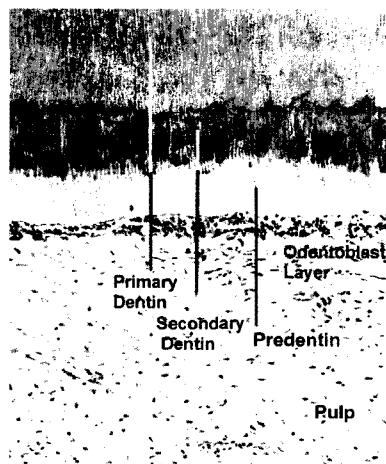
Figure 2: *Histological image of the dentin-pulp complex. A layer of odontoblasts secretes the predentin matrix, which later mineralizes. Primary dentin is formed during tooth development, secondary dentin throughout our lifetime. Adapted from [2].*

The root dentin is covered with yet another species of mineralized tissue, the cementum. Tendon-like fibers insert both into the cementum and the surrounding alveolar bone, thus anchoring the tooth in its socket. This periodontal ligament is important for proprioception and cushions large forces during mastication.

The complex architecture of teeth and a unique structural composition provides durability for a lifetime. Teeth can withstand enormous abrasive forces, large temperature changes, varying pH and a moist and corrosive environment. Despite their strength, teeth

are susceptible to damage caused by bacterial infection, chemicals or mechanical trauma. A common cause for the loss of hard tissues in teeth is dental caries, a degradative disease process fuelled by sugars in the diet and cariogenic microorganisms. Over time, these oral bacteria deposit complex biofilms on the tooth's surface. Their metabolites create an acidic environment, resulting in demineralization of the inorganic matrices and cavitation, progressing from the enamel to the dentin. Subsequently, bacterial toxins can enter the pulp chamber and cause inflammation and degeneration of the underlying soft tissue.
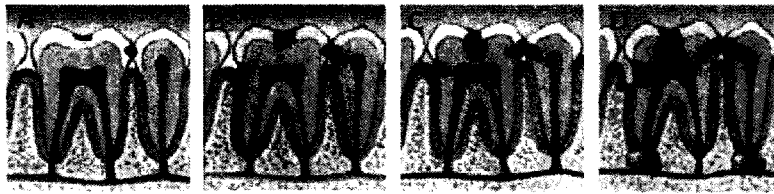
Figure 3: *Development and progression of dental caries.* *Initial lesions are restricted to the enamel (A). As demineralization continues, it reaches the underlying dentin. At this stage, bacterial toxins can diffuse through the dentinal tubules and cause an inflammatory reaction in the pulp (B, C). Further demineralization leads to exposure of the pulp, bacterial invasion, necrosis of the pulp tissue and migration of bacteria into the surrounding bone via the apical dental foramen. Adapted from [3].*

During therapeutic intervention, infected enamel or dentin can be removed and replaced with an inert filling material, thus maintaining vitality and function of the dental pulp. In the face of ongoing insult, necrosis ensues and the tissue has to be removed completely.

Besides caries, erosion can lead to destruction of dental enamel or dentin; furthermore fractures after traumatic impact. If the dental pulp is exposed after loss of dental hard tissues, contamination and necrosis of the soft tissue follow, and the inflammatory process can spread into the surrounding bone, oftentimes resulting in tooth loss.

2.   Current Treatment Methods

To date, treatment strategies rely on the insertion of synthetic materials such as metal alloys, ceramics, cements and composite resins to restore defects in enamel and dentin. An interesting aspect is that the use of malleable or carved materials for tooth replacement reaches far back in human history, and thus dentists were among the first to apply material science in a biological setting.

Amalgam, a mixture alloy of mercury and at least one other metal, used to be the golden standard for dental restorations. Recently, it has been exchanged for highly sophisticated materials such as dental resin composites, which settle esthetic claims and aim at high quality material properties. Over the last decades, companies have invested heavily in the development and improvement of dental materials, involving research efforts of mainly chemists and material scientist.

Detected early, infected enamel or dentin can be removed and replaced with a filling material, thus maintaining vitality and function of the dental pulp. Even after exposure of the pulpal tissue, regeneration is still possible. Application of calcium hydroxide or mineral trioxide as a pulp capping material stimulates defense mechanisms and reparative dentin formation. Despite these advances, problems remain. In composite filling materials, marginal gaps often form due to polymerization shrinkage, which leads to tensile stress between the cavity wall and the restoration. These gaps facilitate the invasion of bacteria and bacterial products into the dentinal tubules and the dental pulp, leading to post-operative sensitivity, secondary caries and pulpal damage [4]. If intervention comes too late, necrosis of the soft tissue ensues. After loss of the dental pulp, thorough debridement,

disinfection and subsequent obturation of the pulp chamber and root canal system are necessary to prevent reoccurrence of infection. While root canal fillings have been utilized as replacements for decades and show high success rates of over 90% over 8 years [5], they fail to restore physiological form and function of lost tissues and are incapable of remodeling and repair as a response to ongoing stimulation or injury.

The loss of dental pulp after traumatic impact poses another serious problem to patients and dentists. The incidence of tooth fracture, mainly of the incisors, is highest in children and young adults [6] and is associated with considerable challenges since root formation is not complete until 3 years after the tooth has fully erupted. After complicated tooth fractures with exposure of the soft tissue in immature teeth, bacterial contamination leads to inflammation and subsequent tissue necrosis, and root formation comes to a halt as the mineralizing cells are lost. If the condition is not treated, the inflammation will spread into the surrounding alveolar bone and eventually the tooth will be lost. Treatment with calcium hydroxide or mineral trioxide aggregate (MTA) can induce a continuation of hard tissue formation in the apical region. In order to control infection, calcium hydroxide, for example, has to be applied frequently over a prolonged period of time of 5 to 20 months [7]. The procedure is often complicated by divergent root canals, making debridement difficult. Failure to control infection can result in root resorption, apical radiolucencies or root fracture, and eventually tooth loss [6]. This, in turn, leads to an arrest of bone development in that area of the dental arch, as the teeth transmit load into the bone and thus trigger bone and jaw growth and remodeling. Insertion of a dental titanium implant covered with a ceramic crown, which can substitute for a lost tooth, might be severely

complicated if the bone in the area of supposed implantation is underdeveloped and thin, requiring alveolar bone augmentation before an implant can be placed. Furthermore, implantation is considered only after growth is completed and is usually not performed before the age of 18.

Overall, restoration of lost tooth tissue, whether from disease or trauma, represents a significant proportion of the daily routine for practicing clinicians. The 2003 WHO World Oral Health Report [8] as well as a recent follow-up [9] identified oral diseases as a major and continuing public health problem. This is based on their impact in terms of pain, impairment of function and thus effect on quality of life along with their high prevalence and global incidence. Treatment costs are estimated as accounting for 5-10% of the healthcare budget in industrialized countries, leaving us with a daunting challenge to minimize the burden of restoring teeth.

3.   Regenerative Dentistry

Regenerative dentistry strives for the development of innovative treatment strategies which lead to true regeneration rather than replacement and repair. Two distinct approaches can be distinguished to achieve this goal: whole tooth regeneration and the regeneration of partial tooth structures.

In order to engineer a whole tooth, researchers are investigating events occurring during tooth development. Tooth formation is initiated and progresses through cross talk and reciprocal interactions between two morphologically different tissues from different germ layers, the ectoderm and the underlying mesenchyme. Understanding the molecular

mechanisms responsible for these events is not only interesting to developmental biologists, but is key for tissue engineers who aim to reiterate these processes *in vitro* in order to regenerate a whole biotooth [10]. This biology-based strategy provides a viable alternative to the use of today's state-of-the-art titanium implant.

Whereas replacement of whole teeth remains a challenge, regeneration of partial tooth structures might be a more achievable short-term goal. In general, newly developed dental biomaterials have not capitalized on the intrinsic regenerative capacity of oral tissues. Such natural resources could be taken advantage of for more biologically-driven treatment strategies. Formation of new dentin and partial regeneration of periodontal ligament can be stimulated through therapeutic intervention. In either case, the healing process is thought to involve the recruitment of uncommitted progenitors or stem cells, which hold the capacity to differentiate and produce the respective matrices to repair and restore damaged tissues. The recent isolation of postnatal stem cells from a variety of oral tissues marks a milestone in regenerative dentistry, and these cells provide a promising tool for future treatment strategies. On the other hand, tissue engineering scaffolds are transitioning from passive cell delivery systems to bioactive matrices, which allow for incorporation of biomolecules and can thus elicit a desired cellular response. The combination of dental stem cells with novel scaffolding materials might enable us to engineer oral tissues in the near future.

4. Tissue Engineering

Tissue engineering is an emerging interdisciplinary field that integrates principles of developmental, cellular and molecular biology, genetics, medicine, chemistry, material sciences and engineering. The term was first coined in 1985, and defined as "the application of principles of engineering and life sciences toward fundamental understanding of structure-function relationships in normal and pathological mammalian tissues, and the development of biological substitutes to restore, maintain or improve tissue functions" [11]. The emergence of the field has resulted from the need for tissue and organ replacements [12]. Significant progress has been made over the last decades in understanding and harnessing those structure-function relationships, and tissue-engineered products are already commercially available and used for novel and improved treatment methods in medicine.

The concept of tissue engineering is based on the combination of the following: (1) *ex-vivo* expanded (stem) cells, (2) a biocompatible carrier or scaffold material and (3) bioactive molecules to induce cellular differentiation and tissue formation. Thus, tissue engineering strategies utilize the functional triad of cells, scaffold and biomolecules to recapitulate physiological processes of development and regeneration. This important challenge presents itself to biologists and bioengineers, chemists and material scientists who must design biomimetic and bioactive scaffolds to drive the field forward.

4.1. Stem Cells

The most valuable cells for regenerative medicine are stem cells. These cells possess the capability for self-renewal and can differentiate into various lineages, a characteristic called plasticity. Stem cells are commonly defined as either 'embryonic' or 'postnatal' [13]. Stem cells are also subdivided into pluripotent and multipotent categories according to their plasticity. Embryonic stem cells, which are comprised in the inner cell mass of the blastocyst (5-14 days after conception), are pluripotent, which means each cell can form any cell type of the body. However, the use of embryonic tissues is afflicted with legal and ethical issues. The recent creation of "induced pluripotent stem cells" (iPS) by re-programming somatic cells to re-activate characteristics of embryonic stem cells set a new milestone and promises to revolutionize regenerative medicine [14, 15].

In contrast, postnatal stem cells possess a limited capability to differentiate but can still form a number of lineages and are readily accessible. Mesenchymal stem cells, which have commonly been isolated from bone marrow, give rise to osteoblasts, chondrocytes, myocytes, adipocytes, neuronal cells, or beta-pancreatic islets cells, any pathway can be induced by addition of adequate cell culture supplements or differentiation factors. Many researchers focus on postnatal stem cells in order to bypass the legal and ethical issues associated with embryonic stem cells. In fact, postnatal stem cells are a promising tool as an alternative source for clinical applications, both in regards to their accessibility and lack of immunogenicity, despite their reduced plasticity.

Postnatal stem cells have been successfully utilized for bone marrow transplants for certain types of cancer [16], injection into heart muscle after infarction to produce

cardiomyocytes [17], re-growth of damaged neuronal axons [18], bone and cartilage regeneration [19, 20], or skin and vascular grafts [21, 22]. Recently, postnatal stem cells have been isolated from tissues such as umbilical cord, peripheral blood or adipose tissue. Today, stem cells can be isolated from various sources, including the oral cavity.

4.1.1. Tooth-Derived Mesenchymal Stem Cells

A long-standing obstacle in regenerative dental medicine is to obtain progenitor cells that will continually divide and produce cells or tissues suitable for implantation in the oral cavity. Cells could either come from an allogenic source, e.g. as a disease- and pathogen-free human pulp stem cell line, or from the same patient as autologous stem cells from oral tissues, such as mucosa or dental pulp. The latter might cause constraints, since expansion of sufficient cell numbers could be time-consuming, regarding the fact that many adult tissues contain only 1-4% stem cells [23].

Since dentin-producing odontoblasts are terminally differentiated, postmitotic cells, they cannot proliferate to replace lost cells after injury. The ability of both young and old teeth to respond to injury by induction of reparative dentinogenesis suggests that a small population of competent progenitor pulp stem cells may exist within the dental pulp throughout life. For many years, possible sources of replacement cells had been discussed controversially. Progenitor cells were thought to reside in the cell-rich zone subjacent to the odontoblast layer, in the core of the pulp as undifferentiated mesenchymal cells, or in the perivascular niche [24]. Today, several different sources of dental stem cells have been

identified. Stem cells can be isolated from mixed cell populations by four commonly used techniques:

1) Fluorescence activated cell sorting (FACS) using a flow cytometer,

2) Immuno-magnetic bead selection,

3) Immuno-histochemical staining,

4) Physiological and histological criteria including phenotype, chemotaxis, proliferation, differentiation and mineralizing activity.

4.1.2. Dental Pulp Stem Cells

Teeth are an easily accessible source to harvest postnatal stem cells from different tissues, including dental pulp, periodontal ligament, or dental follicle and apical papilla of developing teeth. The most applicable for our approach are stem cells derived from dental pulp. Gronthos et al. first isolated stem cells from the pulp of developing third molars, DPSC (dental pulp stem cells). These cells are highly proliferative, differentiate into various lineages, and are able to form dentin-pulp-like complexes, but not lamellar bone, after transplantation *in vivo* [25, 26]. Three years later, Miura et al. were able to harvest clonogenic cells from exfoliated deciduous teeth, SHED (stem cells from human exfoliated deciduous teeth), and differentiated them into odontoblasts, adipocytes or neural cells [27]. Interestingly, both SHED and DPSC are located in the perivascular niche, they express the mesenchymal stem cell marker STRO-1 and the pericyte marker CD146 [28].

However, SHED are considered distinct from DPSC for several reasons. Compared to DPSC or bone marrow stromal stem cells (BMSSC), SHED display increased numbers of

population doublings and higher proliferation rates [27]. Although both cell types show calcium accumulation after osteogenic induction *in vitro*, DPSC cells are able to form dense mineralized nodules, indicating a higher potential to mineralize. After transplantation *in vivo*, SHED develop into odontoblast-like cells associated with a dentin-like structure, but are unable to regenerate a complete dentin-pulp complex as observed with DPSC. On the other hand, SHED show a strong osteoinductive capacity and promote host cell differentiation into bone-forming cells [25, 27]. The behavior of these cells reflects their physiological function *in vivo*. Deciduous teeth are significantly different from permanent teeth with regards to their development, tissue structure and function. Whereas pulp cells in deciduous teeth fail to generate new dentin after injury, this can commonly be observed in adult pulp. Due to the strong osteoinductive capacity of SHED it has been suggested that these cells not only guide the eruption of permanent teeth, but furthermore induce bone formation during the eruption process [27]. SHED therefore represent a population of stem cells that might be more immature and is distinct from DPSC with respect to their higher proliferation rates, increased population doublings, sphere-like cluster formation, osteoinductive capacity and a failure to reconstitute a dentin-pulp like complex *in vivo*.

Both dental stem cell lines have been demonstrated to retain their multipotential differentiation ability after cryopreservation [29, 30]. SHED and DPSC used in studies described in this dissertation were kindly provided by Dr. Songtao Shi at USC.

4.2.   Scaffolds

In order to provide a three-dimensional microenvironment to accommodate cells and guide their adhesion, growth and subsequent differentiation, we are in need of suitable scaffolding systems. In one scenario, cells can be seeded onto the scaffold and cultured *in vitro* to generate the desired tissue before transplantation. A slightly different approach is the design of materials for transplantation of a primarily cell-free system, which will, due to a combination of signaling molecules incorporated in the scaffold, induce the homing of stem cells residing in the respective tissues, and promote their differentiation to support regeneration. Cell-free biocompatible scaffolds are especially attractive because of an easier handling process that eliminates the issues associated with the use of stem cells and their expansion *in vitro*, with storage and shelf-life, cost aspects, immunoresponse of the host and transmission of diseases.

In any case, an ideal scaffold material has to be non-toxic, biocompatible and non-immunogenic to avert any damage to neighboring cells. The scaffold should be degradable by enzymes or hydrolysis at a rate that allows for replacement with newly formed tissue. As a carrier for drugs and differentiation factors, the material should be versatile enough to enable the incorporation and controlled release of bioactive molecules.

A variety of materials has been designed and constructed for tissue engineering approaches, namely natural and synthetic polymers or inorganic materials and composites, which have been fabricated into porous scaffolds, nanofibrous materials, microparticles and hydrogels.

Natural materials include collagen, elastin, fibrin, alginate, silk, glycosaminoglycans such as hyaluronan, and chitosan. They offer a high degree of structural strength, are biocompatible and biodegradable, but are often difficult to process and afflicted with the risk of transmitting animal-associated pathogens or provoking an immunoresponse. Collagen has been of special interest and has been used for manifold tissue engineering approaches in bone and tooth tissue engineering; it has been fabricated as gels, nanofibers, porous scaffolds and films. However, it is mechanically weak and undergoes rapid degradation [31].

Synthetic polymers on the other hand provide excellent chemical and mechanical properties and allow for high control over the physicochemical characteristics, such as molecular weight, configuration of polymer chains, or the presence of functional groups. Disadvantages of synthetic polymers can be a chronic or acute inflammatory host response, and localized pH decrease due to relative acidity of hydrolytically degraded byproducts. Commonly used synthetic scaffolds are fabricated from poly lactic acid (PLLA), poly glycolic acid (PGA), and their copolymer, poly lactic-co-glycolic acid (PLGA). PLLA is a very strong polymer and has found many applications where structural strength is important. PGA has been used as an artificial scaffold for cell transplantation, and degrades as the cells excrete extracellular matrix. Both PLLA and PGA are nontoxic and biocompatible; they degrade by simple hydrolysis and have gained FDA approval for a number of applications [32, 33].

Hydrogels made from collagen, poly ethylene glycol, fibrin, glycosaminoglycans or self-assembling peptide molecules have recently been explored for tissue engineering applications in more detail. They offer numerous interesting properties including high

biocompatibility, a tissue-like water content, viscoelastic properties similar to soft tissues, efficient transport of nutrients and metabolic products, uniform cell encapsulation, and the possibility of injection and gelation *in situ*. Based on their chemistry, they can be chemically or physically crosslinked, and modifications such as incorporation of biofunctional molecules or growth and differentiation factors are possible [34, 35]. In our laboratory, we focus on hydrogel systems made from short peptide building blocks, and the development of a peptide-based scaffold conducive for dental stem cell proliferation and differentiation was the objective for Specific Aim 1 of this research.

4.2.1. Peptide-Based Hydrogels

The ECM network, which is the physiological microenvironment of cells, is mainly composed of fibrillar proteins; their construction as a well-organized matrix is achieved though self-assembly. In order to provide optimized matrices for tissue engineering approaches, novel materials are required to generate supramolecular structures which resemble natural ECM and display biological functions. Self-assembly is a process that is mediated by non-covalent weak chemical bonds, namely ionic bonds, hydrogen bonding, hydrophobic interactions or van der Waals interactions. In the past decade, many synthetic self-assembling peptides have been developed for tissue engineering approaches [36 – 41]. Typically, they are 8–16 amino acids long and contain alternating hydrophilic and hydrophobic residues. Hydrophilic modules consist of alternatively repeating units of positively charged amino acids, such as lysine or arginine, and negatively charged aspartic or glutamic acid. The peptides form stable β-sheets in water, but upon exposure to physiological salt concentration or pH they

self-assemble into nanofiber networks, which form self-supporting gels with a water content of more than 99%. Self-assembling peptides can be synthesized by solid phase chemistry, but are also commercially available, such as RAD16-I peptides (Puramatrix). A slightly different concept is used for peptide amphiphile (PA) molecules, where a peptide segment is coupled to a fatty acid chain. The process of self-assembly is driven by formation of a hydrophobic core composed of closely packed alkyl tails, fibrous strands can build because of hydrogen bond formation between the amino acids of adjacent PA molecules. Whereas the PAs remain amorphous aggregates at neutral pH due to the repulsive negative charge which prevents self-assembly, addition of polyvalent ions eliminates the negative net charge and allows self-assembly into cylindrical micelles, which undergo physical crosslinking to provide the gelled macrostructure. Self-assembly can be triggered by mixture of PA solutions with cell culture media or other physiological fluids that contain polyvalent metal ions.

It has been shown that cells can move, proliferate and differentiate within the hydrogel [39, 40, 42, 43]. The compatibility of self-assembling peptides with cells may be related to the size of the fibers. Most biopolymers used for tissue engineering have fiber sizes ranging from 10 to 100 μm, which is similar to the size of most mammalian cells. Essentially, cells grow in these polymers on a curved two-dimensional surface. In contrast, self-assembling peptides form nanofibers of 6–20 nm in diameter, which mimics the structure of extracellular matrix, allowing true three-dimensional cell culture. Cells can bind to self-assembling peptides with their adhesion molecules, but the size of the nanofibers does not inhibit interaction with other cells in all three dimensions [44].

Another advantage of self-assembling peptides is the extreme flexibility with which they can be designed and modified, following a modular conception. The molecules can be functionalized by adding adhesion motifs, such as RGD, enzyme-cleavable sites, or heparin-binding domains to tether growth factors, such as vascular endothelial growth factor (VEGF) or fibroblast growth factor 2 (FGF2). Optimization for specific cell types and targeting towards defined applications are possible. Immunohistochemical analysis after injection of self-assembling peptides *in vivo* did not show obvious inflammation or immune response [45 – 47].

4.2.2. Multidomain Peptides

Recently, a peptide architecture was developed in our laboratory that undergoes self-assembly in water to form short nanofibers [48]. The peptide molecules are designed to display distinct regions of function or "domains" arranged in an ABA block motif, and they self-assemble into nanofibers which feature similarity to the make-up of natural ECM. The process of supramolecular assembly is driven by a core motif (B) of alternating hydrophilic (glutamine or serine) and hydrophobic (leucine) amino acid residues. In an aqueous environment, the side groups segregate to opposing sides of the backbone, and two peptide molecules form a sandwich upon hydrophobic packing between leucine residues. The fiber elongate as the dimers string together and hydrogen bonding occurs along the fiber axis. Charged amino acid residues in the flanking region (A) provide water solubility, but counteract fiber assembly via electrostatic repulsion and can thus be utilized to control fiber length [48]. However, addition of multivalent ions screens the charge and results in physical

crosslinking, fiber elongation, entrapment of water and gelation.

With a fiber diameter of 6 nm, hydrogels created from MDPs mimic the nanoscale dimensions and structure of natural ECM, where cells can bind to the fibers via adhesion molecules, but still interact with other cells [44]. True three-dimensional cell growth within the nanofibrous gels makes these materials promising candidates as scaffolds for cell delivery. Incorporation of bioactive sequences in either the central block or the flanking regions of MDPs can further enhance cell-matrix interactions and promote desired cellular responses.

In Specific Aim 1 of this project, multidomain peptide hydrogels were modified and optimized for compatibility with dental stem cells.
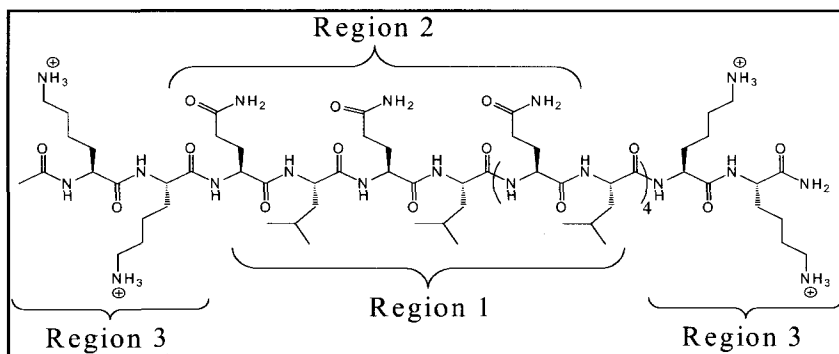
Figure 4. Chemical structure of peptide $K_2(QL)_6K_2$. The three key regions that control the peptides' self-assembly into a nanostructured fiber are shown. The peptides making up these nanofibers have three key regions that control their assembly: 1) a hydrophobic face, which is the energetic driving force for self-assembly in water; 2) a hydrophilic face, which provides water solubility and opposition to region 1, creating a facial amphiphile; and 3) charged peripheral groups that limit the extent of self-assembly via electrostatic repulsion and also aid in solubility. Regions 1 and 2 are formed from a pattern of alternating hydrophobic and hydrophilic amino acids such that when the peptide is in a fully extended conformation, the amino acid side chains alternate between one side of the peptide and the other. This arrangement results in one face of the peptide being hydrophobic (region 1) while the other is hydrophilic (region 2).
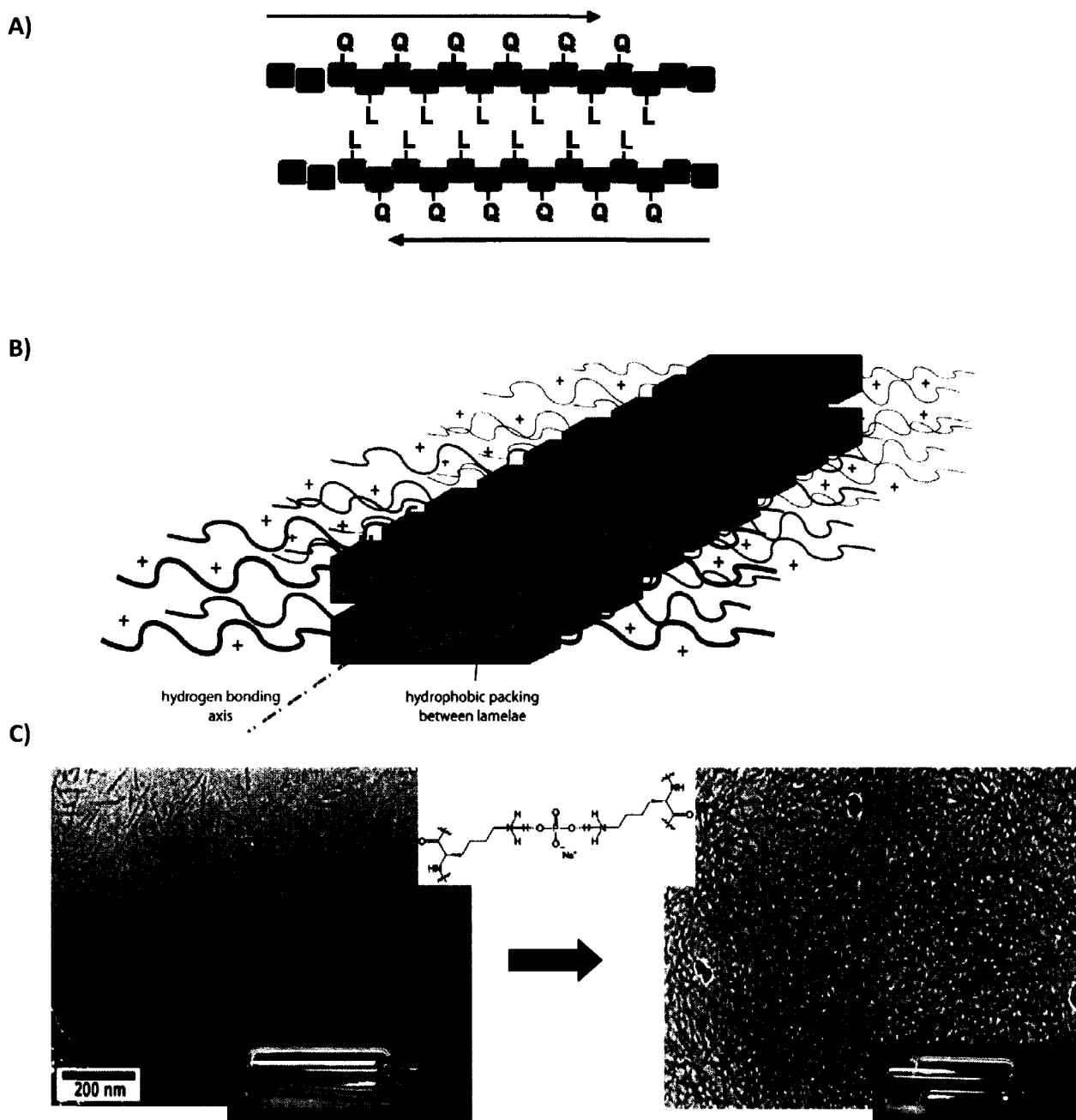
Figure 5: Mechanism of nanofiber formation. *The hydrophilic and hydrophobic amino acid residues assemble on either side of the peptide backbone to form a facial amphiphile. Hydrophobic packing occurs between leucine residues, and a hydrophobic sandwich forms (A). Model of nanofiber self-assembly, indicating the hydrophobic packing region, hydrogen bonding axis and repulsive positive charges (B). cryoTEM images of nanofibers before and after addition of phosphate, which eliminates the repulsive positive charges, resulting in increased fiber length and gelation (C).*

4.3. Bioactive Molecules and Dental Stem Cell Differentiation

Increased understanding of the biological processes mediating tissue repair has allowed some investigators to mimic or supplement tooth reparative responses. Dentin contains many proteins capable of stimulating these processes. Demineralization of the dental tissues can lead to the release of growth factors entrapped in the dentin matrix, following the application of cavity etching agents or restorative materials and even caries [49]. Once released, these growth factors may play key roles in signaling many of the events of reparative dentin formation [50, 51]. Growth factors, especially those of the transforming growth factor-beta (TGFβ) family, are important in cellular signaling for differentiation and stimulation of dentin matrix secretion. These growth factors are secreted by dentin-forming cells during tooth development and deposited within the organic matrix preceding the mineralized tissue [52 – 54], where they remain protected in an active form through interaction with other components [55]. The addition of purified dentin protein fractions has stimulated an increase in dentin matrix secretion [56]. The TGFβ superfamily of ligands furthermore includes another important group of growth factors in tooth development and regeneration, the bone morphogenetic proteins (BMP's). Recombinant human BMP-2 stimulates differentiation of adult pulp stem cells into an odontoblast-like morphology in culture [57, 58]. Recombinant BMP-2, -4, and -7 induce formation of reparative dentin *in vivo* [57, 59]. Besides growth factors, other molecules have been shown to stimulate pulp cell differentiation. Dentin matrix protein-1, a non-collagenous protein involved in the mineralization process induced cytodifferentiation, collagen production and calcified deposits in dental pulp in a rat model [60]. Dexamethasone, a synthetic glucocorticoid,

reduced cell proliferation and induced expression of the differentiation markers alkaline phosphatase and dentin sialophosphoprotein in primary human pulp cells [61]. Addition of β-glycerophosphate to the cell culture medium in explants from human teeth induced a change in cell morphology, collagen synthesis and mineral formation [62]. Whereas combinations of inorganic phosphate and dexamethasone are used as standard osteogenic supplements to drive differentiation of bone-forming osteoblasts, it has also been proven to induce dental stem cell differentiation followed by mineral deposition [26, 27]. This may be explained by the fact that osteogenesis and dentinogenesis are highly similar processes, and osteoblasts and odontoblasts are closely related cell lineages. However, they remain distinct cell types, as observed by their slightly different gene expression profile and the structural differences of their respective products, bone and dentin. Optimal conditions permissive for dental stem cell differentiation into odontoblasts rather than osteoblasts remain to be elucidated.

The increasing knowledge about these biological processes enables us to develop materials which go beyond the basic requirements of biocompatibility. Whereas in the past, biomaterials were designed to be bioinert as not to damage the tissues around the implantation site, we are now striving to make scaffolding systems bioactive, where incorporation of growth factors or other drugs actively stimulate a desired response. For Specific Aim 2 of this project, we started customizing multidomain peptide hydrogels by incorporation of growth factors and bioactive molecules relevant for dental stem cell differentiation and tissue formation.

4.4. Engineering of Partial Tooth Structures

Several groups have begun to develop strategies to engineer dental pulp. In 1996, a pulp-like tissue was first engineered *in vitro* after seeding pulp fibroblasts on PGA scaffolds, where cells formed new tissue after 60 days in culture [63]. Using a similar approach, the ability of different scaffold materials to support pulp tissue formation from pulp fibroblasts was evaluated two years later. PGA, collagen hydrogels and alginate were tested. Culturing cells on PGA resulted in tissue formation and collagen synthesis, whereas only moderate cell proliferation was observed on collagen and no proliferation on alginate [64].

Recently, formation of pulpal tissue could be demonstrated *in vivo*. Dental stem cells were seeded on PLLA scaffolds and inserted into the pulp cavity of tooth slices after removal of the original tissue. These constructs were implanted subcutaneously into immunodeficient mice. It could be shown that dental stem cells differentiate into odontoblast-like cells, and that the resulting tissues contained newly formed blood vessels [65]. Mobilization and release of growth factors and proteins from the dentin due to locally decreased pH by degradation of PLLA scaffolds might promote the differentiation process [65].
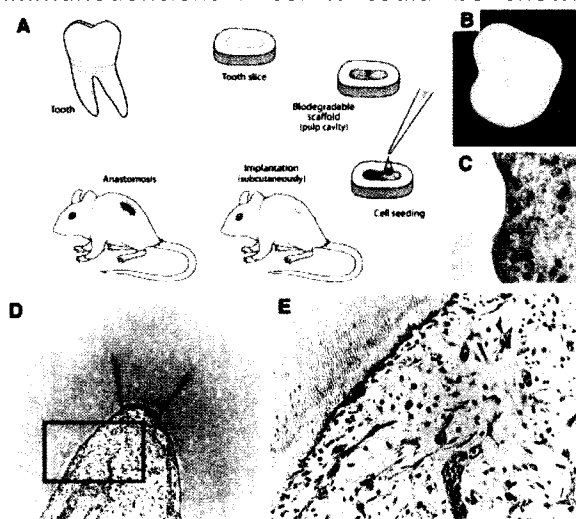
Figure 6: Engineering of dental pulp tissue. (A) Schematic of the strategy for dental pulp engineering. (B) Biodegradable scaffold prepared within the root canal and seeded with dental stem cells, subsequent subcutaneous implantation. (C) Scaffold-dentin interface. (D) Low magnification (100x) of a dental pulp engineered with dental pulp stem cells 14 days after implantation. (E) High magnification (400x) of the boxed area. Adapted from [65].

In a similar approach, dentin cylinders were prepared from human teeth for Specific Aim 3, and hydrogels laden with dental stem cells and growth factors were implanted into immunocompromised mice to evaluate the potential of this system to form a tissue similar to dental pulp.

CHAPTER II: PILOT STUDY

1.   SHED in Peptide Amphiphile Hydrogels

A detailed description of this work can be found in Appendix B, which contains a copy of the manuscript which was published in *Tissue Engineering* in 2008. The following paragraph provides a brief overview, whereas a thorough description of the material's chemistry, the methods used and the results obtained can be found in the paper.

2.   Introduction

To establish general parameters for the compatibility of dental stem cells with peptide-based hydrogels, a set of experiments was performed on a modification of peptide amphiphile (PA) hydrogel developed in our laboratory [66]. The structure of the molecules used in this study can be divided into four regions of function: the peptide sequence contains an MMP-2 specific enzyme-cleavable site to enable cell-mediated degradation; a glutamic acid to assist in calcium binding for self-assembly; and the cell adhesion motif RGDS. The fourth region of functionality is added after peptide synthesis by N-acylation with palmitic acid, which provides the driving force for self-assembly. Whereas the PAs remain amorphous aggregates at neutral pH due to the repulsive negative charge which prevents self-assembly, addition of divalent ions eliminates the negative net charge and allows self-assembly into cylindrical micelles, which undergo physical crosslinking via calcium-ions to provide the gelled macrostructure.

In order to investigate the potential of peptide amphiphile hydrogels to accommodate dental stem cells, SHED and DPSC were seeded in peptide amphiphiles and cultured either with or without osteogenic supplements (0-control, β-glycerophosphate + dexamethasone, KH_2PO_4 + dexamethasone). Cell proliferation and alkaline phosphatase activity were monitored via MTT and quantitative DNA and ALP assays. Real-time PCR experiments were performed using RNA extracted from SHED and DPSC after a four-week culture period with different osteogenic supplements. Marker genes of osteoblast and odontoblast differentiation were chosen to assess the differentiation potential of both cell lines in peptide amphiphiles under different culture conditions. The panel of genes included collagen α I (I) (Col I), collagen III (Col III), alkaline phosphatase (ALP), bone sialoprotein (Bsp), osteocalcin (Oc), Runx2 and dentin sialophosphoprotein (Dspp), which have been used as markers of mineralization and odontoblast differentiation before [27, 28, 67 – 69]. Besides the markers for cell differentiation, we included MMP-2, which is the main gelatinase secreted by human pulp cells [70], to assess whether proteinase activity was in accordance with cell proliferation and matrix degradation. A list of primer sequences for real-time PCR can be found in Appendix C. For histologic analysis, we stained with hematoxilin & eosin (H&E), Masson's trichrome and von Kossa to detect mineral deposition.

3.   Results and Discussion

PA hydrogels were easy to handle, and continuous cell proliferation of SHED and DPSC was observed over a 4-week culture period. However, SHED proliferated at a higher rate compared to DPSC. Addition of β-GP + dex resulted in slightly increased proliferation rates

in both cell lines, whereas potassium phosphate + dex showed the opposite effect. Quantitative measurements of alkaline phosphatase activity showed a dramatic increase in alkaline phosphatase activity in both cell lines over time, but whereas SHED responded to treatment with βGP + dex with a considerable increase in enzyme activity, DPSC showed a different profile, where potassium phosphate + dex evoked higher ALP levels.

Gene expression studies of markers for osteoblast and odontoblast differentiation revealed increased expression except for dentin-specific Dspp, which ceased to be expressed in DPSC treated with potassium phosphate + dex. βGP + dex appears to have a positive effect mainly on expression of extracellular matrix components (Col I, Col III), especially in SHED. At the same time, MMP-2 levels were increased. On the other hand, potassium phosphate + dex stimulated increased expression of genes typically found in the osteoblast lineages, which are involved in matrix mineralization, such as osteocalcin, bone sialoprotein and Runx2.

Histologic analysis revealed degradation of the PA gel and replacement with extracellular matrix. Whereas SHED formed clusters of cells, DPSC were more sparsely distributed within the gel, they showed a round, osteoblast-like morphology, and a higher tendency of mineral deposition. CryoTEM images showed no mineral in gels without cells and gels with cells cultured without osteogenic supplements (0-control). Mineral can be seen in treated groups, to a higher degree in DPSC versus SHED, and higher with potassium phosphate + dex versus βGP + dex.

This data set provides evidence that the two stem cell lines are able to proliferate within the gel, to remodel it by enzymatic degradation and deposition of a collagenous

matrix, to change their morphology and gene expression profile as a sign of differentiation, and to induce calcium deposition and the formation of a mineralized matrix.

4.   Drawbacks

Whereas PA hydrogels provide a suitable matrix for proliferation and differentiation of dental stem cells, a few drawbacks remain:

1) The relatively rapid gelation of PAs (2-3 sec) might prevent thorough mixing and homogenous cell distribution within the gel. *In-situ* gelation of this material is possible, but a gel undergoing shear-recovery might be advantageous for *in vivo* applications.

2) Addition of a fatty acid is necessary to induce self-assembly of PAs, which reduces the possibilities to add biofunctional ligands to one end of the molecule.

The development of a system of self-assembling multidomain peptides (MDP) in our laboratory led to transition to MDP hydrogels for further work on this tissue engineering project. MDPs offered the opportunity of working with a novel, innovative and highly versatile system. The above mentioned drawbacks of PAs are not present in MDPs, and an iteration process of varying a parent MDP peptide sequence led us to the development of a customized peptide-based hydrogel system specifically targeted to for dental stem cells in an approach to engineer the dentin-pulp complex.

CHAPTER III: SPECIFIC AIMS

1.   Overview

There are two major causes for the loss of mineralized matrices with subsequent loss of soft connective tissue in teeth. During cavity formation, demineralization of enamel and dentin allows for penetration of bacterial toxins to the dental pulp, causing inflammation and eventually tissue necrosis, leaving a devital tooth. Traumatic impact and tooth fracture lead to bacterial contamination and cause a similar situation. After loss of hard or soft tooth tissues, conventional treatment methods rely on replacement with biologically compatible materials alone. Amalgam, gold or resin composites are used to fill defects of the tooth crown. After necrosis of the dental pulp, debridement and obturation of the root canal and pulp chamber are necessary.

However, the latest developments in the area of tissue engineering make it feasible to strive for biology-based approaches and true regeneration. Only recently, stem cell niches have been accessed, tooth-derived postnatal stem cells have been isolated, and their differentiation potential has been studied *in vitro* as well as after transplantation into immunocompromised animals. In order to utilize these cells for tissue engineering purposes *in vivo*, we are in need of suitable delivery systems. Novel technologies in scaffold design and synthesis make it possible to develop customized matrices, which will specifically promote proliferation and differentiation of dental stem cells to form and replace tooth tissues. An interesting class of biomaterials is peptide – based hydrogels. Following a bottom-up approach, peptide molecules can be designed to self-assemble into nanofibrous

networks highly similar to natural ECM, and form hydrogels. The system is highly versatile since peptide molecules can be designed following a modular concept and therefore be modified and optimized for specific applications. Bioactive peptide sequences and small molecule drugs can be incorporated in the peptide matrix, and living cells can be entrapped and cultured in the hydrogel. An injectable system is particularly interesting for application into small defects in the oral cavity.

The overarching goal of this project was to explore future treatment strategies to preserve or regenerate a functional dentin-pulp complex. A synthetic, peptide-based scaffold should be optimized and customized for the growth and differentiation of dental stem cells for further applications in regenerative dentistry. The scaffold should 1) create an environment permissive for cell adhesion, proliferation and migration; 2) allow for cell-mediated matrix degradation and remodeling; 3) stimulate new blood vessel formation via incorporation of vascular endothelial growth factor (VEGF); and 4) induce cell differentiation and mineralization through incorporation of growth or differentiation factors.

2. Hypothesis

Combining dental stem cells with a specifically modified peptide hydrogel might provide us with an applicable system to form the soft connective tissue for the regeneration of dental pulp. Directional cues for the cells can lead to deposition of new dentin, and thus formation of a functional dentin-pulp complex. Since dental pulp-derived stem cells have been demonstrated to differentiate into odontoblasts and form dentin after transplantation *in vivo* [26, 27], it seems most feasible to utilize these cells for our approach. DPSC (dental

pulp stem cells) are derived from dental pulp of extracted wisdom teeth; they possess multilineage differentiation and are capable of forming dentin-pulp-like complexes after transplantation [25, 26]. SHED (stem cells from human exfoliated deciduous teeth) are derived from deciduous teeth after exfoliation, they show higher proliferation rates compared to DPSC, and present a more heterogeneous and immature cell population [27]. An optimized and customized peptide-based hydrogel should accommodate the cells in a three-dimensional environment for cell delivery. Incorporation of an adhesion sequence and an enzyme-cleavable site can result in cell attachment, cell-mediated degradation and cell migration through the synthetic matrix. Bioactive molecules and differentiation factors can stimulate new blood vessel formation and promote cell differentiation and subsequent tissue formation. Through an iteration process and synthesis of different peptides, an optimal sequence will be identified. The resulting hydrogels can be characterized regarding gel formation and handling aspects as well as mechanical properties. *In vitro* cell culture of dental stem cells with different peptide hydrogels can be used to assess cytocompatibility, cell proliferation rates, adhesion, spreading and migration as well as cell differentiation. For evaluation of this system *in vivo*, dentin cylinders will be a suitable carrier for the cell-laden hydrogels. Contact with the dentin walls will provide orientational cues to the cells and closely mimic a physiological situation. Transplantation of these constructs into a host will allow us to evaluate the system's potential to induce tissue formation, ideally production of the soft connective tissue of dental pulp and deposition of a dentin matrix in a directional manner towards the existing dentin.

3. Specific Aim 1

To design and synthesize a peptide library in an iteration process to find an optimized sequence to accommodate dental stem cells and promote cell proliferation.

The first part of this research project describes a rational process of design and synthesis of peptide sequences based on a parent peptide. Starting point is a 14 amino acid peptide, which undergoes self-assembly at physiological pH after addition of multivalent ions to form a hydrogel. The material is easy to handle, but does not provide sufficient gel strength. A step-by-step variation of this parent peptide is described, in which changes of single amino acids lead to a mechanically stronger gel, which furthermore features shear recovery. Incorporation of an enzyme-cleavable site and the cell adhesion motif arginine-glycine-aspartic acid (RGD) improve cytocompatibility, which can be seen from cell proliferation rates in different gels, cell morphology and spreading as well as cell migration in the hydrogels. At the same time, rheological and chemical characterization of the peptides provides information about gel strength and degradation characteristics. Specific Aim 1 is completed after identification of a peptide sequence which fulfills the requirements in terms of optimized rheological and gelation properties for cell encapsulation, is cytocompatible and biodegradable, and allows for cell proliferation and spreading comparable to commercially available hydrogel systems.

4.   Specific Aim 2

To assess the potential of this system for cell differentiation after application of growth and differentiation factors. In a second step, bioactive factors are incorporated into peptide hydrogels, which will aid in cell differentiation and tissue formation.

Biologically active compounds can be added to the media in cell culture, and the first part of this section shows the effect of combinations of differentiation factors on dental stem cells in monolayer or three-dimensional culture in peptide hydrogels. Evaluation of cell proliferation rates, expression of differentiation markers and matrix formation and mineralization provide information about lineage commitment and tissue formation.

However, an *in vivo* application requires these molecules to be an integral part of the delivery system. Two bioactive factors, dexamethasone and β-glycerophosphate, were incorporated into peptide hydrogels. Whereas dexamethasone loses its bioactivity after covalent linkage to peptide molecules, β-glycerophosphate induces gelation and aids in mineral formation in three-dimensional cultures. Furthermore, the peptide sequences can be designed such that heparin, a negatively charged glycosaminoglycan, stabilizes the self-assembled nanofibers. At the same time, heparin can be used for binding and slow release of growth factors. This mechanism was utilized to incorporate vascular endothelial growth factor (VEGF), a potent stimulator of new blood vessel formation. Slowed release of VEGF from heparin-containing hydrogels is demonstrated.

5.   Specific Aim 3

To test the potential of the generated system for engineering of the dentin-pulp-complex in an appropriate animal model.

The optimized peptide-hydrogel system laden with VEGF and β-glycerophosphate was used as a carrier system for either SHED or DPSC cells. The gels were injected into small standardized dentin cylinders prepared from the roots of human molars. These constructs were transplanted subcutaneously into immunocompromised mice. After 2 and 5 weeks, the implants were harvested and examined for tissue formation in the dentin cylinders. Histological analysis revealed the formation of vascularized soft connective tissues inside the dentin cylinders for both cell lines. Immunohistochemistry allowed for the localization of microvessels. The presence of VEGF stimulated formation of significantly higher numbers of blood vessels compared to controls. Better nutrition in VEGF-containing gels in turn allowed for much improved cell growth and tissue formation. DPSC furthermore formed small and dense collagen deposits, and islands of cells dispersed throughout the tissue express dentin sialoprotein, a dentin-specific marker.

Combination of the dental stem cells in this customized hydrogel system promoted vasculogenesis and formation of a soft connective tissue with localized matrix deposits. These results indicate that we have an applicable system for the regeneration of dental pulp at hand; however, directional deposition of dentin remains to be resolved.

CHAPTER IV: SPECIFIC AIM 1

To design and synthesize a library of peptide sequences in an iteration process to find an optimized sequence to accommodate dental stem cells and promote cell proliferation.

1.   Summary

Control over fiber length, various mechanisms for physical crosslinking, resemblance to natural ECM, versatility, biocompatibility and biodegradability along with the possibility to incorporate additional bioactive motifs for a custom-made scaffold make hydrogels assembled from multidomain peptides (MDPs) promising candidates for cell encapsulation and further use in tissue engineering [48, 71]. However, our first generation peptide architecture, the parent $E(QL)_6E$ (for peptide molecules see Table 1, for amino acid nomenclature and properties see Appendix A), had to undergo an optimization process to develop a sequence with a set of desired properties, which could accommodate dental stem cells. Therefore, a library of peptide sequences was designed, synthesized, characterized and tested for compatibility with dental stem cells during an iteration process. Specifically, the peptide should

1) incorporate the cell adhesion motif RGD,

2) contain an enzyme-cleavable site to enable cell-mediated degradation and cell migration,

3) offer sufficient viscoelastic properties (storage modulus $\geq$ 100 Pa), and

4) form a matrix conducive for dental stem cell viability and proliferation.

Cell adhesion, the first step of cell-matrix interaction, can be mediated by a variety of short peptide sequences, which can be incorporated into bioscaffolds to mimic ligands on

molecules abundant in natural ECM. The most common sequence incorporated into tissue engineering scaffolds is the integrin-binding tripeptide RGD, which was first detected in fibronectin [72]. Presentation of RGD in combination with another site, PHSRN, in close proximity mimicking their distance in fibronectin results in a synergistic effect and enhances cell spreading [73]. Therefore, the first step of optimization was to modify the parent peptide with RGD or a combination of RGD and PHSRN in the flanking region. Proliferation rates of dental stem cells were higher in these modified peptides compared to the parent peptide, indicating that this was a step in the right direction. However, we did not observe an improvement after addition of PHSRN, and decided to continue our work by attaching RGD only.

Although conducive for cell proliferation, the hydrogels formed from $E(QL)_6E$ were mechanically weak and therefore difficult to handle. Alternative sequences were designed, and exchange of glutamine (Q) with serine (S) in the central block turned out to improve the mechanical properties of the gels substantially. The resulting $E_2(SL)_6E_2$ and its counterpart $K_2(SL)_6K_2$ were then modified to carry RGD in their flanking regions. Cell proliferation assays confirmed that the presence of the adhesion motif resulted in increased cell numbers.

Biodegradability was another important feature to be incorporated into our hydrogels. The organization of MDP molecules into β-sheet aggregates with poor water solubility and a fiber assembly process reminiscent of amyloid raises concerns that the material cannot be degraded *in vivo* and might not be suitable as a tissue engineering scaffold. This is underscored by the devastating effects of amyloid aggregates in brain, causing Alzheimer's disease and dementia, or other organs such as heart, kidney and the

vascular system. By programming susceptibility to proteolytic degradation into these β-sheet forming peptides, MDPs can be adapted to requirements for biological applications. Based on the peptide $K_2(SL)_6K_2$, a hexapeptide containing the MMP-2 consensus cleavage motif LRG [74] was incorporated into the central block. To confirm that modification resulted in susceptibility to degradation, a weight loss study was conducted and loss of gel mass over time after incubation with the enzyme was monitored. Furthermore, disintegration of the peptide molecules and the nanofibrous network was confirmed by mass spectrometry and cryoTEM, respectively.

The mechanical properties of the hydrogels from all the sequences designed and synthesized were analyzed by oscillatory stress sweep rheometry. Based on experience and handling aspects, e.g. for the gels to withstand a series of processing steps for histologic analysis, sufficient gel strength for our application was defined for gels with a storage modulus (G′) of ≥ 100 Pa.

In order to test for compatibility with dental stem cells, proliferation rates were assessed in hydrogels prepared from the different peptide sequences in comparison to two commercially available hydrogel systems. Cell morphology and spreading were observed by confocal microscopy to visualize the effect of different matrix chemistries on cellular behavior. For hydrogels prepared from peptides with enzyme-cleavable site, a cell migration study was conducted, where cells were seeded on top of the hydrogels, and migration of cells into the matrix was observed.

At this point, we considered the iteration process completed. The peptide $K(SL)_3RG(SL)_3KGRGDS$, which features both the cell adhesion motif and an enzyme-cleavable

site, provided the most suitable environment to accommodate dental stem cells, resulting

in cell proliferation rates comparable to commercially available systems, and allowing for

cell spreading and migration into the hydrogel matrix.

2. Peptide Design

The following table gives an overview of all sequences synthesized during the course of this

Ph.D. The mechanism of crosslinking is indicated, and a brief summary of the material

properties is provided.

Peptide Sequence	MDP	Crosslinking	Properties (/Con)
EQLQLQLQLQLQLE EQLQLQLQLQLQLE GEQLQLQLQLQLQLEG	1 1A 1B	Mg $^{2+}$, Ca $^{2+}$	Mechanically weak
EESLSLSLSLSLSLEE	2		Insufficient cell compatibility
KKSLSLSLSLSLSLKK	3	PBS, β-GP, Heparin	
EESLSLSLSLSLSLEEG RGDS KKSLSLSLSLSLSLKKG RGDS	2A 3A	Mg $^{2+}$, Ca $^{2+}$	Non degradable
		PBS, β-GP, Heparin	
EESLSLS SLSLSLEE	2B	Mg $^{2+}$, Ca $^{2+}$	no gelation
KKSLSLS SLSLSLKK KSLSLSL LS SLSLSLK KSLSLS SLSLSLK	3B 3C 3D	PBS, β-GP, Heparin	
KSLSLS SLSLSLKG RGDS	3E		
KSLSLSL LRGSLSLSLK	3D-1 3D-2	-	Expected cleavage fragments

Table 1: Peptide Library. For single-letter amino acid code see Appendix A.

The original parent multidomain peptide $E(QL)_6E$ (*MDP1*) was modified to contain the cell adhesion motif G-RGD-S (*MDP 1A*) or a combination of both G-RGD-S and G-PHSRN (*MDP 1B*), where glycine serves as a linker, and the C-terminal serine in the tripeptide increases specificity of this motif [75]. These peptides were designed and synthesized by He Dong in our laboratory. We intended to identify the best candidate for cell survival among sequences with and without cell adhesion motifs. Cell culture studies showed comparable results for PHSRN + RGD versus RGD alone; therefore we decided to continue with peptides carrying RGD only. Although the cell compatibility studies with this series of peptides were promising, the mechanical strength of the hydrogels was insufficient. Another student in our laboratory, Lorenzo Aulisa, modified the sequences in an attempt to improve the mechanical properties. The exchange of glutamine (Q) for serine (S) in the central block motif resulted in the two peptides $E_2(SL)_6E_2$ and $K_2(SL)_6K_2$. Whereas the negatively charged glutamic acid (E) in the flanking region allows for crosslinking with positively charged ions, such as Ca^{2+} or Mg^{2+}; the antagonistic peptide with positively charged lysine (K) in the flanking region can utilize negatively charged ions, such as phosphate, to induce gelation. The increased number of amino acids in the flanking region provided improved water solubility. An additional advantage of this peptide architecture was the fact that the resulting hydrogels possess shear-thinning behavior and undergo quick shear-recovery.

The peptide $K_2(SL)_6K_2$ was modified further to create four different variants with MMP-2 specific cleavage motifs and either one or two lysine residues in the flanking region. In general, specificity of enzymatic cleavage by endopeptidases arises from the amino acid sequence. Occurrence of specific residues 5 positions N-terminal and 3 positions C-terminal

from the scissile bond (P5 – P3′) has been demonstrated to affect recognition and increase the specificity of an enzyme for its substrate [74]. Two hexapeptides were designed, in which the consensus MMP-motif LRS (leucine-arginine-serine) C-terminally of the actual cleavage site was modified to LRG (leucine-arginine-glycine). Whereas glycine, similarly to serine, can be observed frequently in position P3′ in MMP-2 susceptible substrates, this amino acid appeared more favorable as to maintain the pattern of alternating polar and nonpolar residues in the central block motif. The three amino acid residues N-terminally of the scissile bond were chosen based on cleavage site motifs described previously [74]. The sequences SLS-LRG (*MDP 3B, 3D*) and VLS-LRG (*MDP 3C*) were incorporated into the central block of $K_2(SL)_6K_2$ (*MDP 3*), where addition of valine (V) 3 positions N-terminally of the scissile bond was expected to increase the specificity of the site. In order to compensate for the unfavorable influence of the hydrophobic residue in this position on self-assembly and gel formation, the peptide was elongated and this motif was flanked by an additional SL-repeat on either side. Furthermore, a version of $E_2(SL)_6E_2$ (*MDP 2*) with the cleavage motif SLS-LRG was synthesized (*MDP 2B*).

After assessment of solubility, gelation properties and confirmation of enzymatic cleavage of these peptides, the sequence KSLSLSLRGSLSLSLK (*MDP 3D*) was chosen for further analysis. The expected fragments after enzymatic cleavage (*3D-1, 3D-2*) were synthesized to exclude that these could still assemble and form β-sheet structures. For cell culture studies, this peptide was synthesized with the cell adhesion motif RGD, and compared to $K_2(SL)_6K_2$ both with and without RGD.

3.   Materials and Methods

3.1.   Peptide Synthesis

All peptides, including the expected cleavage fragments were synthesized by solid phase chemistry on an Advanced Chemtech Apex 396 peptide synthesizer using a modified protocol specifically for MDPs as described previously [71]. After acylation of the N-termini and cleavage from the resin, the crude peptides were dissolved in de-ionized water at 5 mg/mL and purified by dialysis in semipermeable membranes with a molecular weight cut-off of 100-500 Da (Spectra/Por, Spectrum Laboratories Inc., Rancho Dominguez, CA). The water was changed every 12 hours for 5 days, the peptides were lyophilized and the resulting products were used for further analysis and cell culture experiments. The correct masses of all peptides were confirmed by matrix-assisted laser desorption/ionization time-of-flight (MALDI-TOF) mass spectrometry.

3.2.   Gel Formation and Rheological Properties

The lyophilized peptides were dissolved in de-ionized water containing 298 mM sucrose at 20 mg/mL, and the pH was adjusted to 7.4. For E-series peptides, gelation was induced by addition of Mg^{2+} or Ca^{2+} ions (ratio of peptide molecules to ions of 1:4). For K-series peptides, phosphate buffered saline (1 x PBS, phosphate concentration of 10mM) was added, where lysine-containing peptides are cross-linked due to the presence of negatively charged phosphate ions. The final peptide concentration amounted to 10 mg/mL (1 % by weight).

To evaluate viscoelasticity and gelation behavior of MDP hydrogels, and in how far incorporation of bioactive motifs would affect these properties, oscillatory stress sweep analysis was performed 24 hours after induction of gelation on an AR-G2 rheometer (TA Instruments, NE). Fifty µL of gel were pipetted onto the center of the bottom plate, and the upper plate (parallel plate, 8 mm) was lowered to the default gap of 250 µm. Storage moduli (G') and loss moduli (G") were measured as a function of oscillatory stress ranging from 0.01 to 1000 Pa at an angular frequency 0.5 rad/s and 10 points/decade.

In order to evaluate shear recovery of the hydrogels, time sweep analysis was performed. This experiment contains three phases. During the first phase, a constant and low oscillatory stress is applied, followed by application of a very high load 5 min into the experiment. It finishes with a third phase, where the oscillatory stress goes back to the original level. The material undergoes shear recovery if its storage modulus returns to the original value within seconds.

3.3. Cell Viability

To assess the compatibility of the different peptide hydrogels with cell cultures, MTT assays for cell viability were conducted. For experiments with E(QL)₆E, a previously developed immortalized cell line from human pulp-derived cells was utilized [76]. The cells were cultured in αMEM supplemented with 15% fetal bovine serum (FBS), 50 µg/mL L-ascorbic acid 2-phosphate, 100 U/mL penicillin and 100 µg/mL streptomycin, and incubated at 37°C with 5% CO_2. Subconfluent cells were detached using trypsin-EDTA (Invitrogen, Carlsbad, CA), and 1 x 10^5 cells were encapsulated per gel. Gelation was induced by adding Mg^{2+} to

the cell suspension. Gels containing cells were seeded in 96-well plates with a gel volume of 100 μL, and 200 μL of medium were added on top of each gel 30 min later. Culture medium was changed every other day, and MTT assay for cell viability was performed on triplicate samples at different time points of the incubation period. Briefly, gels were incubated with 200 μL of medium without serum containing 2 mg/mL of 3-(4,5-dimethylthiazol-2-yl)-2,5-diphenyltetrazolium bromide (MTT) (Sigma-Aldrich, St. Louis, MO) for 3 hours. The solution was removed, and gel and cells were lysed in 200 μL DMSO (Sigma-Aldrich, St. Louis, MO), the plates were shaken thoroughly on a shaker for 5 min. Absorbance was measured in a 96-well plate reader at 570 nm against a blank reading prepared from gels without cells.

3.4.   Cell Proliferation

Actual cell numbers in hydrogels were determined by fluorometric quantification of DNA content using CyQuant cell proliferation assay kit (Invitrogen, Molecular Probes, Carlsbad, CA). For these proliferation studies, SHED from exfoliated deciduous teeth were used. Cells were cultured under conditions as listed above. Subconfluent cells of passage 5 were detached using trypsin EDTA (Invitrogen, Carlsbad, CA) for encapsulation. Several E- and K-series peptides were included in these proliferation studies, as well as two commercially available hydrogels for three-dimensional cell culture: collagen type I (Rat Tail Collagen, Invitrogen, Carlsbad, CA) and PuraMatrix™, a peptide-based hydrogel system (BD Biosciences, San Jose, CA).

Hydrogels were prepared as follows: A peptide stock solution was made in de-ionized water containing 298 mM sucrose at 2 % by weight (20mg/mL). This solution was

mixed with an equal volume of cell suspension with a final peptide concentration of 1 % by weight, a cell number of 1 x 10^5 and a volume of 100 µL per gel. For E-series peptides, the cells were suspended in de-ionized water with 298 mM sucrose to maintain the appropriate osmolarity for cell culture, and with Ca^{2+} to induce gelation. For K-series peptides, the cells were suspended in 1 x PBS. All hydrogels with serine in the central block motif show shear-thinning behavior. Therefore, the total volume of hydrogel needed for a particular experiment was prepared and 100 µL of gel were pipetted into a well of a 96-well plate for each sample. For each assay to be performed and for each time point and culture condition, 3 or 5 samples were seeded. After 30 min, 200 µl of media were added to each well, and subsequently changed every 48 hrs. After 3, 7, and 14 days, samples were diluted in 1 mL PBS and pipetted up and down to disrupt the hydrogel. After centrifugation (3 min at 1000 rpm), the supernatant was removed and cell pellets were frozen down at -80°C for further analysis. After completion of sample collection, these were thawed, and assays and measurements were performed on all samples at the same time. The number of cells in all samples was determined by fluorometric quantification of DNA content using CyQuant cell proliferation assay kit (Invitrogen, Carlsbad, CA) and a FLUOstar Optima fluorescence plate reader (BMG Laboratories, Durham, NC). Actual cell numbers were calculated based on a standard curve created from suspensions of known cell densities. Several proliferation studies were performed, and data were collected from at least 10 samples resulting from two independent experiments. One way analysis of variance (ANOVA) followed by Tukey test was performed to determine differences in cell numbers between different hydrogel systems using Kaleidagraph 4.03 software. The significance level was set to $\alpha = 0.5$.

3.5. Hydrogel Degradation and Weight Loss

Gels were prepared from the three peptides containing an enzyme cleavable site: $K_2(SL)_3RG(SL)_3K_2$ (*MDP 3B*), $K(SL)_3VLSLRG(SL)_3K$ (*MDP 3C*) and $K(SL)_3RG(SL)_3K$ (*MDP 3D*). Their viscoelastic properties were assessed by oscillatory stress sweep rheometry. Whereas *MDP 3B* formed mechanically stable hydrogels around pH 9, its storage modulus at pH 7.4 was lowest among the 3 cleavage peptides (G' = 42.7 Pa). Since this value did not meet our requirement for sufficient gel strength, *MDP 3B* was excluded from further experiments. The degradation profile of the remaining *MDP 3C* and *D* was determined, and $K_2(SL)_6K_2$ (*MDP 3*) was used as a control. For each sample, 50 µL of gel were transferred to a centrifuge tube after weighing the empty tube. After 30 min of equilibration, 200 µL PBS was added on top of each gel, and samples were stored at 37°C for 2 hrs. The PBS solution was then removed, and the weight of each gel was determined on an analytical balance as the difference between the weight of the empty tube and the tube containing the gel. Samples were 200 µL of 1) collagenase IV (Sigma-Aldrich, St. Louis, MO) at 3mg/mL in PBS, or 2) PBS as a negative control. Samples were run in triplicates, solutions were changed and the sample weight was determined every 24 hrs for 14 days.

3.6. MMP-2 - Specific Cleavage

To assess MMP-2 specific cleavage, gels of the cleavage-peptides *MDP 3C* and *D* and of *MDP 3* as a control were prepared at a concentration of 20 mg/mL, and then mixed with MMP-2 (Sigma-Aldrich, St. Louis, MO) in PBS, with the final concentrations being 10 mg/mL peptide

and 100 ng MMP-2 in a total volume of 100 µL. Samples were incubated at 37°C for 48 hrs, and enzymatic cleavage was assessed by mass spectrometry.

Disintegration of the nanofibrous network formed from *MDP 3D* was furthermore visualized by vitreous ice cryo-transmission electron microscopy (cryoTEM) at pH 7.4 and a peptide concentration of 1 % by weight. A small quantity of the sample solution (2-3 µL) was applied to a TEM copper grid with holey carbon film purchased from Quantifoil (400 mesh Cu grid, 1.2 µm hole diameter), and blotted with filter paper using a Vitroblot type FP 5350/60 under 100% relative humidity for two seconds to create a thin layer of sample on the surface of the grid. The grid was plunged into liquid ethane and quickly transferred to liquid nitrogen. Samples were analyzed using JEOL 2010 TEM at an accelerating voltage of 200 kV under low-dose imaging conditions. cryoTEM analysis of the samples was done by Lorenzo Aulisa.

3.7. Circular Dichroism Spectroscopy

Secondary structures were analyzed by measuring ellipticity spectra from 250 to 190 nm on a CD spectrometer. The full length peptide *MDP 3D* as well as the fragments *MDP 3D-1* and *MDP 3D-2* were dissolved in de-ionized water at 1% by weight, sonicated for 30 sec, the pH was adjusted to 7.4 and the solutions were left overnight. The peptides were then diluted to 0.25 % by weight with de-ionized water and pipetted into a cuvette with 1mm path length for acquiring spectra. A blank reference of water was subtracted from the raw data before molar ellipticity was calculated. The calculation was based on the equation $[\theta]$ = $(\theta*MW)/(c*10*l*n)$, where $[\theta]$ = molar ellipticity at λ in mdeg, MW = molecular weight of

the peptide, c = concentration of the peptide in g/L, l = path length in cm, and n = number of amino acids in the peptide.

3.8. Cell Migration and Spreading

To determine whether the presence of the enzyme-cleavable site would encourage cell migration into the hydrogels, SHED were incubated with membrane-permeant fluorescein diacetate (Cell Tracker Green CMFDA, Invitrogen, Carlsbad CA) for 30 minutes, then washed with PBS, detached and seeded on top of hydrogels MDP *3A* and *3E* at a density of 5 x 10^4. Samples were fixed in 2 % paraformaldehyde and embedded for cryosectioning after 1 and 5 days in culture. Sections of 10 μm thickness were prepared on a cryostat microtome, mounted on slides and stored at -20°C. Before use, cells were permeabilized with 5 % triton X in PBS, and cell nuclei were stained with DAPI (4',6-diamidino-2-phenylindole). Cells and hydrogels were visualized using a Zeiss LSM 510 Meta confocal microscope with an attached PMT.

4. Results and Discussion

4.1. Cell Viability

The cell viability studies for the first E-series peptides (MDP *1, 1A* and *1B*) revealed an increase of metabolic activity over a culture period of 14 days. Viability was lowest in hydrogels without RGD. The presence of both RGD and PHSRN did not result in better cell viability compared to peptides with RGD alone, and PHSRN was excluded from further studies.
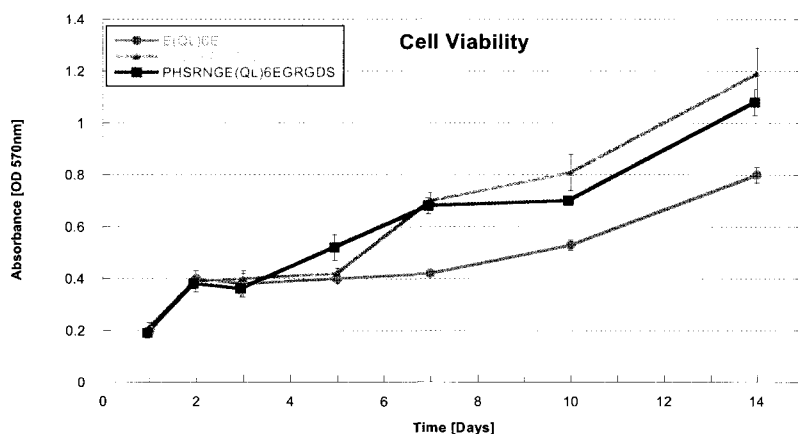
Figure 7: Cell viability in E-series peptides. *Whereas addition of the cell adhesion motif RGD increased viability, the combination of both RGD with its synergistic site PHSRN did not result in further improvement of cell compatibility.*

4.2. Rheological Properties

Oscillatory stress sweep and time sweep experiments were conducted to evaluate the viscoelastic properties of the described hydrogels. Storage (G′) and loss modulus (G″) are obtained, where G′ is a measure of the deformation energy stored in the sample, and the loss modulus (G″) a measure of the energy which is lost during the process and dissipated as heat. Results from oscillatory stress sweep analysis for E- and K-series hydrogels are visualized in Figure 8; additionally, a summary of all measurements is provided in Appendix E. For a comparison, data obtained from commercially available collagen type I at a concentration of 3mg/mL was plotted. Whereas gels from E(QL)$_6$E are mechanically weak, exchange of glutamine for serine increased gel strength considerably. Addition of the cell adhesion motif RGD and the MMP-2 cleavage site resulted in a decrease of mechanical strength, but it remains well above our defined threshold for G′ of 100 Pa, and is comparable to the gel strength of collagen at commonly used concentration for 3D cell culture.
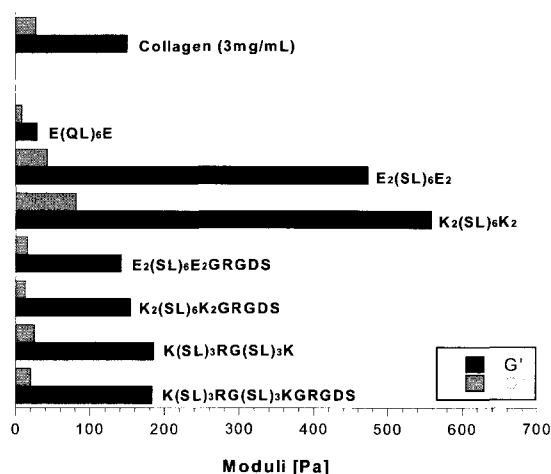
Figure 8: Viscoelastic properties of MDP hydrogels. *Storage (G') and loss moduli (G") for hydrogels prepared from different peptide sequences.*

Besides increased gel strength, hydrogels prepared from peptides with serine in the central block revealed another useful characteristic. They were found to undergo shear-recovery and possess shear-thinning behavior, where the viscosity decreases with increasing load. This was first detected by handling and pipetting the gels, and later confirmed by oscillatory time sweep analysis.

Figure 9 depicts shear recovery for *MDP 2A, 3A* and *3E*. After application of a high load, the gels almost immediately return to the storage moduli observed during the first phase. This behavior makes MDPs an excellent injectable material and ideal for application into small defects in the oral cavity.
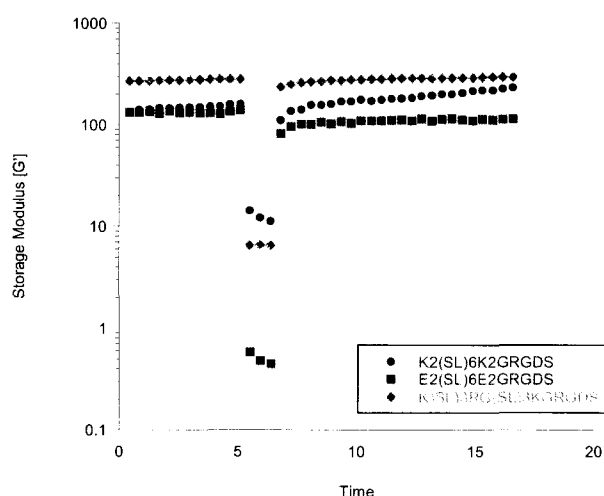
Figure 9: Shear recovery of MDP hydrogels. *A time sweep experiment shows shear-recovery properties of MDP 2A, 3A and 3E. After application of a high load 5 min into the experiment, the hydrogel returns to the original storage modulus (G') within seconds.*

4.3. Cell Proliferation

Figure 10 summarizes proliferation data from several independent experiments. The graph shows cell numbers in two commercially available systems, collagen type I and PuraMatrix™, compared to different MDPs.

For both the E- and K-series peptides, addition of RGD increased proliferation rates significantly ($p \leq 0.05$ at D7 and 14). Whereas E-series with and without RGD seemed to be more conducive for cell proliferation than K-series, addition of the enzyme-cleavable site to K-series peptides resulted in higher proliferation rates, which were comparable to both commercially available systems as well as E-series. The difference between K(SL)$_3$RG(SL)$_3$KGRGDS and either collagen I or PuraMatrix was statistically not significant. MDPs offer the possibility of modification and design of customized scaffolds, which does not exist for the commercially available systems.

A summary of the statistical analysis of differences between the hydrogel systems at the different time points of the incubation period can be found in Appendix D.
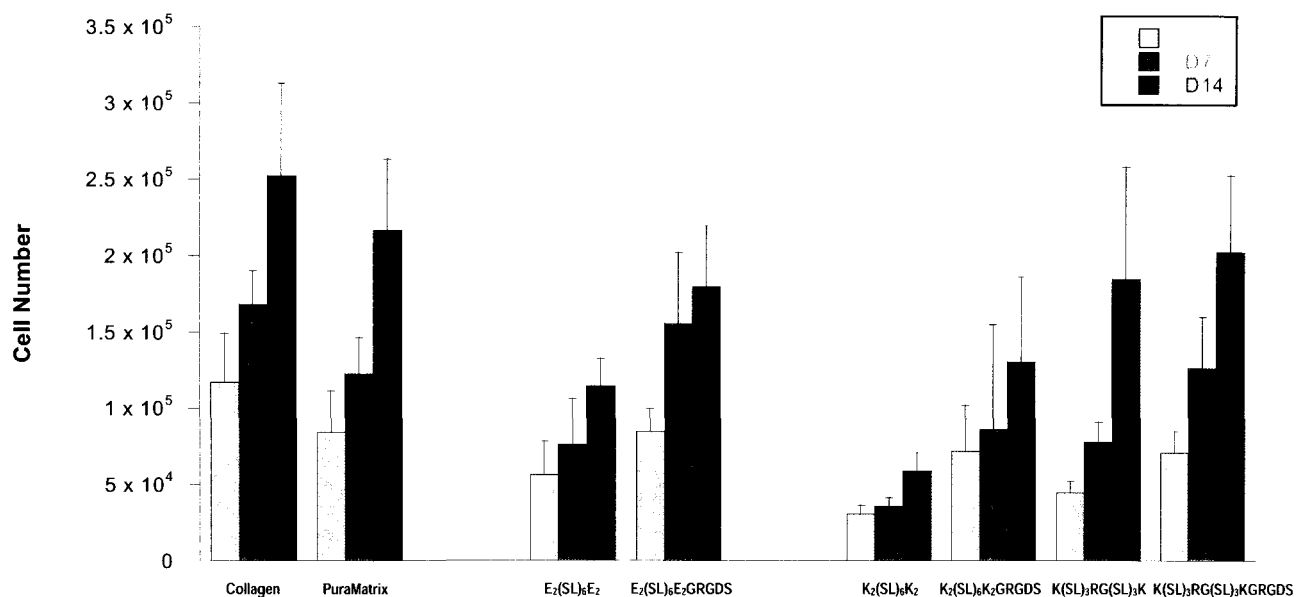
Figure 10: Comparison of cell proliferation in different hydrogels. Cell numbers were determined after 3, 7 and 14 days in culture. Columns represent means, error bars depict standard deviations (n = 10).

4.4. Hydrogel Degradation and MMP-2 - Specific Cleavage

Figure 11 shows weight loss of the cleavage peptides K(SL)₃VLSLRG(SL)₃K (*MDP 3C*) and K(SL)₃RG(SL)₃K (*MDP 3D*) as well as from K₂(SL)₆K₂ (*MDP 3*) when incubated with either collagenase IV or PBS (control). For all gels, incubation with PBS resulted in a weight loss of 5 – 10% over a 2-week period, where a small amount of peptide was washed off due to daily changes of the supernatant. Incubation with collagenase IV resulted in complete digestion of both cleavage peptides after 14 days, whereas the control peptide hydrogels were reduced by only 25 % of their original weight.
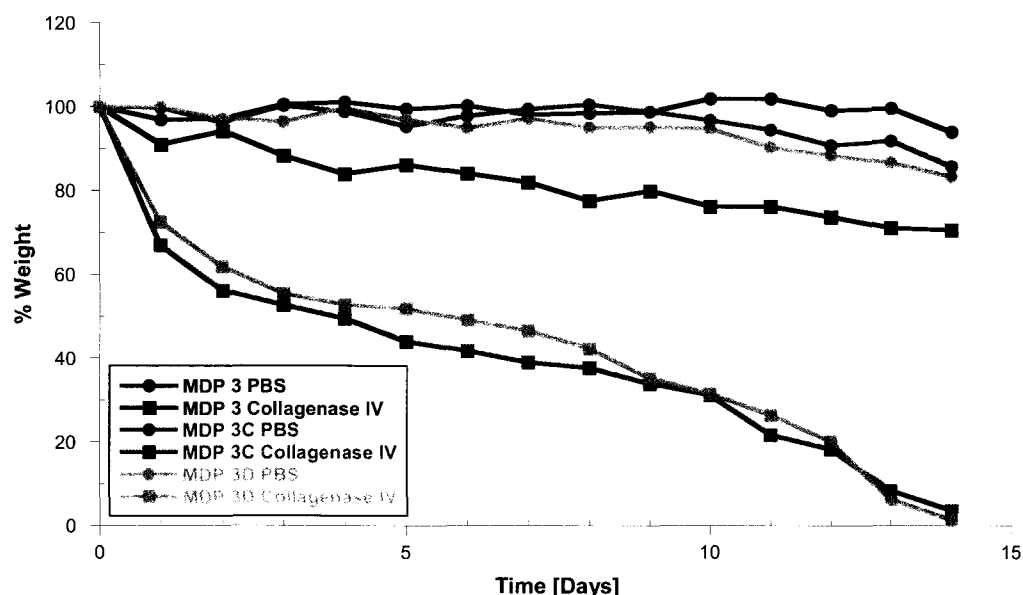
Figure 11: Weight loss after enzymatic degradation. *Hydrogels from MDP 3C and 3D with cleavage sites as well as from MDP 3 (control) were incubated with collagenase IV or PBS. The weight of each hydrogel was determined every day. Data points show averages of three samples (n = 3). Weight loss is depicted as a percentage where the weight at the beginning of the experiment was set to 100 %. Whereas MDP3 without a cleavage site is reduced by 25 % of its original weight with collagenase IV, both cleavage peptides are degraded completely within 14 days. Control samples in PBS show little weight loss.*

To test specific degradation, MMP-2 was used for the following experiments. Upon mixture of a 2 % by weight hydrogel of *MDP 3C, 3D* or *MDP 3* (control) with MMP-2 in PBS at a ratio of 1:1, the hydrogels reform, but cleavage peptides are degraded after 48 hrs of incubation at 37°C. After MALDI-TOF mass spectrometry, the control $K_2(SL)_6K_2$ showed the expected peak before as well as after incubation with MMP-2. The results for both cleavage peptides were nearly identical. One peak according to the mass of the peptide molecule could be observed before incubation, but several fragments afterwards. The peak with the highest intensity was identified as the smaller fragment KSLSLS, a small peak represented the larger fragment, LRGSLSLSLK. Several additional peaks were present, part of which

corresponded to smaller peptide fragments present in the mix. This might be attributed to the fact that after cleavage into the two main fragments, the smaller peptide molecules are more susceptible to further degradation. Some of the peaks could not be identified as cleavage fragments, which might be due to the enzyme digesting itself. Figure 12 shows the data after mass spectrometry for *MDP 3* and *3D*.
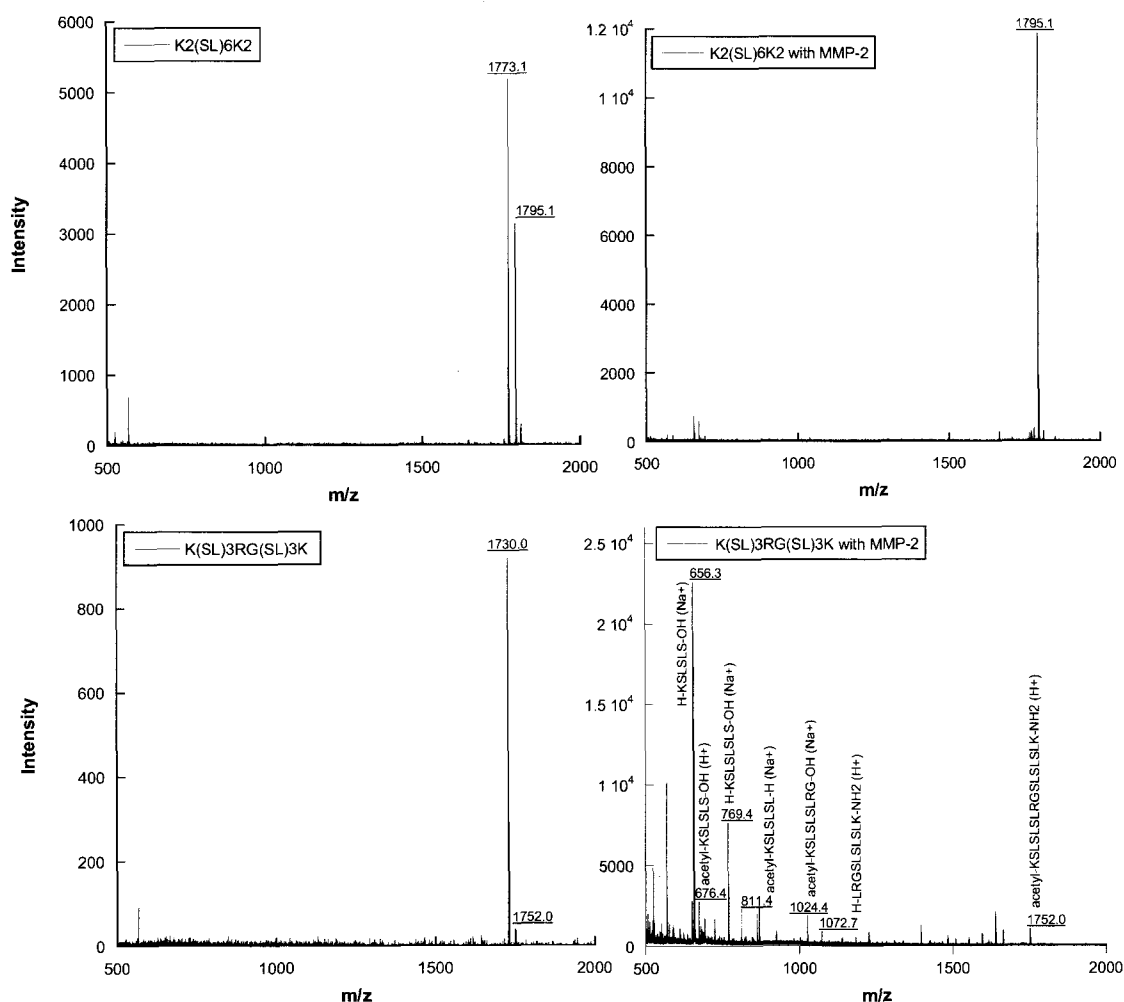
Figure 12: Mass spectrometry before and after enzymatic degradation. The control peptide MDP 3 shows a single peak before and after digestion, the cleavage peptide is degraded and multiple fragments can be observed. The expected fragments after cleavage KSLSLS and LRGSLSLSLK are both present. Some of the fragments could be identified as cleavage products, whereas some of the peaks remained unidentified.

To characterize the profile of enzymatic digestion, two different procedures were chosen. Addition of collagenase IV on top of the hydrogels resulted in a degradation profile showing continuous mass loss, indicating surface erosion of the material. For bulk degradation, an initial plateau phase would be expected, followed by a rapid drop of the curve. In this case, the enzyme would diffuse into the gel and start breaking up peptide molecules internally, but the initial mass of the material would be maintained for some time after the start of exposure, until it collapses rapidly at a critical point of weakened internal architecture. Surface degradation is the preferred mechanism for biological applications, as it will allow migrating cells to locally degrade the matrix as they move along while overall mechanical integrity of the scaffold is maintained until sufficient amounts of ECM have been produced to replace the synthetic material. Mixture of hydrogels with MMP-2 resulted in more rapid disruption of the fibrous network, as can be expected due to the largely increased surface area for the enzyme to attack, and higher specificity of MMP-2. The preparation of collagenase IV contains a varying mixture of enzymes and digests a wider range of substrates. The first results after incubation with collagenase IV therefore show that the designed peptide with cleavage site is susceptible to enzymatic degradation. Digestion with MMP-2 confirms specificity of this enzyme towards the substrate we created. The fast degradation of the hydrogel with MMP-2 compared to collagenase IV might be explained by the difference in preparation (mixing the solutions rather than adding the enzyme on top), and the higher specificity of MMP-2 for the substrate.

This series of experiments confirmed that specific digestion of MDPs occurs when required amino acid residues are present in certain positions relative to the scissile bond: a

hydrophobic amino acid at P1′ followed by a basic amino acid and a small residue. Although specificity of the region N-terminally of the cleavage site has been shown to arise from proline, valine or isoleucine preferred in P3 [74], we did not observe more efficient cleavage for *MDP 3C*. Due to the almost identical profile of degradation for *MDP 3D* and *C* from the weight loss experiment and from mass spectrometry, we concluded that the additional valine in the sequence did not increase the specificity or accelerate the degradation process. Therefore, *MDP 3D*, which is preferable due to its shorter sequence, better water solubility and higher storage modulus, was chosen for further analysis.

Degradation of *MDP 3D* nanofibers was visualized by cryoTEM as depicted in Figure 13. The dense fibrous network changed after 48 hrs of incubation with MMP-2 and transformed into amorphous aggregates, indicating cleavage and subsequent disintegration of the hydrogel. CryoTEM images were taken by Lorenzo Aulisa.
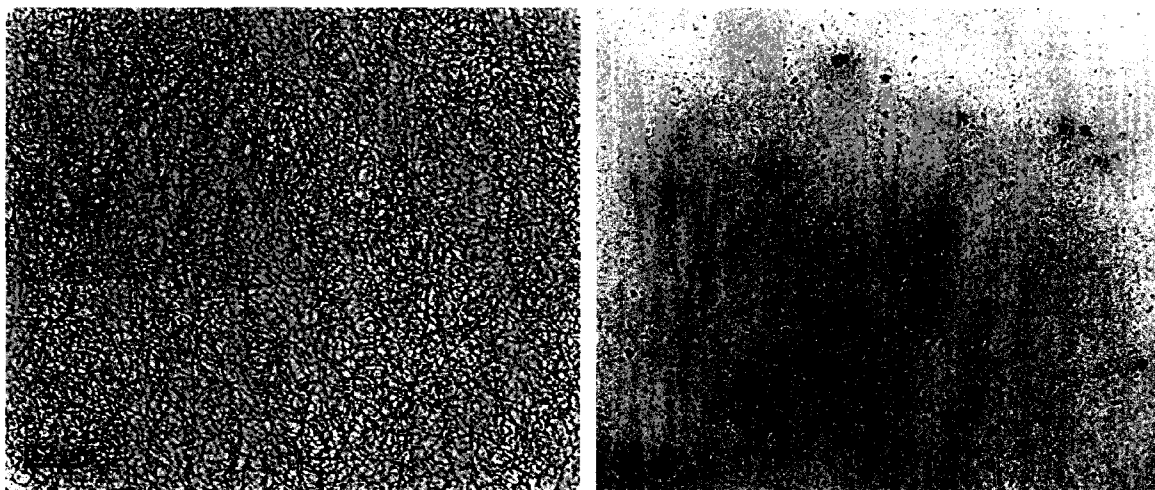
Figure 13: CryoTEM before and after enzymatic degradation. Images were taken before and 48 hrs after incubation with MMP-2. MDP 3D forms a dense fibrous network, after cleavage the nanofibers disintegrate and amorphous aggregates remain. Macroscopically, the gel turns into liquid.

Both peptide sequences synthesized analog to the expected C- and N-terminal cleavage fragments did not form gels and remained as liquid solutions capable of flowing. To exclude that the fragments could still adopt β-sheet conformation, circular dichroism spectroscopy was performed on both fragments *MDP 3D-1* and *3D-2* and the full length *MDP 3D*. Profiling the secondary structures of these peptides by CD and examining the presence of β-sheets can provide basic information on their assembling capability. The CD spectra of β-sheets are characterized by a minimum at 216 nm and a maximum at 195 nm, while these of random coils show a maximum at 218 nm and a minimum at 198 nm [77]. The profiles for *MDP 3D* and its fragments can be seen in Figure 14. Whereas the full length peptide clearly showed β-sheet conformation with the described maximum and minimum, both fragments displayed the profile of random coils. This data suggests that the truncated peptides after degradation of the starting material will no longer be able to assemble and form insoluble aggregates, which is a critical point for any *in vivo* applications.
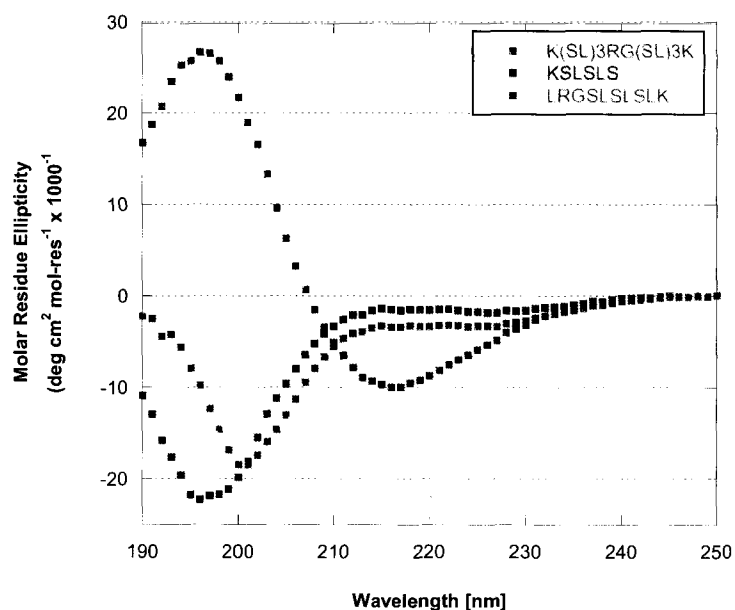
Figure 14: Circular dichroism spectra. The full length MDP 3D (blue) adopts β-sheet conformation, the shorter N-terminal fragment (red) and the C-terminal fragment (green) remain as random coils.

4.5.   Cell Spreading and Migration

To assess cellular morphology in different hydrogel systems, green-fluorescent SHED were seeded into collagen, PuraMatrix™, and E-and K-series of MDPs. Figure 15 shows the cells in these different matrices. The natural collagen matrix proved highly conducive for cell spreading, resulting in a spindle-shaped morphology (15 A). Cells in peptide hydrogels without cell adhesion motif appeared round and balled up (15 B, C, E). When RGD was present, the cell bodies were more spread out (15 D, F). Presence of the cleavage site seemed to enhance spreading (15 G). However, presence of both the enzyme-cleavable site and the cell adhesion motif RGD resulted in a synergistic effect, with visibly different cell morphology and spread-out cell bodies (15 H). This is in accordance with previous work, which demonstrated that initial cell spreading is dependent on proteolytic susceptibility of the matrix [78].

Furthermore, we hypothesized that the possibility of cell-mediated degradation would enable migration and result in penetration of the cells into the hydrogels. Therefore, we seeded green-fluorescent SHED on top of MDP 3A and 3E (Figure 16). After 1 day in culture, the cells could be seen covering the top as a monolayer in both cases (16 A, C). 4 days later, MDP 3A still looked similar (16 B), whereas cells on MDP 3E had started to migrate into the matrix (16 D), indicating that if the cells were able to degrade the matrix around them, cell movement was facilitated.
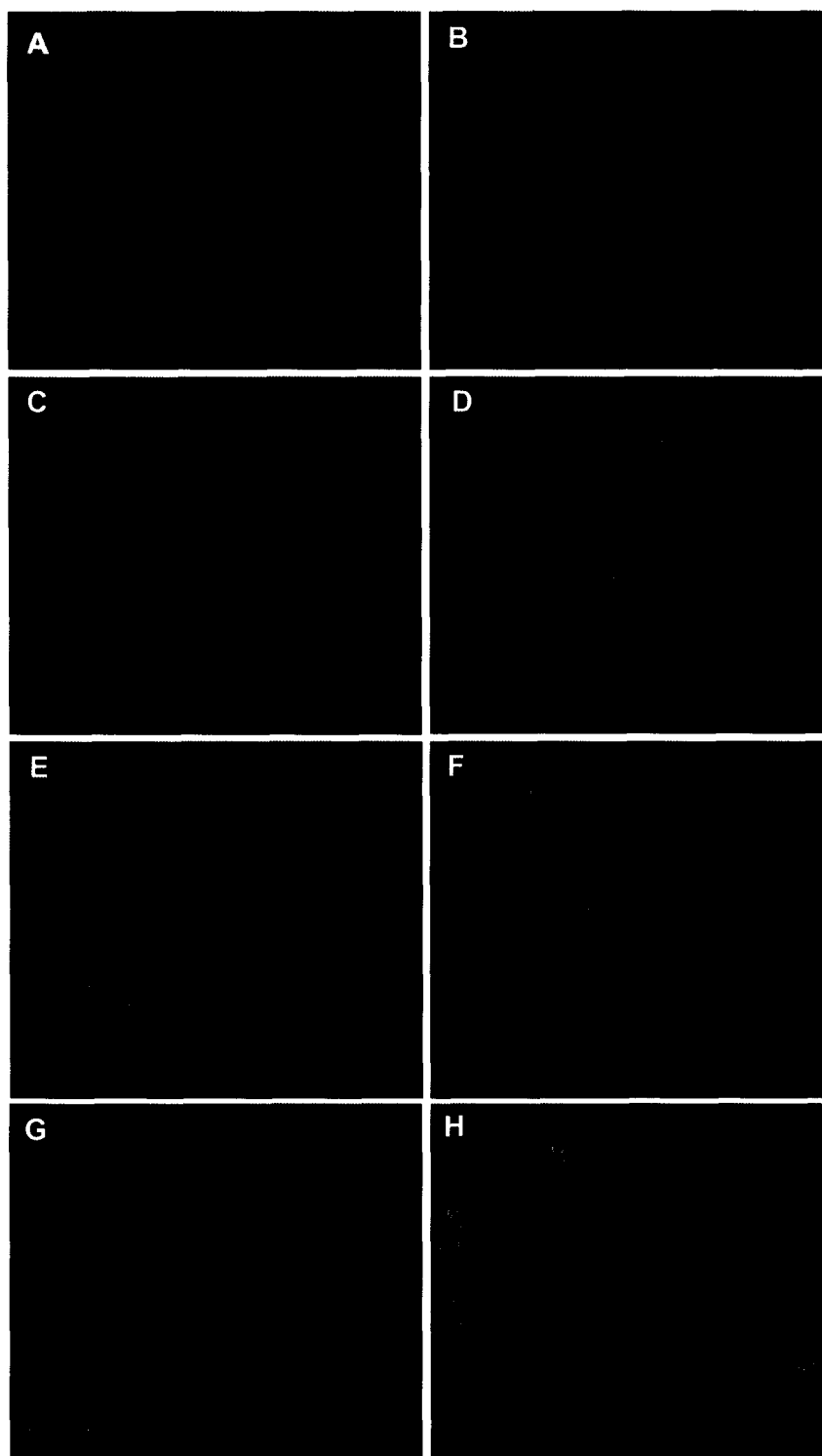
Figure 15: Confocal Microscopy of cells in different hydrogels. *Images A − H show green-fluorescent SHED cells encapsulated in Collagen I (A), PuraMatrix™ (B), $E_2(SL)_6E_2$ (C), $E_2(SL)_6E_2GRGDS$ (D), $K_2(SL)_6K_2$ (E), $K_2(SL)_6K_2GRGDS$ (F), $K(SL)_3RG(SL)_3K$ (G) and $K(SL)_3RG(SL)_3KGRGDS$ (H).*
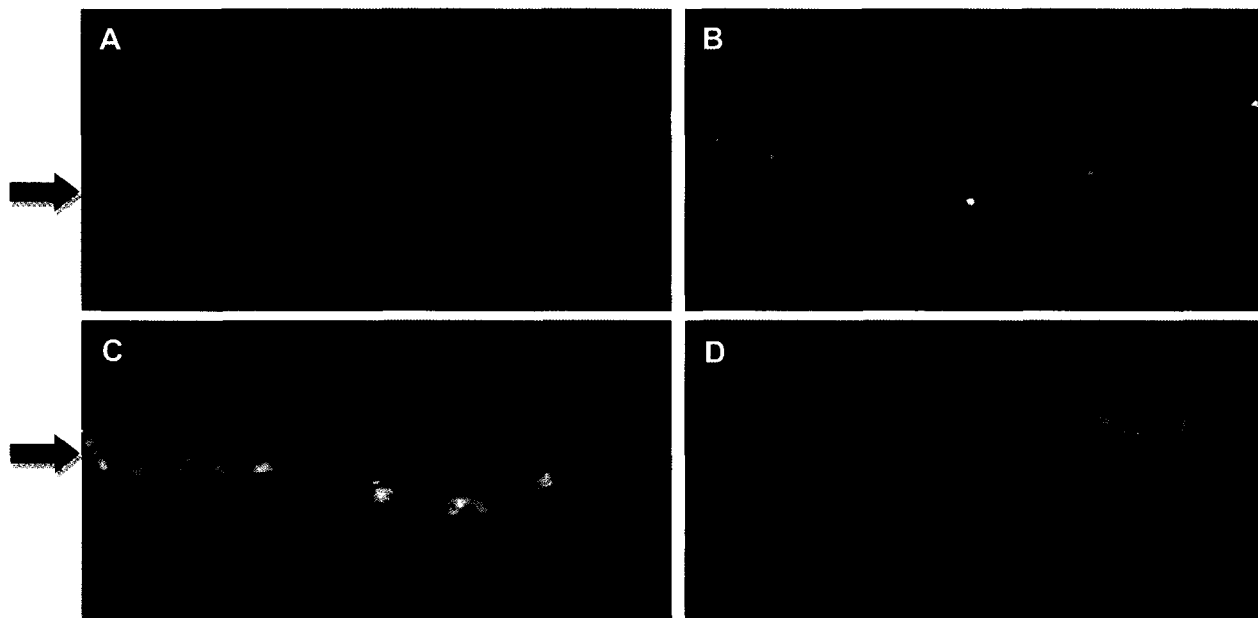
Figure 16: Cell migration into hydrogels. *Green-fluorescent cells were seeded on top of MDP 3A without cleavage site (A, B) and MDP 3E where the cleavage motif is present (C, D). Both peptides carry the cell adhesion motif RGD. Images show cells after 1 day (A, C) and after 5 days (B, D) in culture. Whereas cells remain as a monolayer on top of MDP 3A (B), they migrate and spread into MDP 3E (D) The red arrows indicate the top of the gel.*

In conclusion, incorporation of an MMP-2 specific cleavage motif in β-sheet forming peptides resulted in enzyme-mediated digestion and collapse of the hydrogel due to disruption of the nanofibrous network. Although similar effects have been demonstrated for other hydrogel systems including gels prepared from modified PEG [79 – 81] or self-assembling peptide amphiphiles [82], only one report has shown proteolytic susceptibility of β-sheet-forming peptides [83]. In this case, incorporation of the cleavage motif required elongation of the starting peptide of 16 amino acid residues to a length of 30 to ensure β-sheet formation and gelation.

Furthermore, we demonstrate an immediate effect of the peptide design on cellular behavior, where incorporation of the cleavage site markedly enhanced cell viability,

spreading and migration. This specific interaction of cells with the synthetic matrix surrounding them is another step towards the development of ECM-mimics. The versatility of MDPs leaves a variety of possibilities for further modifications and the design of custom-made scaffolds for regenerative medicine.

5. Troubleshooting

5.1. Cell Compatibility and Purification

After resolving the problem of mechanically weak hydrogels by changing from QL to SL-series peptides, an issue arose as the cell viability in the new gels was comparably low, which was confirmed by repeated measurements. Since E-series peptides are difficult to purify by HPLC due to the charge effect, which results in binding of the molecules to the column and a low yield, alternative purification methods were explored. A comparison using K-peptides revealed that purification by HPLC resolved the toxicity issues. In order to circumvent loss of material in E-peptides, we tried dialysis for purification. Whereas this method resulted in markedly increased cell viability, another advantage of this procedure was that after dissolving the purified peptide powder in water, the pH was already at 7.0, and further adjustment was usually not necessary.

5.2. Gelation Conditions

The protocol for gelation and cell encapsulation was changed after switching from QL- to SL-series. For QL-series, the peptide stock solution as liquid, it was pipetted into the wells of a

96-well plate, and individually mixed with an equal volume of cell suspension containing the ions to induce gelation. Gels formed within 3-5 minutes.

For SL-series, the peptide stock solution already forms a gel. Pipetting the peptide stock, mixing it with the cell suspension and keeping all volumes constant was therefore challenging. The procedure was changed such that instead of mixing gels individually in the 96-well plates, the required volume of gel containing the cells was prepared in a centrifuge tube, and transferred to the wells in 100 uL aliquots. Switching to a 1000 uL - pipette instead of a 200uL - pipette made it easier to handle the gels due to the larger opening at the tip.

5.3.   Cell Proliferation Assays

Whereas the CyQuant cell proliferation assay worked well with E-series peptides, problems occurred when it was used with the K-series, and the results were implausible. This might be due to interference of positive charges on these peptides with the DNA-binding dye used for this assay. A WST - Quick cell proliferation assay kit (BioVision, Mountain View, CA) was tried as an alternative, and a series of experiments was conducted with collagen gels, which worked well. However, in K-series hydrogels, the WST dye, which indicates cell metabolic activity was not properly released from the gels, and the absorbance readings were likely to be too low. Other procedures we tried included cell counts using a hemacytometer and trypan blue stain, or a coulter counter. However, the trypan blue stained the gels as well, and the cells and gel remnants formed lumps, which made it impossible to obtain accurate cell counts. Therefore, we returned to the MTT assay we had worked with initially. This

turned out to work with K-series peptides, as after the incubation period, the gels and cells

lysed in dimethyl sulfoxide, an organic solvent which dissolves the peptides. Measurements

were now possible.

CHAPTER V: SPECIFIC AIM 2

To assess the potential of this system for cell differentiation after application of growth and differentiation factors. In a second step, bioactive molecules are incorporated into peptide hydrogels, which will aid in cell differentiation and tissue formation.

1.   Summary

Dental stem cells have been shown to possess plasticity [25, 27], and osteogenic supplements in the cell culture media promote cell differentiation towards an odontoblast-like phenotype [60 – 62]. In our earlier work on peptide amphiphiles, we demonstrated that both SHED and DPSC differentiate in the hydrogel matrix after addition of inorganic phosphate and dexamethasone. After 4 weeks in culture, the cells express osteoblast- and odontoblast- marker genes, increase their alkaline phosphatase activity, form collagen and initiate mineral formation. To confirm that multidomain peptides are equally conducive for dental stem cell proliferation and differentiation, a similar set of experiments was conducted where cells were grown in *MDP 1A*. The results were comparable to those from our pilot study, indicating that multidomain peptide hydrogels are a suitable scaffold for these cells.

In a next step, we evaluated the effect of dexamethasone and β-glycerophosphate alone and in combination in monolayer cell cultures to get a better idea of their role in promoting cell differentiation. Whereas both compounds decreased cell proliferation and

increased alkaline phosphatase activity, it remained questionable whether a synergistic effect existed for the combination of both.

In order to customize our system for future *in vivo* applications, we attempted to incorporate these differentiation factors into the hydrogel matrix. Dexamethasone was covalently linked to the peptide molecule via a succinyl linker. However, when used in cell culture studies, no effect on cellular behavior could be observed. This might be due to the fact that dexamethasone, a small and hydrophobic molecule, does not act via cell membrane receptors, but induces intracellular changes after passing the plasma membrane. Covalent linkage of dexamethasone to the peptide might prevent the molecule from reaching its intracellular target. Alternative ways to incorporate dexamethasone into multidomain peptides are currently investigated in the Hartgerink laboratory. The incorporation of β-glycerophosphate was successful, as the molecule can be used to induce gelation in positively charged multidomain peptides, resulting in comparable gel strength to previously used PBS. At the same time, β-glycerophosphate can act as a bioactive factor.

Another mechanism we explored for growth factor incorporation was via heparin-binding. Heparin, a negatively charged glycosaminoglycan, is present in natural extracellular matrix, where it can bind growth factors, protect them from proteolytic degradation and prolong their activity. This effect can be mimicked by incorporating heparin into synthetic matrices. Heparin was utilized for gelation of K-series peptides and was successfully integrated into the gels, at the same time increasing gel strength. Heparin was exploited to bind vascular endothelial growth factor (VEGF), a potent differentiation factor for the induction of new blood vessel formation, which is a critical process for any tissue

engineering approach. Prolonged release of VEGF from heparin-containing gels compared to controls could be demonstrated.

The work summarized in Specific Aim 1 led to the development of a peptide sequence which features the cell adhesion motif RGD and an MMP-2 specific enzyme-cleavable site. As established in Specific Aim 2, this peptide is furthermore capable of binding β-glycerophosphate and heparin. With these building blocks, we constructed a customized scaffold for dental stem cell delivery. *In vitro* cell culture with SHED and DPSC followed by histologic analysis demonstrated that the cells deposit collagen and mineral, both indicators for cellular differentiation. This work laid the basis for the *in vivo* experiments described in Specific Aim 3.

2.   Proliferation and Differentiation in Multidomain Peptides

To confirm that multidomain peptides allow for cell proliferation and differentiation comparable to peptide amphiphiles, a similar set of experiments was performed to what had been done before [84]. SHED and DPSC cells were encapsulated in multidomain peptide hydrogels and cultured for four weeks after addition of osteogenic supplements of inorganic phosphate and dexamethasone. Samples were taken at different time points to determine cell numbers and alkaline phosphatase activity. After 28 days, RNA was extracted from the cells in gels, and quantitative real-time PCR was performed to analyze the expression profile of marker genes of matrix deposition and mineralization in treated and control cells.

3. Materials and Methods

3.1. Cell Culture

SHED and DPSC were cultured in αMEM supplemented with 10% fetal bovine serum, 50 μg/mL L-ascorbic acid 2-phosphate, 100 U/mL penicillin and 100 μg/mL streptomycin, and incubated at 37°C with 5% CO_2. Subconfluent cells of passage 4 were detached using trypsin-EDTA (Invitrogen, Carlsbad, CA), resuspended in PBS, and cells were encapsulated in *MDP 1A* hydrogels at a density of 1 x 10^5 cells per gel as described in Chapter IV: *3.3*. Both control and treated groups received αMEM with an increased serum concentration of 20% FBS, and the other supplements as listed above. For treated groups, 10 mM β-glycerophosphate and 10 nM dexamethasone were added. Culture medium was changed every other day for a culture period of 4 weeks. Samples for cell proliferation assays and alkaline phosphatase activity were seeded in triplicates. For Real-time PCR analysis, 6 gels per group were pooled to get sufficient amounts of RNA.

3.2. DNA Content and Alkaline Phosphatase Activity

After 3, 7, 14, 21 and 28 days, cells were harvested by diluting the peptide hydrogels in 1 mL PBS and mechanical disruption of the gels by pipetting up and down. Cell pellets were collected after centrifugation (5 min at 1000 rpm), and frozen at -80°C. As soon as the collection of all samples was completed, these were thawed, and assays and measurements were performed on all samples at the same time. DNA content was determined by fluorometric quantification using CyQuant cell proliferation assay kit (Invitrogen, Molecular

Probes, Carlsbad, CA) and a FLUOstar Optima fluorescence plate reader (BMG Laboratories, Durham, NC). Actual cell numbers were calculated based on a standard curve created from suspensions of known cell densities.

Samples for the detection of alkaline phosphatase (ALP) activity were prepared as described for the DNA assay. Cell pellets were resuspended in 60 μL PBS. After addition of 60 μL alkaline buffer and 100 μL alkaline substrate solution (SIGMA-Aldrich, St. Louis, MO), samples were incubated at 37°C for 60 min and the liberated p-nitrophenol was measured spectrophotometrically at 410 nm. Samples were compared to a dilution series of p-nitrophenol standard (SIGMA-Aldrich, St. Louis, MO) and ALP activity was normalized to the corresponding cell numbers obtained from the proliferation assay.

3.3. Quantitative Real-time PCR

To assess the effect of osteogenic induction on the expression of genes involved in differentiation, matrix formation and mineralization, real-time PCR was performed on samples after 28 days of culture. RNA was extracted using RNA Stat 60 (Tel-Test Inc., Friendswood, TX) from 6 gels per group, which were pooled to get sufficient amounts. Reverse transcription was performed according to standard protocols for cDNA synthesis using an oligo-dT primer. One μg of RNA was used for one reaction of reverse transcription, which provided cDNA for 10 real-time PCR reactions. Primer sets for marker genes of osteoblast and odontoblast differentiation were designed using primer 3 software [85] from mRNA sequences published in GenBank as follows: collagen α(I)I (Col I) (NM_000088),

alkaline phosphatase (ALP) (NM_000478), bone sialoprotein (Bsp) (NM_000582), osteocalcin (Oc) (X_53698), Runx2 (NM_004348), dentin sialophosphoprotein (Dspp) (NM_014208), and glyceraldehyde 3 phosphate dehydrogenase (GAPDH) (M_33197) as an internal control. Primer efficiency was determined prior to quantification by running a dilution series of cDNA from differentiated cells for each primer pair. Conditions for real-time PCR were as follows: After a denaturation step at 95°C for 15 minutes, 60 cycles were run with 95°C (15 sec), 60°C (30 sec), 72°C (30 sec), with a final dissociation step to generate the dissociation profile of the PCR products. Reactions were run in triplicates (ABI Prism 7900HT), gene expression was quantified using SYBR green (QuantiTect SYBR green PCR kit, Qiagen Inc., Valencia, CA) and normalized to GAPDH activity in respective samples. Calculations of fold-change in gene expression between controls and treated samples were performed according to the Pfaffl-method for relative quantification in real-time PCR [86].

4.   Results and Discussion

4.1.   Cell Proliferation

The results from the cell proliferation assays are depicted in Figure 17. Both cell lines show an increase in cell numbers over the four-week culture period, where proliferation rates in SHED are markedly higher than in DPSC. This is in accordance with our previous work on peptide amphiphiles [84], and with the literature, where SHED and DPSC proliferation rates were compared in monolayer cultures [27]. Proliferation is slightly reduced when

osteogenic supplements are added, which is to be expected due to the inverse relationship between cell proliferation and differentiation.
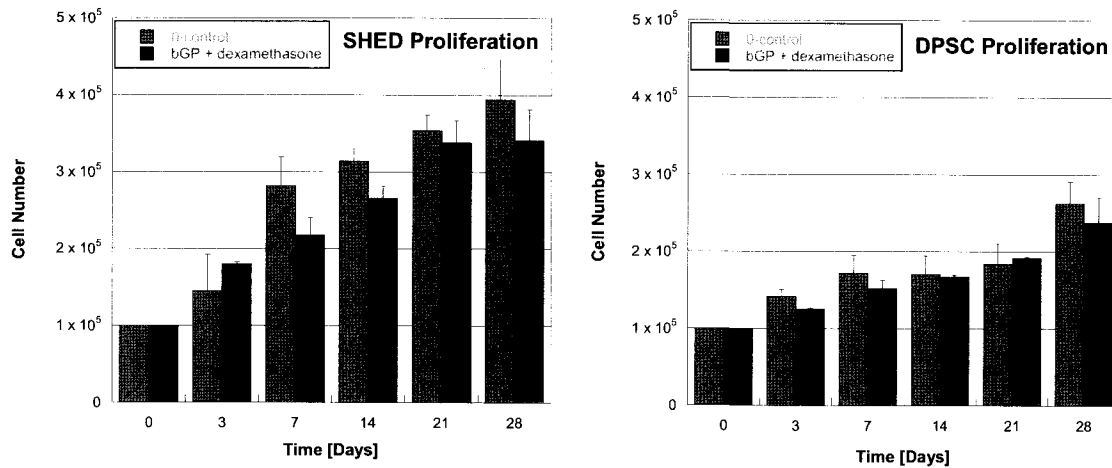
Figure 17: *Cell proliferation for SHED and DPSC in E(QL)₆EGRGDS. SHED proliferate faster. A slight decrease in proliferation can be observed for cells treated with osteogenic supplements. Columns and bars show means and standard deviations (n = 3).*

4.2.   Cell Differentiation

To evaluate indicators of cellular differentiation, we first determined alkaline phosphatase (ALP) activity in treated and control cells. In mineralizing tissues, the enzyme ALP cleaves extracellular pyrophosphate, an inhibitor of hydroxyapatite crystal formation, to inorganic phosphate, which is needed for matrix calcification [87]. ALP is commonly quantified as an early differentiation marker and indicator of lineage commitment towards a mineralizing cell type. Figure 18 shows ALP levels in treated cells and controls at different time points of a four-week culture period. ALP activity was elevated in treated cells, and markedly higher

in DPSC compared to SHED, which is in accordance with our observations in peptide

amphiphiles, reflecting a higher potential for mineralization in DPSC [84].
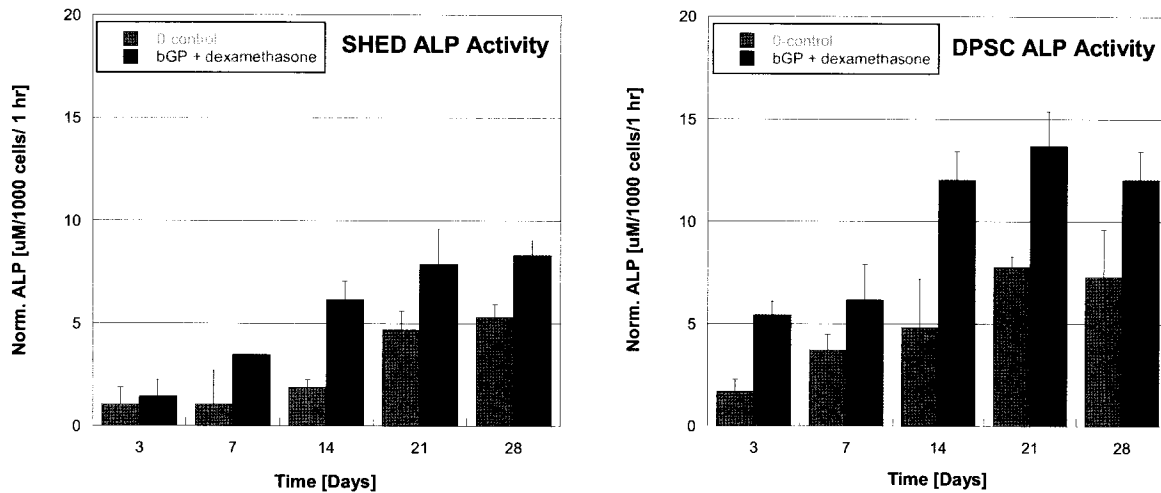
Figure 18: Alkaline phosphatase (ALP) levels in SHED and DPSC. Cells were cultured in regular media (control in grey) or treated with ß-glycerophosphate (bGP) in combination with dexamethasone (blue) (n = 3). ALP activity is increased in treated groups for both cell lines, and highest in DPSC, indicating their tendency towards mineralization.

For real-time PCR analysis, the following markers of matrix deposition and mineralization were chosen: collagen I (Col I), bone sialoprotein (Bsp), osteocalcin (Oc), Runx2, and dentin sialophosphoprotein (Dspp). These genes are commonly used as markers of mineralization [88, 89, 27]. Col I is the major component of extracellular matrix in dentin [90]. The acidic proteins Bsp and Dspp share common expression in bone and teeth and induce mineral nucleation [91]. Runx2, a transcription factor, is known as the master regulator of osteoblast differentiation, exhibiting similar roles in dental development and

odontoblast cytodifferentiation [92]. Oc is considered a marker of differentiated osteoblasts [93], but can also be detected in pulp-derived cells [88].

Expression of all the genes we examined was increased in cells treated with β-glycerophosphate and dexamethasone. The difference in gene expression in treated cells and controls are depicted in Figure 19. The change compared to control groups was not dramatic (for example, for DPSC the fold-increase of marker gene expression ranged from 1.3 to 5.1), which might be due to the fact that growth factors in the serum, which was added at a fairly high concentration of 20% to support three-dimensional growth, might induce differentiation in control groups to some extent. Although the results have to be looked at with caution, they indicate that cellular differentiation in peptide hydrogels is possible, which confirms results from earlier experiments in peptide amphiphiles (see Appendix B). In order to evaluate the differentiation potential of SHED and DPSC thoroughly, experiments should be conducted under serum-free or low-serum conditions.
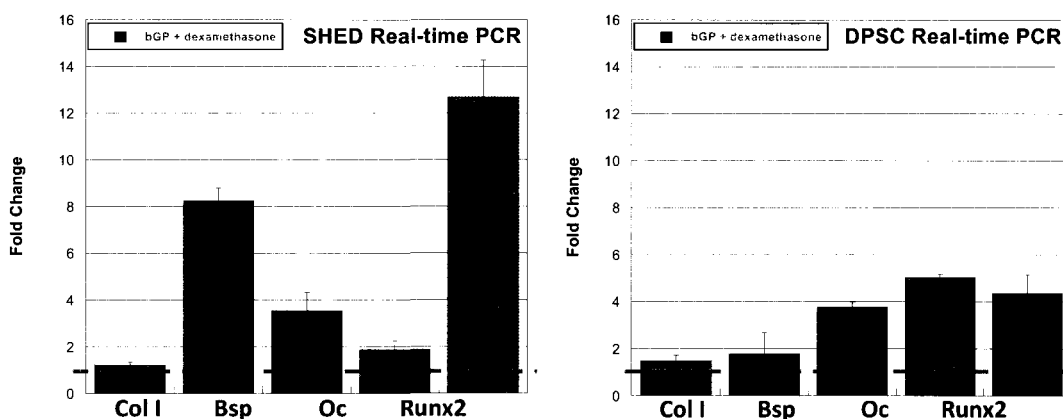
Figure 19: Gene Expression in SHED and DPSC. Fold increase of marker genes of osteoblast and odontoblast lineages. Results are normalized to GAPDH levels in each sample. An increase can be observed for all genes after treatment with β-glycerophosphate (bGP) with dexamethasone. Control groups were set to 1, which is indicated by the dashed line.

In summary, we were confident that multidomain peptides were conducive for cells proliferation and differentiation, similar to peptide amphiphiles. These data were important, as they led us to continue working with this peptide architecture and start modifications to improve the properties of multidomain peptides. The first concern to be addressed was the problem of mechanically instable hydrogels. Although cells were seeded for fixation and processing for histologic analysis for this set of experiments, the gels did not withstand the manipulation for processing and embedding, and this attempt remained unsuccessful.

4.3. Studies with Dexamethasone and β-glycerophosphate

To evaluate the effect of dexamethasone and β-glycerophosphate alone and in combination on cell cultures, a simple experiment was performed in which SHED proliferation and ALP activity were determined at different time points of a 2-week culture period.

SHED were grown in monolayer cultures and treated with these supplements. Cells of passage 4 were seeded at a density of 2500 cells/well into 96 well-plates and cultured in αMEM with 5% FBS and antibiotics as described before. The reduced serum concentration should minimize the effect of growth factors contained in the serum. All samples were seeded in triplicates. After 3, 7, 10 and 14 days, a Quick cell proliferation assay (BioVision, Mountain View, CA) was performed to determine cell numbers. Alkaline phosphatase activity was quantified as described in *3.2*. Figure 20 summarizes the results. All supplements slightly decreased cell proliferation rates and increased alkaline phosphatase

levels. However, based on our results it was not possible to identify a candidate supplement or combination with the highest potential to effect cell differentiation. Therefore, our goal was to incorporate both compounds into multidomain peptides.
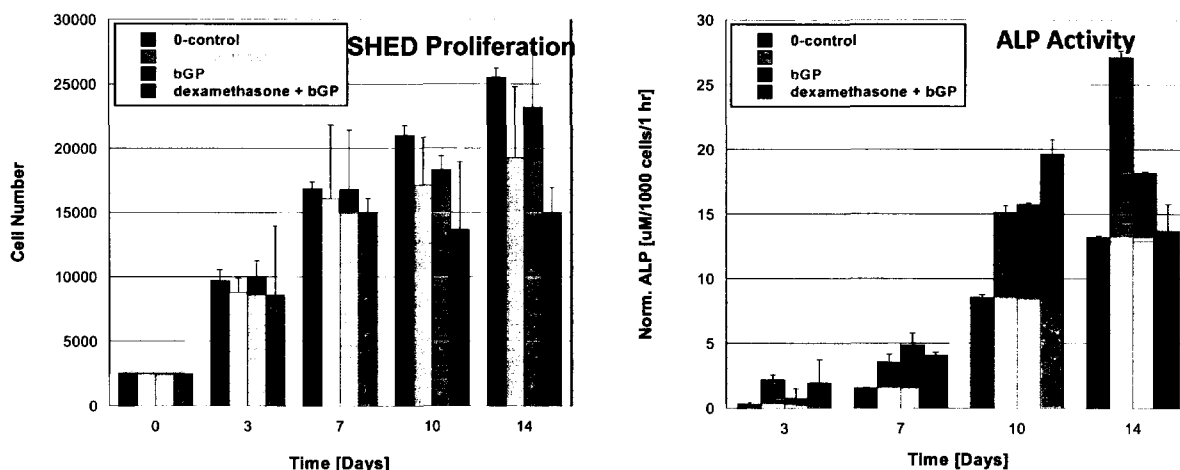
Figure 20: Proliferation and ALP activity in monolayer SHED cells. *Treatment with osteogenic supplements slightly decreased cell proliferation, whereas alkaline phosphatase levels were increased.*

4.4. Incorporation of Dexamethasone into Multidomain Peptides

Dexamethasone, a synthetic glucocorticoid, has been used to induce osteogenic differentiation in osteoblasts [93 - 96], and it is known to stimulate differentiation of odontoblast-like cells in dental pulp cultures [61]. The experiments described in the previous sections demonstrate that dental pulp stem cells treated with dexamethasone and inorganic phosphate decrease their proliferation rates and increase alkaline phosphatase activity and expression of genes associated with matrix deposition and mineralization. Furthermore, dexamethasone not only promotes cellular differentiation, but exerts an anti-

inflammatory effect. In dentistry, it is commonly administered to counteract inflammation and swelling after dental surgery. This could be useful for *in vivo* applications of peptide hydrogels, where inflammation will be present at the site of injury due to tissue damage either by traumatic impact or caused by bacterial toxins.
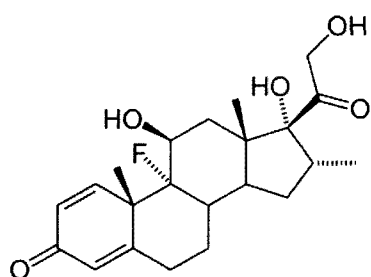
Figure 21: *Chemical structure of dexamethasone.*

Our goal was to incorporate dexamethasone into our multidomain peptides by covalently linking the molecule to the peptide chain. The entire work on dexamethasone coupling to the peptide $K_2(QL)_6K_2$, purification and confirmation of covalent linkage was done by Erica Bakota in our laboratory. Dexamethasone was reacted with succinic anhydride to produce a 4-carbon linker molecule. The carboxylic acid group at the end of the linker allowed her to couple this molecule to the N-terminus of the peptide using standard peptide coupling chemistry, resulting in amide bond formation between the peptide and the succinate linker. The coupling of dexamethasone to succinic anhydride was monitored by thin layer chromatography (TLC), and the product was purified using silica chromatography. The final product was purified by high-performance liquid chromatography (HPLC), and the expected mass was determined by mass spectrometry to confirm successful coupling.

Since dexamethasone is hydrophobic, it could be expected that attachment of this molecule to the peptide chain will affect the gelation properties dramatically. Indeed this was the case; $K_2(QL)_6K_2$, which forms stable hydrogels at basic pH, does not form a gel when dexamethasone is covalently linked to the peptide. However, the concentration at which

dexamethasone is used as an osteogenic supplement is 10 nM. Two peptides of the same sequence with and without dexamethasone can thus be mixed to form a gel. In the case of $K_2(QL)_6K_2$ with dexamethasone attached, the molecular weight of the molecule is 2410.75 Da. Only 24.11 ng/mL are needed to prepare a 10 nM solution, as compared to 10 mg/mL peptide stock concentration (1 % by weight or 5 mM) without dex. This small amount is not expected to interfere with gelation or mechanical stability.

However, the effect of dexamethasone on cellular behavior when bound to a peptide molecule was first evaluated in a monolayer experiment with analogous set-up as described in section 3, where dexamethasone was covalently linked to $K_2(QL)_6K_2$. Peptide stock solution was added to cell culture media to obtain dexamethasone concentrations of 10 nM, 100 nM and 1000 nM. Media containing supplements were changed every other day. The results are summarized in Figure 22. We could neither detect an influence on cell proliferation nor alkaline phosphatase activity after addition of peptide-bound dexamethasone. This might be explained by the fact that this compound, due to its small size and hydrophobicity, is able to pass the cell's lipid bilayer membrane and directly activate intracellular targets rather than acting via membrane-bound receptors. Covalent linkage of dexamethasone to the peptide might prevent the molecule from reaching its intracellular target. Whereas my work on dexamethasone was put on halt at this point, alternative ways to incorporate this compound into multidomain peptides are currently investigated in the Hartgerink laboratory.
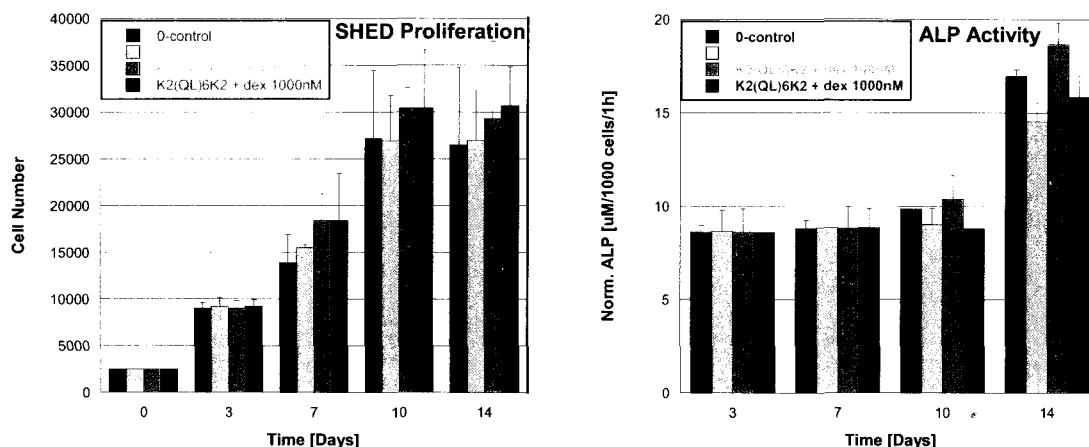
Figure 22: Treatment with peptide-bound dexamethasone. *Proliferation rates and alkaline phosphatase activity after treatment with peptide-bound dexamethasone seemed unaffected and similar to controls.*

4.5. Incorporation of β-glycerophosphate into Multidomain Peptides

Inorganic phosphate is commonly used as an osteogenic supplement. In mineralizing tissues, PO_4^{3-} is needed to build the crystal lattice in combination with calcium- and hydroxyl-ions to form hydroxyapatite, the predominant mineral in bone and teeth. The fact that gelation of multidomain peptides carrying positively charged lysine residues can be induced by addition of phosphate led to the idea that PBS could be exchanged with a solution of β-glycerophosphate. Therefore, mechanical strength of *MDP 3* was tested after gelation with either PBS or β-glycerophosphate. 1x PBS has a phosphate concentration of 10mM, which in our system is reduced to 5mM as peptide stock solution is mixed with the cell suspension in PBS. In order to maintain osmolarity, β-glycerophosphate was dissolved in de-ionized water with sucrose and brought to a concentration of 10 mM. After mixture with the peptide stock solution, the final concentrations were as follows:

- Gel with PBS: 1 % by weight of peptide, 0.5 x PBS (5 mM phosphate), 149 mM sucrose

- Gel with β-GP: 1 % by weight of peptide, 5 mM β-glycerophosphate, 298 mM sucrose.

Stress sweep analysis was performed to compare differently prepared gels (Figure 23). Both

PBS and β-glycerophosphate were equally suitable to produce mechanically stable gels.
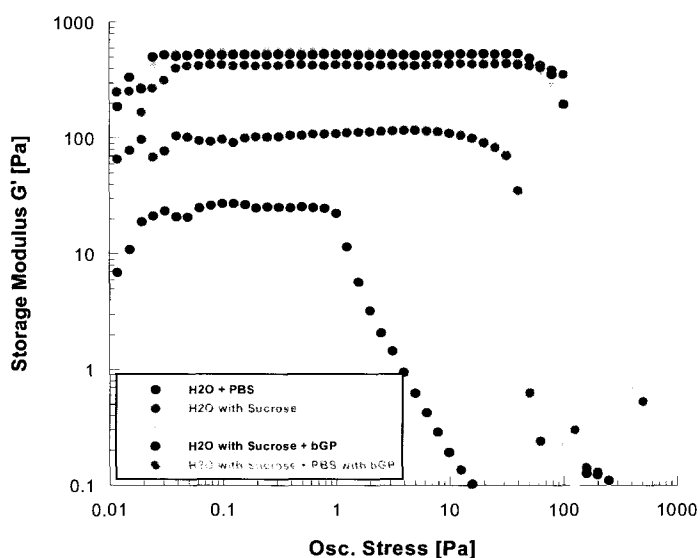
Figure 23: Mechanical strength of $K_2(SL)_6K_2$ prepared with different solutions. When the peptide is prepared in water alone, the gel strength is lowest (black). Dissolving the peptide in water with sucrose increases gel strength (brown). Addition of PBS results in a further increase of mechanical stability (green). A similar effect can be observed with β-glycerophosphate (red). If PBS and βGP are combined, gel strength decreases slightly, indicating that the optimum phosphate concentration is exceeded (blue).

4.6. Incorporation of Heparin into Multidomain Peptides

In order to provide proper nutrition for cells seeded in the scaffold and delivered to the site

of injury, it is absolutely essential to provide sufficient blood supply. It has been shown that

growth factors, such as vascular endothelial growth factor (VEGF) or fibroblast growth

factor -2 (FGF2), can boost signaling for new blood vessel formation and induce sprouting of

new capillary networks from existing microvessels [97 – 99]. A common strategy of

incorporation uses the ability of the glycosaminoglycan heparin to bind growth factors. Heparin is a biopolymer of variably sulfated repeating disaccharide units of iduronic acid and glucosamine, which is present in natural ECM. It has the highest negative charge density of any know biological molecule. Heparin has been found to not only bind growth factors, but to protect them from enzymatic degradation and prolong their bioactivity [100]. Slow and continuous release of growth factors bound to synthetic systems via heparin has been demonstrated over a time period of 10 days to up to 42 days [101, 102]. Thus we hypothesized that inclusion of small amounts of heparin would regulate growth factor release.

Heparin can be bound to the hydrogels via specific peptide sequences. Consensus heparin-binding domains follow the pattern XBBBXXBX or XBBXBX, where X is a hydrophobic amino acid and B a basic amino acid [103]. Heparin-binding sequences have been utilized in peptide amphiphile systems [101, 104] or other hydrogels such as hyaluronan [102]. Stimulation of extensive new blood vessel formation after binding and slow release of angiogenic growth factors from peptide hydrogels via heparin-binding has been demonstrated recently in a rat corneal assay [101]. Since growth factor binding to these heparin-binding domains seemed most likely to be due to a charge effect, we hypothesized that it would be possible to incorporate heparin into K-series multidomain peptides without specific heparin-binding domains.

A series of experiments with heparin (heparin sodium salt from porcine intestinal mucosa, SIGMA-Aldrich, St. Louis, MO) was performed. In order to identify optimum concentrations of both heparin and peptide, heparin concentrations between 1 and 10

mg/mL in water with 298 mM sucrose or in PBS were tested with peptide stock solutions with concentrations from 1 % to 3 % by weight. After preparation of the peptide stock, the heparin-containing solution was added and gently mixed with the peptide. Gels were left to equilibrate for 30 min, and proper gelation was evaluated. At too high heparin concentrations, a precipitate would form, which was evident after centrifugation of samples for 1 min at 14,000 rpm. An increase of peptide concentration would allow for the incorporation of higher concentrations of heparin. Oscillatory stress sweep analysis was performed after proper gelation to evaluate the mechanical properties. We were able to form stable hydrogels from $K_2(SL)_6K_2$, $K_2(SL)_3RG(SL)_3K_2$ and $K(SL)_3RG(SL)_3KGRGDS$ with heparin. The hydrogel chosen for further analysis was $K(SL)_3RG(SL)_3KGRGDS$ with heparin in PBS at final concentrations of peptide at 1% by weight and heparin at 1 mg/mL. Heparin contributed to hydrogel stabilization, and the storage modulus in the resulting hydrogel was determined at 505 Pa.

In a next step, we wanted to assess binding and release of VEGF from heparin-containing hydrogels. Recombinant human vascular endothelial growth factor (VEGF) (SIGMA-Aldrich, St. Louis, MO), was incubated with the heparin solution for 30 min at room temperature prior to mixing it with the peptide stock. Hydrogels were seeded into 96-well plates at a volume of 100 uL per well, with final concentrations of 1 mg/mL of heparin and 10 ng of VEGF per gel. After 30 min of equilibration, 200 μL PBS containing 1% BSA were added on top of each gel. Control gels were prepared with VEGF in PBS without heparin. Gels for both groups were seeded in triplicates for growth factor release to be measured over 14 days of incubation at 37°C. For sample collection, the supernatant from each gel

was removed and stored at -80°C, and new supernatant was added. After 14 days, VEGF content was measured in all samples using a VEGF ELISA kit (Quantikine Human VEGF Immunoassay, R&D Systems, Minneapolis, MN). VEGF concentrations were calculated based on standard samples, and the percentage of daily VEGF release was calculated and plotted in Figure 24.
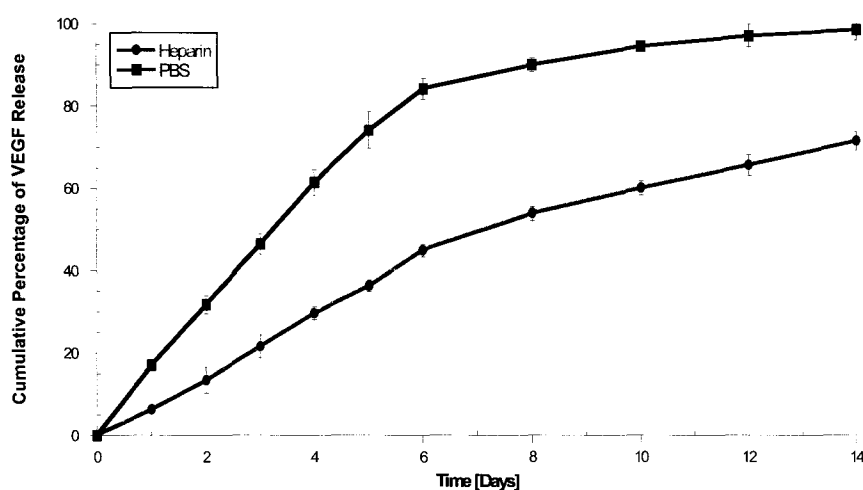
Figure 24: VEGF release profile. Release of VEGF from MDP 3E with heparin (blue) and control gels with PBS (black). Data points and error bars show mean values and standard deviations (n = 3). Heparin retains VEGF in the gel with a slowed release, where 50% of VEGF are still bound after 1 week. In contrast, a burst release is observed for gels prepared with PBS.

Slowed release of VEGF from heparin-containing gels could be observed, where 50% of VEGF are still bound after 1 week, whereas VEGF in control gels is depleted by 90%.

In heparin-containing hydrogels, PBS is interchangeable with β-glycerophosphate in water containing 298mM sucrose, resulting in an equally stable gel. These promising results allowed us to incorporate two bioactive factors, VEGF to induce angiogenesis and β-glycerophosphate to promote mineralization, into a hydrogel permissive for cell adhesion and cell-mediated degradation. An *in vitro* compatibility check with dental stem cells was

the last step that had to be performed before applying these customized hydrogels in an *in vivo* setting.

4.7.　*In Vitro* Study with Dental Stem Cells

To assess the behavior of dental stem cells in the established system, both SHED and DPSC were seeded into hydrogels of K(SL)$_3$RG(SL)$_3$KGRGDS containing β-glycerophosphate and VEGF. Whereas VEGF was not expected to promote dental stem cell differentiation, we wanted to test the system exactly the way we planned to use it for the *in vivo* studies. In this case, 5 x 10^5 of either SHED or DPSC were seeded into 100 µL hydrogels, and medium was added on top and changed every other day. After 4 weeks, gels were fixed in 4% PFA for 2 hours, dehydrated through ethanol series and embedded in paraffin. Sections were prepared at 5 µm thickness, and mounted to glass slides. Cells and gels were stained with H&E, Masson's trichrome (Trichrome Stain (Masson) Kit, Sigma-Aldrich, St. Louis, MO) and von Kossa stain to gain information about cellular morphology and distribution, collagen deposition and mineral formation.

Figure 25 displays the results. Both SHED and DPSC were evenly distributed throughout the matrix. Whereas SHED showed a more spindle-shaped morphology, DPSC appeared mostly round. Collagen deposits could be observed for both cell lines. Von Kossa stain revealed that the cells started to form mineral around their cell bodies.

Our histologic analysis provides evidence that the cells not only survive in this customized synthetic matrix, but that a differentiation process is stimulated, which results in collagen deposition and mineral formation.
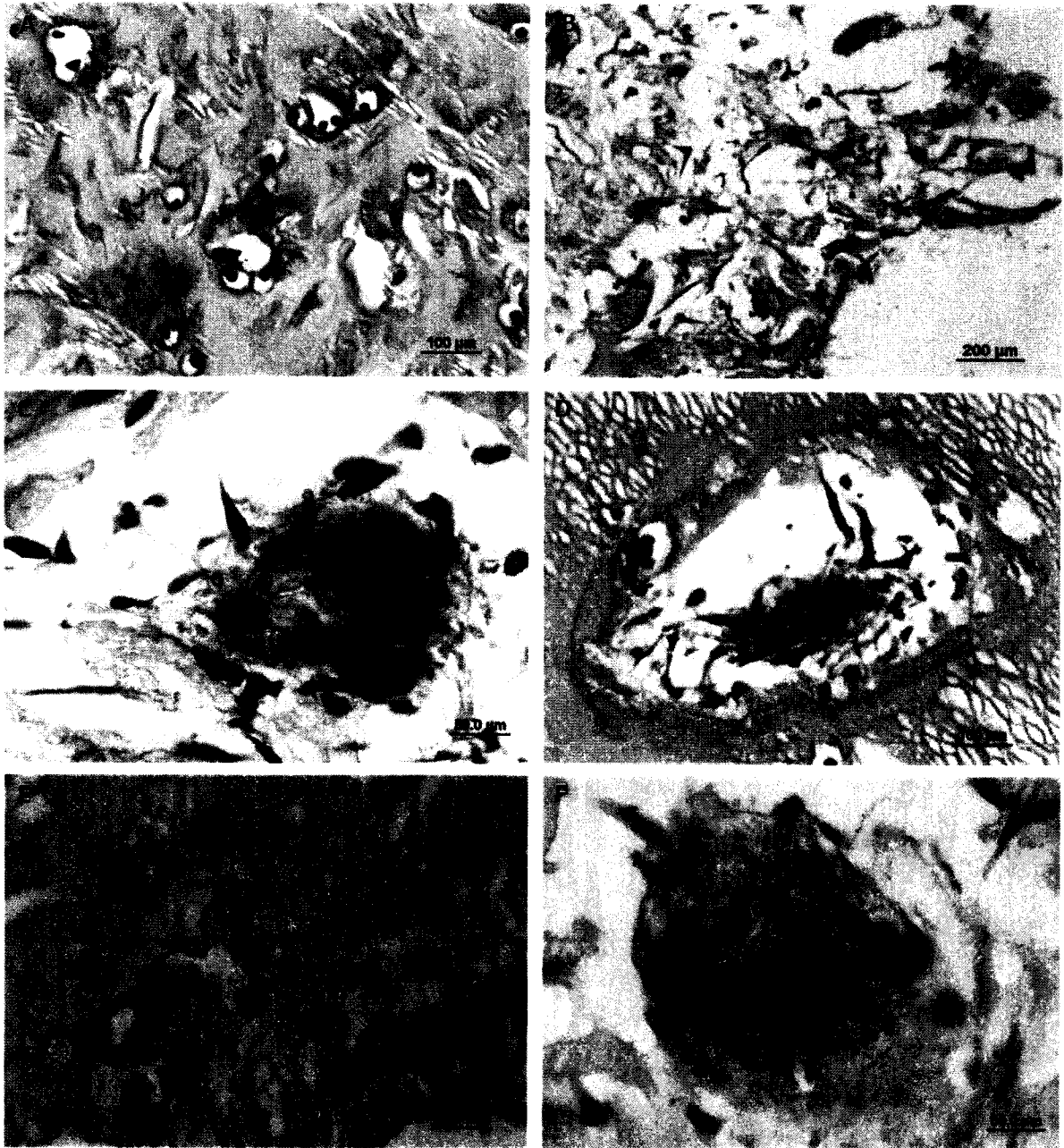
Figure 25: Histologic analysis of SHED and DPSC in a customized multidomain hydrogel. The left column shows DPSC (A, C, E), the right column SHED (B, D, F) in MDP 3D. DPSC appear round, SHED more fibroblast-like and spindle-shaped (A: H&E, B: Masson's Trichrome). Both cell lines deposit clusters of collagen throughout the matrix visible as blue deposits around the cell bodies after Masson's Trichrome stain (C, D). The remaining hydrogel matrix takes on a light blue color. Mineral formation can be seen as dark brown stain after von Kossa (E, F).

Looking back at the data acquired in Specific Aim 1 and 2, we certainly had numerous ideas for further optimization and customization of this system. The effect of RGD ligand densities on dental stem cells could be assessed, and alternative cleavage motifs might be tested. The influence of the mechanical properties of the hydrogels on dental stem cell migration and differentiation could be evaluated. It has been demonstrated for osteoblasts that stiffness of the matrix alone can affect cellular differentiation [105, 106]. Effects on dental stem cells could be similar, given the close relatedness of the osteoblast and odontoblast lineages.

Series of tests to evaluate the optimal concentrations of heparin and VEGF for prolonged release would be a next step. Additional growth factors could be included, such as basic fibroblast growth factor (FGF-2) or transforming growth factor beta (TGF-β), which have been shown to increase proliferation rates of dental stem cells and promote cell differentiation into an odontoblast-like phenotype [107]. Both growth factors can be bound via heparin [102]. Another interesting field of exploration would be incorporation of peptide sequences which can promote crystal nucleation and mineral formation. Several of these sequences have been described in the literature [107 – 109]

However, with promising results on our hands, we decided to stop the optimization process for this project, and apply this scaffold combined with the two dental stem lines in our animal studies described in Specific Aim 3.

5. Troubleshooting

5.1. Cell seeding

For cell proliferation and differentiation assays, cells were cultured in 96-well plates. For histology, though, the gels had to be removed from the wells without deformation or damage, which turned out to be difficult. Therefore, a new seeding procedure was established. The top 3 mm of a 0.5 mL PCR reaction tube were cut to form a small ring of 5 mm in diameter. These rings were autoclaved, and placed into 6-well plates. The cells and gels were then directly seeded into the rings, and these could be removed easily to leave an undamaged gel, which was then fixed and processed for histology and only removed from the well before transferring the gels to xylene, the last step before paraffin-embedding. This procedure worked well, and at the same time, we could make sure that even with high cell densities within the gels, nutrients from the cell culture media were available in sufficient amounts. Whereas only 200 µL of medium fit on top of a gel in a 96-well plate, the large 6-well plates allow for much larger volumes of culture medium.

5.2. Processing for Histology

For the first experiments with K-series hydrogels, dehydration and paraffin-embedding did not work well, and the gels shrank as soon as they were immersed in xylene. Prolonged time periods in ethanol series resolved this problem, which was most likely due to insufficient dehydration. Whereas 30 min for each dehydration step (50, 70, 80, 90, 95 and 100 % ethanol) were sufficient for peptide amphiphile gels, K-series peptides were left for 1

hour at each concentration, and the last step in 100 % ethanol was repeated. These changes made it possible to process and embed these gels and obtain satisfactory results from histologic analysis.

5.3.   Heparin Binding

The induction of gelation using negatively charged heparin proved difficult first, where precipitates would form unless the concentration of heparin was low and/or the concentration of peptide was high. These first experiments were performed with heparin dissolved in water. The idea was that negatively charged heparin molecules could replace phosphate ions and induce gelation due to a charge effect. Peptides with two lysines in the flanking region ($K_2(SL)_6K_2$, $K_2(SL)_3RG(SL)_3K_2$) were able to form gels with heparin at a concentration of 2-5 mg/mL, but the peptide concentration had to be increased to 2 % by weight. With only 1 lysine present ($K(SL)_3RG(SL)_3K$), the peptide concentration had to be increased even further to 3 % by weight, which posed a problem, since peptides are time-consuming and expensive to synthesize. For peptides with RGD attached ($K_2(SL)_6K_2GRGDS$, $K(SL)_3RG(SL)_3KGRGDS$), gels did not form even at high peptide concentrations.

However, dissolving heparin in PBS solved this problem, and stable gels could be produced for all peptides. In this case, addition of heparin increased gel strength. PBS is interchangeable with a solution of β-glycerophosphate at the same concentration.

5.4.   VEGF Release Study

An ELISA kit was used to determine the amounts of VEGF released from gels with and without heparin. However, these kits are highly sensitive and detect picogram-quantities. For the first experiments, the amount of VEGF in the samples was too high, and the absorbance readings above the linear range. Test runs were performed to determine amounts of VEGF compatible with this ELISA kit. Incorporation of 10 ng of VEGF per gel and a 1:2 dilution of the samples resulted in reasonable absorbance readings.

CHAPTER VI: SPECIFIC AIM 3

To test the potential of the generated system for engineering of the dentin-pulp-complex in an appropriate animal model.

1.   Summary

The customized peptide hydrogel system generated in the previous Specific Aims now features 1) Sufficient gel strength (storage modulus of approximately 500 Pa),

2) Shear-thinning behavior, which allows for application with a syringe into small spaces,

3) The cell adhesion motif RGD,

4) An MMP-2 specific enzyme-cleavable site,

5) β-glycerophosphate as a source of inorganic phosphate for mineralization, and

6) Vascular endothelial growth factor (VEGF) bound to the hydrogel via heparin.

Extensive characterization and testing of the hydrogel with dental stem cells *in vitro* yielded promising results. However, to get a realistic idea of the cells' behavior in this system, evaluation in an appropriate animal model was necessary. As a first step, we needed a carrier to deliver the cell-laden hydrogels. To mimic the clinical situation, we chose to use standardized dentin cylinders. This environment closely resembles the site which the cell-laden hydrogels should be delivered to as part of a novel treatment strategy for the regeneration of the dentin-pulp-complex. These dentin cylinders were prepared from human molars, and the root canal was enlarged to make space to inject the hydrogels. Since our system contains bioactive factors, an ectopic implantation site was desirable,

where nutrients to the cells would be provided without induction of differentiation by the host tissue. Therefore, the cylinders were implanted subcutaneously in the back of immunodeficient mice. Both cell lines in hydrogels with and without bioactive factors should be tested, with cell-free cylinders as controls, resulting in a total of six groups. The progress of tissue formation was evaluated by harvesting implants after 2 and 5 weeks. Six implants were placed per group and time point. After implant retrieval, the cylinders were fixed, demineralized and prepared for histologic analysis and immunohistochemistry.

Whereas only remnants of the empty hydrogel were present in control cylinders without cells, both SHED and DPSC had formed cellular networks within the cylinders after two weeks. Without VEGF, tissue formation was limited to the entrance of the cylinders, but empty hydrogel was found in the midsection. With VEGF, the united cell structure reached further into the canal. Microvessel counts revealed significantly more blood vessel formation in VEGF-containing hydrogels.

After 5 weeks, the cylinders with growth factor-containing gels were filled with vascularized connective tissue resembling its physiological counterpart. The hydrogel was replaced by natural extracellular matrix. For DPSC, few small and dense collagen deposits could be observed throughout the newly formed tissue. After immunohistochemistry for localization of dentin sialoprotein (Dsp), a dentin-specific protein, small Dsp-positive islands could be detected in DPSC-containing constructs. Collagen deposition and Dsp expression indicate that the cells undergo a differentiation process. However, the deposits and Dsp-positive cells were not predominantly found towards the interface of cells and dentin, but throughout the matrix.

Our results provide evidence that both dental stem cells lines delivered in customized

multidomain peptide hydrogels are suitable for a treatment strategy to regenerate dental

pulp. VEGF proved to be a potent stimulator of microvessel formation and enabled tissue

formation throughout the length of the cylinder. However, directional deposition of

collagen as a template for mineralized dentin remains to be resolved.

2. Materials and Methods

2.1. Treatment Groups

To test both dental stem cell lines with peptide-based hydrogels with and without bioactive

factors, six groups were established (Table 2). Our goals were as follows:

1) To evaluate the amount and quality of new tissue formed by SHED or DPSC cells, and
   to compare the two cell lines regarding cell densities, cell morphology, connective
   tissue formation and collagen deposition within the dentin cylinders.

2) To assess the effect of VEGF on new blood vessel formation and tissue formation.

	Group 1	Group 2	Group 3	Group 4	Group 5	Group 6
Cells **Hydrogel** **Growth Factors**	Empty MDP 3D none	Empty MDP 3D β-GP, VEGF	DPSC MDP 3D None	DPSC MDP 3D β-GP, VEGF	SHED MDP 3D none	SHED MDP 3D β-GP, VEGF
Significance	Cell- and GF-free Control	Cell-free Control	GF-free Control	Treatment Group	GF-free Control	Treatment Group
Number of Implants	6	6	6	6	6	6
Time points	2- and 5 weeks					
Number of Animals	18					

Table 2: Treatment and control groups for implantation

MDP 3D: K(SL)₃RG(SL)₃KGRGDS   SHED: stem cells from human exfoliated deciduous teeth
GF = Growth Factor   DSPC: dental pulp stem cells
VEGF = vascular endothelial growth factor   β-GP = β-glycerophosphate

The decision to place six implants per group was based on previous studies [65, 110], and on consultation with Dr. Scott Baggett at the Department of Statistics at Rice University. A *post hoc* power analysis on data for new blood vessel formation obtained from the two-week experiments confirmed that the number of samples per group was sufficient to detect statistically significant differences between treatment groups with a confidence $\geq$ 95 % (α <= 0.05).

Six implants were placed per group, and four implants were transplanted into each animal, which amounted to a number of 36 implants per time point, 72 implants in total, and a total number of 18 animals.

2.2.   Implant Preparation

Since our cell delivery system is not a solid material, a suitable carrier system for implantation had to be chosen, which would provide stability and allow for implant localization and retrieval after several weeks *in situ*. Hydroxyapatite powder was an option we considered, since this material had been used as a carrier for SHED and DPSC cells in previous studies [25, 27]. However, we envisioned an enclosed space, closely mimicking the situation of the pulp chamber or root canal. A cylindrical system seemed most feasible. Carriers from materials such as polytetrafluoroethylene (PTFA) cylinders or titanium meshes were discussed, both of which are commonly used as implant materials in dentistry [111, 112]. Any material-related effect on the cells had to be avoided, and the carrier should allow for histologic analysis of newly formed tissue. Therefore, we chose the natural material the cells would be in contact with in a clinical setting: dentin.

2.3.   Dentin Cylinders

Extracted human teeth were collected by local oral surgeons and stored in 0.5 % chloramine (chloramine T hydrate, SIGMA-Aldrich, St. Louis, MO; in de-ionized water) at 4°C to avoid bacterial growth and contamination. Dentin cylinders were prepared from the roots of molars using a low speed handpiece and a cylindrical diamond bur (diameter 12 mm) under constant irrigation with water for continuous cooling, as depicted in Figure 26. The size of the cylinders was designed to be small enough for implantation, yet hold a volume of hydrogel of at least 20 µL. Therefore, cylinders were prepared at a height of 4 mm, an inner diameter of approximately 1.5 mm and an outer diameter of 3 mm (volume = 0.028 cm^3 or 28 µL). The root canal was enlarged to prepare the shape of a hollow tube. After preparation of the cylinders, these were stored in chloramine at 4°C until further use. The teeth and cylinders were constantly kept in solution or in a moist environment to avoid drying effects.

Figure 26: Preparation of dentin cylinders. The roots of human molars were used to prepare standardized cylinders with a height of 4 mm and an inner diameter of 1.5 mm.
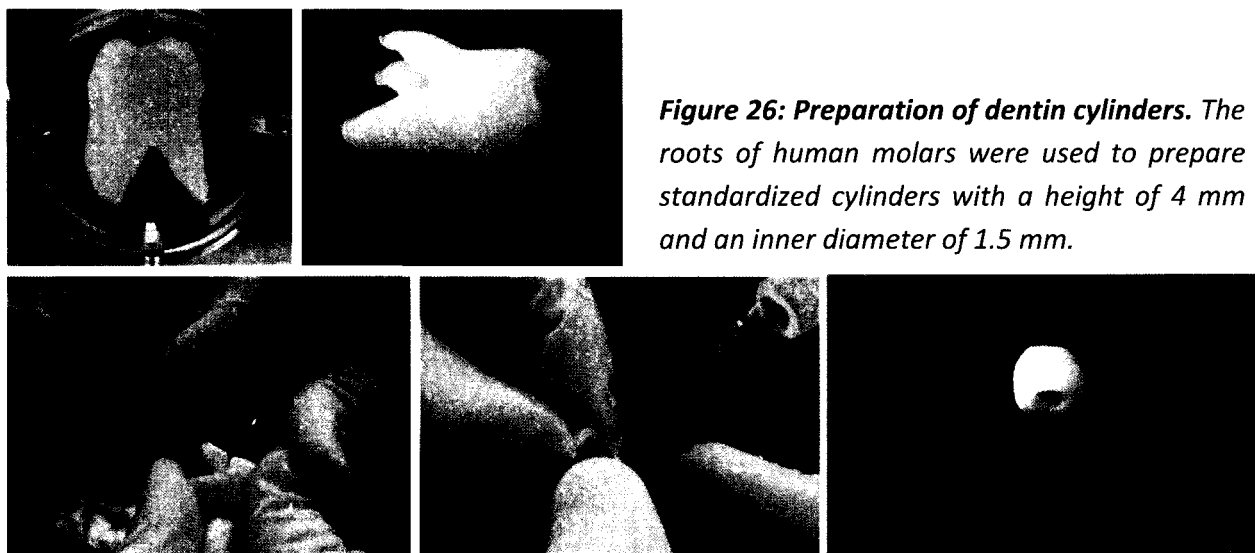
Before cell seeding, the dentin cylinders underwent several steps of a preparatory procedure, which was carried out in a sterile tissue culture cabinet. The cylinders were washed in PBS three times for 1 min per wash, followed by 10 minutes in 5% sodium hypochlorite for disinfection purposes. This procedure was chosen over autoclaving, which has been described to sterilize dentin disks [113]. The goal was to preserve the growth factors which are entrapped in the dentin matrix [54, 114].

After disinfection, the cylinders were washed in PBS three more times, and etched with 10% citric acid for 1 min, followed by three final washes in PBS. Etching demineralizes the dentin surface and exposes the collagen fibrils, which is a well-documented phenomenon, as this procedure is a critical step during the procedure of bonding resin-based dental filling materials to the dentin surface [115]. Furthermore, etching releases growth factors entrapped in the dentin matrix and it has been shown that these stimulate matrix secretion and odontoblast differentiation [49]. After seeding of dental stem cells in pretreated cylinders, collagen could promote cell attachment and growth factors could aid in cellular differentiation. The dentin surface could thus provide directionality, ideally resulting in deposition of new predentin towards the existing walls.

2.4.   Hydrogel Preparation and Cell Seeding

A peptide solution from *MDP 3D* at 2% by weight was prepared in water containing 298 mM sucrose. The peptide stock was mixed with either one of the following solutions:

A) PBS containing 2 mg/mL heparin (for GF-free control groups 1, 3 and 5)

B) De-ionized water containing 2 mg/mL heparin, 298 mM sucrose,

10 mM β-glycerophosphate, and 200 ng/mL VEGF (for groups 2, 4 and 6).

Solution B was prepared 30 min prior to seeding to allow for VEGF-heparin binding.

Subconfluent SHED and DPSC of passage 4 were detached, counted on a hemocytometer, and resuspended in either solution A or B at a cell density of 2.0×10^7 cells per mL. Hydrogels with and without cells and bioactive factors were prepared, and approximately 30 +/- 5 μL of hydrogel were pipetted into each dentin cylinder. The final concentrations were:

A) 1 mg/mL heparin; 149 mM sucrose, 0.5 x PBS

B) 1 mg/mL heparin, 298 mM sucrose, 0.5 mM β-glycerophosphate, 100 ng/mL VEGF.

The cell number per cylinder amounted to 3×10^5 cells.

The hydrogel-containing cylinders were placed into petri-dishes, and cell culture medium was added to cover the bottom of the plate and maintain a moist environment. The cylinders were stored at 37°C in a 5% CO_2 environment until preparations for the surgical procedure were complete, usually not more than 30 min.

2.5.   Transplantation Procedure

Immunodeficient mice (8-to 10-week-old females, strain Crl: NIH-$Lyst\,^{bg}Foxn1^{nu}Btk^{xid}$ or NIH III; Charles River, Wilmington, MA) were used as subcutaneous transplant recipients according to specifications of an approved small-animal protocol (National Institute of Dental and Craniofacial Research). Operations were performed under anesthesia achieved by intraperitoneal injection of 0.35 – 0.4 mL of a mixture of ketamine/xylazine at 50/5

mg/kg. Four midlongitudinal incisions of approximately 0.5 mm in length, two on each side, were made on the dorsal surface of each animal. Subcutaneous pockets were created by blunt dissection, and one implant was placed per pocket, four implants per animal. Incisions were closed with surgical sutures. Local anesthetic (0.5% marcaine at < 0.5 mL/kg) was injected subcutaneously after surgery and once every day for the following three days as part of post-surgical care.

2.6.   Implant Recovery and Processing

Implants *in situ* and after explantation are depicted in Figure 27. Animals were sacrificed two or five weeks after implantation. The implants were retrieved, briefly washed in PBS and fixed in 4% buffered paraformaldehyde (PFA) solution overnight at 4°C. After several washing steps in PBS, the implants were transferred to a Morse's demineralization solution containing 22.5% formic acid and 10% sodium citrate, which has been shown to preserve antigenic sites [116]. The dentin cylinders were decalcified at room temperature on a shaker at 60 rpm for 6 days, and the solution was changed daily. The required time for sufficient demineralization, after which the dentin no longer offered resistance to cutting with a blade during sectioning, was determined prior to implantation on test cylinders.
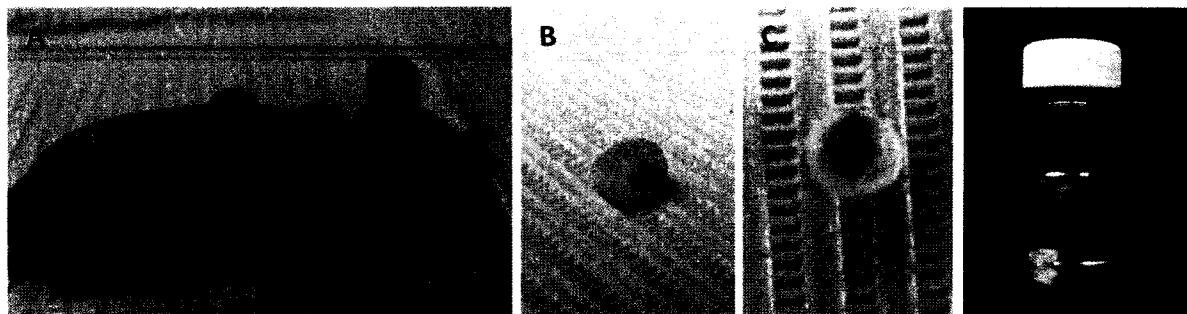
Figure 27: Implants in situ, after explantation and during processing. *Four implants per animal were placed subcutaneously into immunodeficient mice (A). The tissue that formed in hydrogels without VEGF appeared pale (B), in VEGF-containing hydrogels reddish (C). The dentin cylinders were transferred into glass vials for fixation and processing (D).*

After demineralization, the implants were processed through ethanol series for dehydration for a minimum of 1 hour per step at 4°C. The constructs were then embedded in paraffin, sections of 8 μm thickness were prepared on a microtome, and mounted to glass slides (Superfrost/Plus, Fisher Sci, Pittsburgh, PA).

2.7. Histology and Immunohistochemistry

Sections were deparaffinized in xylene and rehydrated though ethanol series. For histology, the tissues were stained with hematoxilin and eosin (H&E), and Masson's Trichrome to visualize collagen formation, (Trichrome Stain (Masson) Kit, Sigma-Aldrich, St. Louis, MO).

To localize microvessels in the newly formed tissues, a dilution of 1:100 of a polyclonal rabbit-anti-human Factor VIII antibody (Lab Vision, Fremont, CA) was used as described previously [65]. Color development was performed with Dako EnVision + system kit (AEC, Dakocytomation), and sections were counterstained with hematoxilin. For controls, one section per group was treated with PBS instead of primary antibody.

The number of microvessels was counted in 2 sections of each of the 6 implants per group, resulting in a total count of 12 sections per treatment condition. Microvessels were identified at 20 x magnification under a light microscope.

For dentin sialoprotein (Dsp), a 1:100 dilution of anti-human Dsp antibody was used, which was kindly provided by Dr. Larry Fisher at the NIH. Color development was performed as described above.

2.8.   Statistical Analysis

To determine differences between groups treated with and without VEGF, paired student's t-test was performed to compare group 1 vs. 2, 3 vs. 4 and 5 vs. 6 at a significance level of α = 0.05. Means and standard deviations were calculated, and power analysis was conducted for two-week samples to calculate the minimum sample size required to accept the outcome of statistically significant differences at a 95% confidence level.

3.   Results and Discussion

The overall strategy for dentin-pulp-complex engineering in this approach consists of manufacturing a root-canal-shaped dentin cylinder filled with a peptide-based hydrogel laden with dental stem cells and bioactive factors. These constructs were implanted subcutaneously into immunodeficient mice. Ideally, we expected to create a vascularized soft connective tissue, degradation of the hydrogel matrix and replacement with natural extracellular matrix, a cell-rich zone adjacent to the dentin wall, collagen deposition

towards the existing dentin wall as template for mineralized dentin, and Dsp-positive cells lining the predentin front.

Following implant retrieval, we wanted to assess the amount and quality of new tissue formed by SHED or DPSC, and to compare the two cell lines regarding cell densities, connective tissue formation and collagen deposition within the dentin cylinders. Furthermore, we wanted to evaluate if the presence of vascular endothelial growth factor (VEGF) can aid in the establishment of microvascular networks, which is of crucial importance for tissue vitality. Histologic stains provided information about overall tissue structure, and the formation of collagenous networks. Immunohistochemistry allowed for the visualization and quantification of newly formed microvessels within the dentin cylinders, and for identification of differentiated cells expressing dentin sialoprotein, a protein specifically expressed by dentin-forming odontoblasts.

3.1.   Results after 2 Weeks

Figures 28 and 29 show images of the constructs after two weeks *in situ*. In cell-free constructs, only remnants of the gel, but no cells were present for both groups 1 and 2 (28 A). When cells, but not bioactive factors were present, tissues formed on either side at the opening of the cylinders, whereas the midsections remained empty (28 B). However, the presence of VEGF seemed to result in better nutrition, allowing the cells to survive throughout the length of the cylinder (28 C). This effect could be observed for both cell lines.

A higher density of blood vessels inside the cylinders in the presence of VEGF was confirmed after microvessel counts. Two examples after immunohistochemical staining for Factor VIII are depicted in Figure 30. For both SHED- and DPSC-laden cylinders, significantly higher numbers of microvessels between constructs with and without VEGF were observed. Our sample size of 6 per group was sufficient to validate statistical significance with 95 % confidence ($\alpha <= 0.05$). For cell-free cylinders, significantly more microvessels were counted at the entrance of the cylinders when VEGF was present, whereas the inside of the cylinders remained empty in both cases.

At the interface between dentin and tissue, some areas revealed higher cell densities towards the dentin wall (29 C, D, F), which might be due to the suggested effects of collagen exposure and growth factor release at the dentin surface. However, it was difficult to localize and analyze these areas. In many cases, processing of the tissues resulted in an artificial gap between the dentin wall and the tissues. Remnants of the gels could be observed for groups 3-6, in areas of high cell density, these were enclosed by cell clusters (28 E, F). In DPSC-laden constructs, small collagen deposits could be observed in bioacive-factor-containing gels. For groups 4 and 6, characteristics of physiological pulp tissue could be observed, including a cell-rich zone at the dentin-pulp-interface (29 C, D), less densely packed fibroblast-like cells making the bulk of the tissue (29 F), and the presence of microvessels (28 F, black arrows). The typical odontoblast phenotype present in dental pulp could not be observed. Morphological characteristics of mature odontoblasts include a columnar shape, a polarized position of the nucleus, and a cellular process reaching into the matrix, which is left behind as the cells produce dentin.

3.1.1. SHED
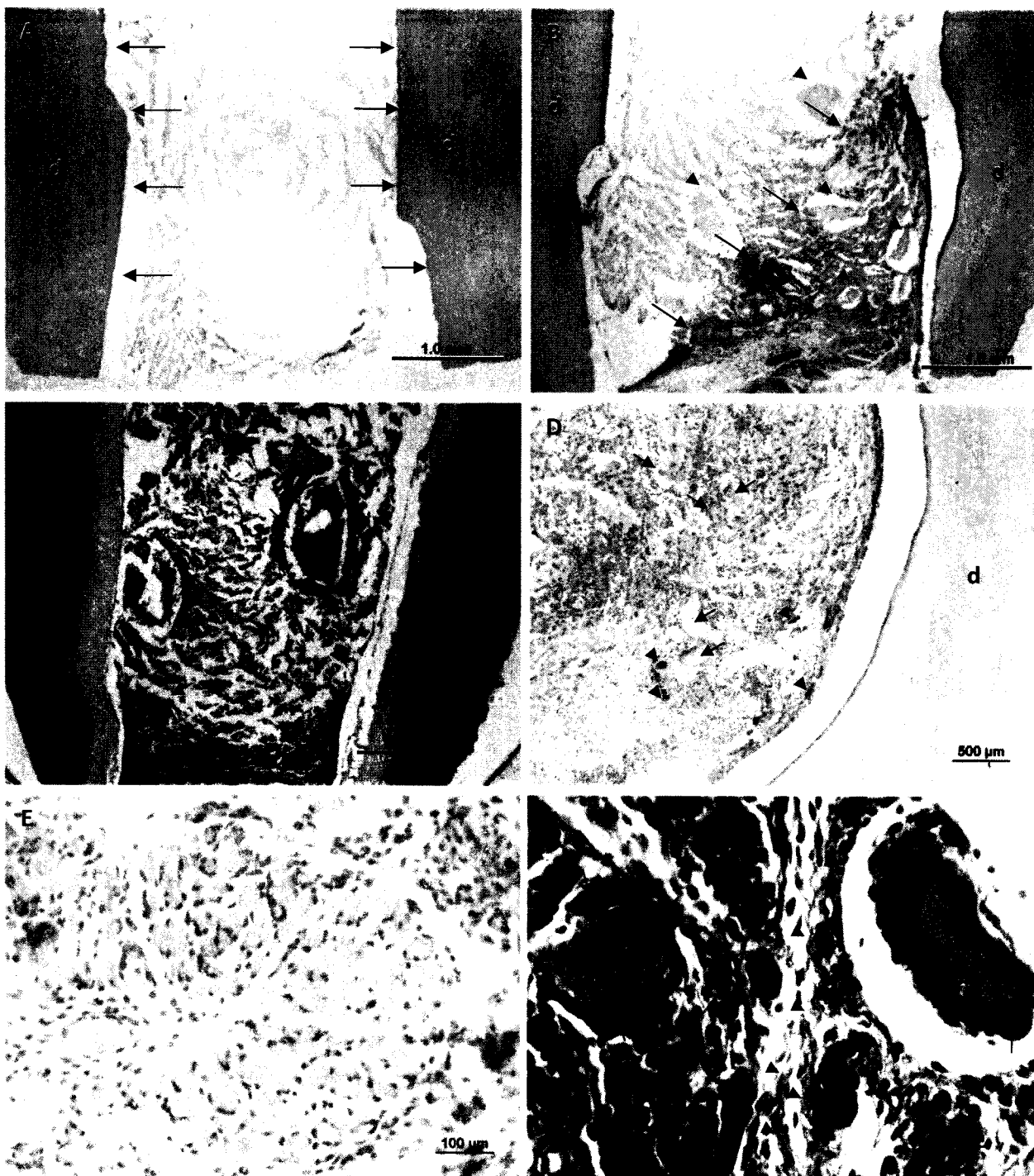
Figure 28: Empty cylinder and cylinders with SHED after 2 weeks.

(A) Overview of a cylinder, arrows indicating the dentin walls. Implantation of cell-free hydrogels (group 1) renders remnants of the gel only, the immigration of host cells cannot be observed. H&E.

(B) SHED in hydrogels without growth factors (group 3) survive only towards the opening of the cylinder, the mid-section remains cell-free, presumably due to insufficient blood vessel formation and therefore lack of nutrients in the center. Arrows indicate the demarcation line. Islands of remaining hydrogel can be seen (arrowheads) H&E.

(C) The presence of VEGF allows for better nutrition (group 4), and cells can be observed throughout the cylinder. Arrows show cell clusters. The dentin walls of the cylinder stain blue for the collagen matrix left after demineralization. Masson's Trichrome.

(D) Tissue formation of SHED cells in hydrogels with growth factor (group 4). Small hydrogel remnants are still present (arrows); microvessels have formed and can be seen throughout the construct (arrowheads). H&E.

(E) Small hydrogel remnants enclosed by the cells visualized at higher magnification. H&E.

(F) Gel remnants visible in homogenous blue after Masson's Trichrome (arrows, black). Newly formed, wavy collagen fibers have been deposited by the cells, replacing the hydrogel carrier (arrowheads). Microvessels filled with erythrocytes (red) can be distinguished. Masson's Trichrome.

d: dentin; h: hydrogel.

3.1.2. DPSC
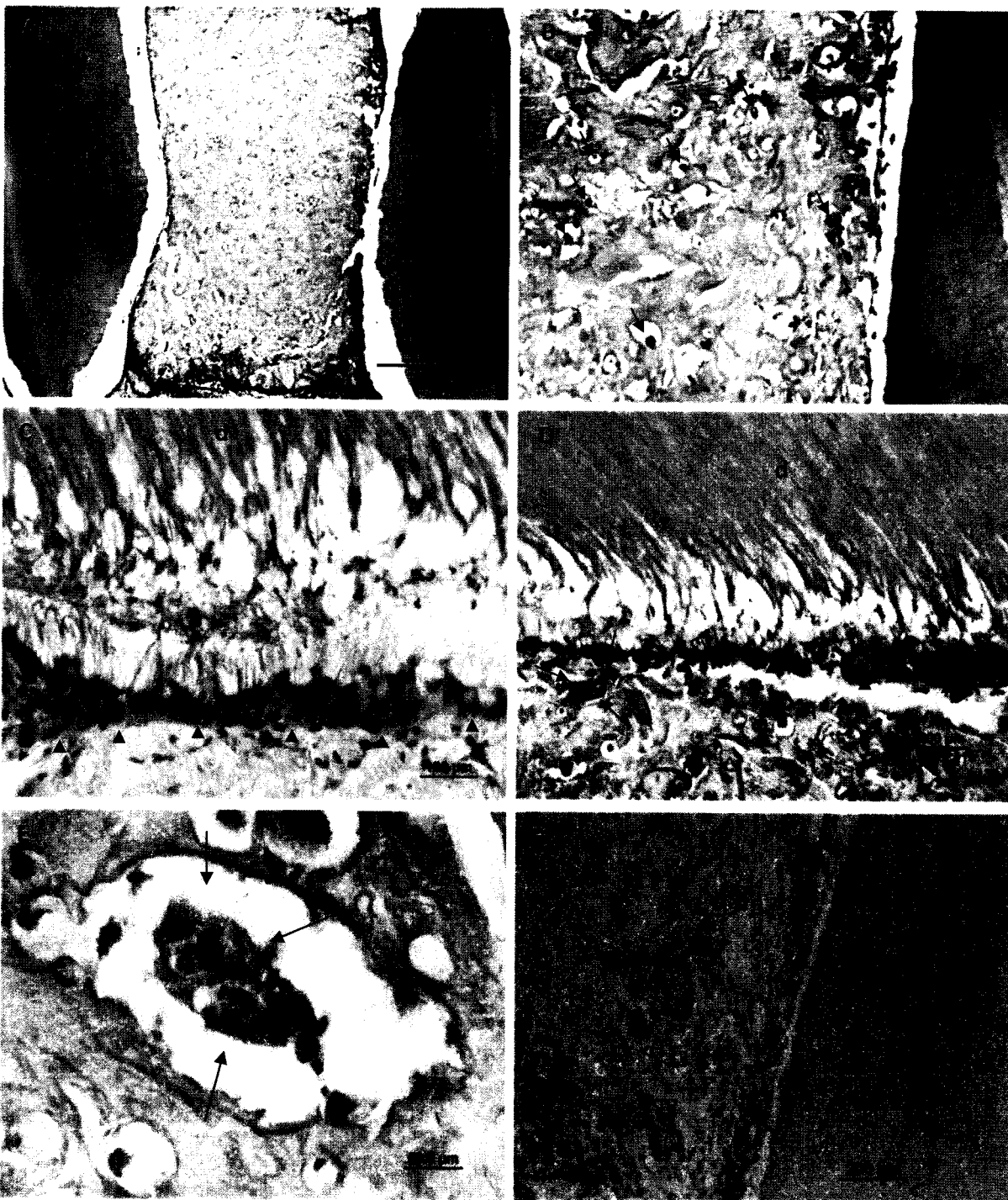
Figure 29: DPSC after 2 weeks.

(A) DPSC in gels with growth factors (group 4). As observed with SHED, in the presence of VEGF, cells can be found throughout the cylinder. Masson's Trichrome.

(B) Higher magnification of the previous image. Single cells are spread out throughout the hydrogel matrix (arrows). The appearance differs from SHED at this time point, which are much more clustered together (compare Fig. 28 C). Masson's Trichrome.

(C) Cell-dentin interface. The top part of the image shows the collagenous matrix left after demineralization, with a recognizable tubular structure. Adjacent to the dentin wall, a zone of higher cell density can be observed, indicating cell clustering towards the dentin wall (arrowheads). H&E.

(D) Consecutive section of (C). The tubular structure of the dentin can be recognized better compared to the previous image. Cells cluster at the cell-dentin interface (arrowheads). Furthermore, a collagen deposit can be seen at the lower left corner, which can be distinguished from the hydrogel matrix by its darker blue color and dense structure. Several smaller collagen deposits can also be observed in the zone of higher cell density. However, a columnar, polarized appearance resembling odontoblasts cannot be confirmed. Masson's Trichrome.

(E) Higher magnification of a collagen deposit (arrows); these can be observed throughout the matrix for DPSC (group 4), but not for SHED (group 6). Masson's Trichrome.

(F) Connective tissue reminiscent of dental pulp. The wall of the dentin cylinder can be seen on the right hand side. A zone of more densely packed cells appears at the cell-dentin interface. Microvessels have formed and can be seen throughout the tissue (arrows). Cells show a fibroblast-like morphology. H&E.

d: dentin.

3.1.3. Microvessel formation
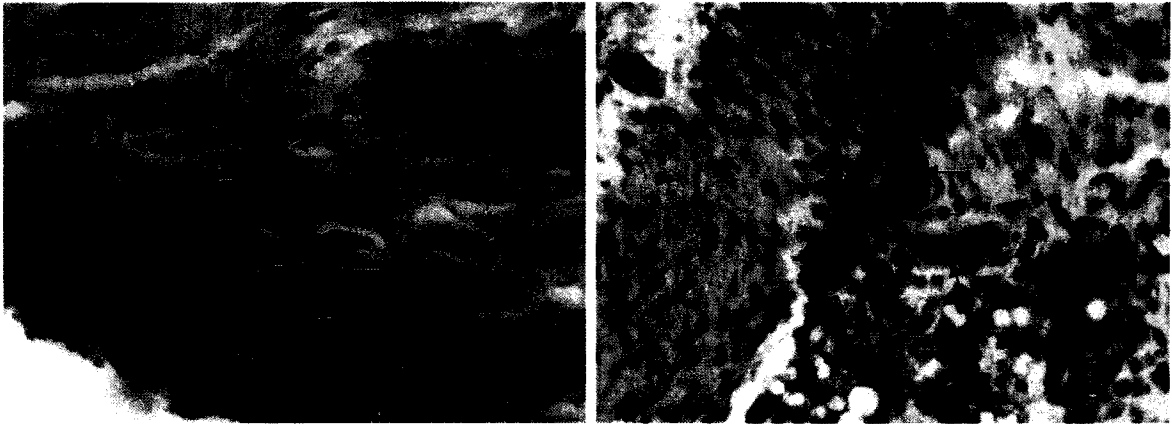
Figure 30: Localization of microvessels by immunohistochemistry. *Example slides for visualization of microvessels using Factor VIII antibody. Endothelial cells appear in dark red (arrows).*

Figure 30 demonstrates visualization of microvessels after immunohistochemistry with Factor VIII antibody, which was performed for both cell lines. Factor VIII is a glycoprotein present in endothelial cells, which is released into the blood stream after activation of the clotting cascade to aid in hemostasis, and its presence identifies endothelial tissue. This method of detection and subsequent counts of vessels in tissue sections was performed after modification of a protocol described in a similar study with SHED in tooth slices [65]. The authors investigated the intrinsic potential of SHED to form microvessels, and they compared SHED alone to SHED mixed with human endothelial cells. Two aspects of this work are highly interesting. Co-transplantation of SHED with endothelial cells did not result in higher blood vessel density in these constructs. Furthermore, SHED cells were transduced with LacZ before implantation to evaluate cell fate in the constructs. The majority of blood vessels in the constructs stained positive for LacZ, indicating that SHED cells had differentiated into endothelial cells and contributed to microvessel formation. In our study,

we did not investigate the origin of endothelial cells in our constructs. The newly formed microvessels could therefore be of murine origin, but also very well be formed by the implanted cells, as indicated by the results described above.

Another aspect, comparing our work to CORDEIRO's [65] is that the tooth slices used for cell seeding in their case were 1 mm thick, allowing connection to the local vasculature more easily. In our work, the cylindrical shape of the constructs makes proper nutrition of the implanted cells more challenging, a fact that bioengineers will face trying to re-colonize the long and narrow space of a root canal with live tissue, which will inevitably depend on sufficient provision of nutrients to the cells. Our results of higher microvessel density and formation of dental-pulp-like tissue in those cylinders mediated by VEGF are promising and make this growth factor a prime candidate for future strategies to engineer dental pulp.

3.2. Results after 5 weeks

3.2.1. Emtpy Cylinders

After 5 weeks *in situ*, the empty cylinders are unaltered and only show remnants of the hydrogel, and encapsulation by fibrotic host tissue, which can be seen in Figure 31. From visual inspection, no difference could be observed between groups 1 and 2.
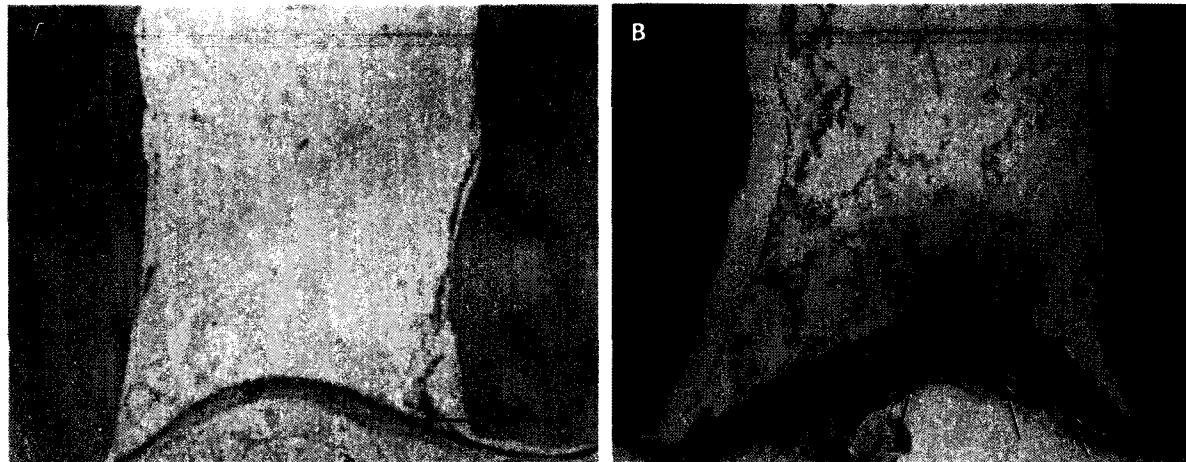
Figure 31: Empty cylinders after 5 weeks.
(A) Faint remnants of the hydrogel can be seen inside the cylinder after 5 weeks. H&E.
(B) Consecutive section of (A). Gel remnants are visualized better. A fibrotic capsule of host
tissue has formed around the implant (arrows). Masson's Trichrome.
d: dentin

3.2.2. SHED

Figure 32 depicts images from transplanted SHED. Without growth factors in the hydrogel,

the cells form tissue to some extent, but large areas containing vacuoles reminiscent of fat

tissue are present (32 A), and big remnants of hydrogel can be observed (32 B). However,

small areas of pulp-like tissue can be found, and a collagenous matrix is formed (32 D). In

growth-factor containing gels, the areas of pulp-like tissues are much larger (32 E). Dense

cellular networks develop for SHED, and these cells synthesize tightly packed collagen (32 E,

F). High proliferation rates of SHED have been reported before [25], and our own work in

peptide amphiphiles demonstrated that these cells grow faster in the hydrogel matrix

compared to DPSC, and deposit more collagen [84].
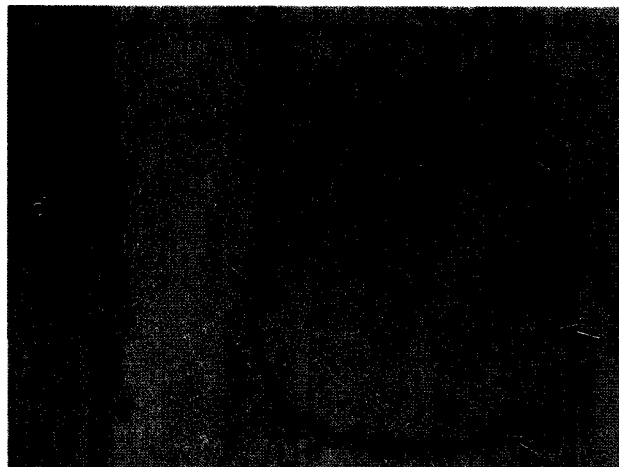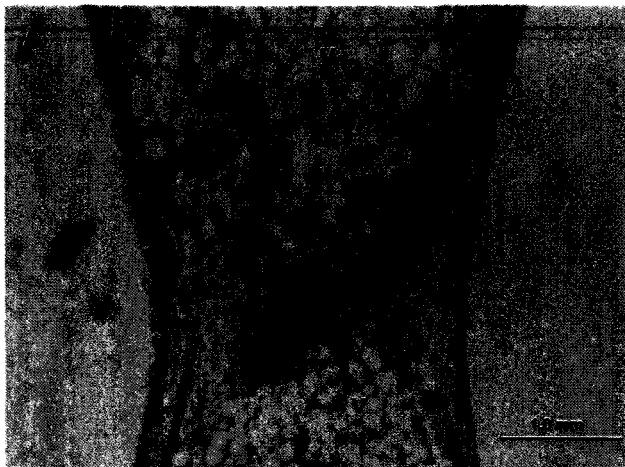
Figure 32: SHED after 5 weeks.

(A) *Tissues in cylinders without growth factors consist mainly of vacuoles reminiscent of fat tissue. H&E.*

(B) *Large remnants of hydrogel surrounded by cell clusters can be observed (arrows). H&E.*

(C) *Between large areas of vacuoles and non-degraded hydrogel, small areas show an organization similar to connective tissue, where the hydrogel has been replaced by collagen fibers, in which the cells are embedded. Masson's Trichrome.*

(D) *Higher magnification of C. The cell clusters and collagen fibers in dark blue are visible. Masson's Trichrome.*

(E) *SHED in hydrogels with growth factors show larger areas of properly organized tissue. Predominant formations show a high cell- and collagen-density. Masson's Trichrome.*

(F) *Higher magnification of E. Densely packed collagen matrix. Masson's Trichrome.*

d: dentin; h: hydrogel, v: vacuoles

3.2.3. DPSC

Compared to SHED, the tissues formed by DPSC resemble more closely dental pulp tissue. The cells form a lose network (33 A, B), and at the interface between dentin and tissue, an intimate association between cells and dentin can be observed (33 A-D). However, in some areas larger cells similar to osteoclasts can be observed, and a rugged dentin might be the result of a resorption process (33E).

The synthetic matrix is replaced by collagen, in most areas appearing like an extracellular matrix, in which the cells are embedded (33 B, D). Apart from that, localized, small and very dense collagen deposits can be observed (33 D). These are usually found in close vicinity to microvessels. These dense deposits can be found only in DPSC in hydrogels with growth factors present. One might speculate whether VEGF plays a role, given their association with microvessels, but the β-glycerophosphate might have an inductive effect, too. Although it is mainly believed to aid in mineral formation, it has been associated with stem cell differentiation as an osteogenic supplement. Unfortunately, after demineralization of the constructs detection of mineral is no longer possible.

200 μm
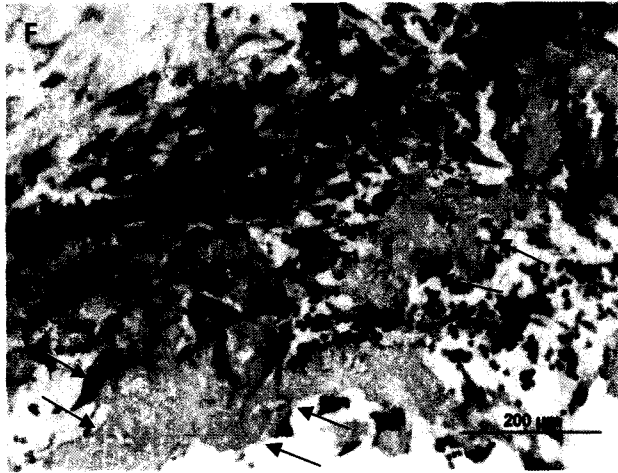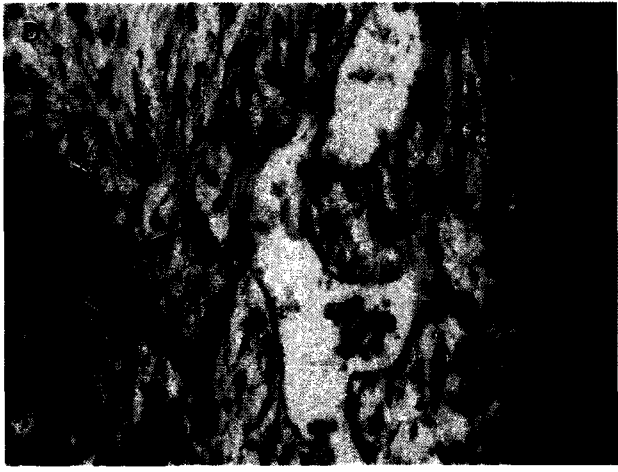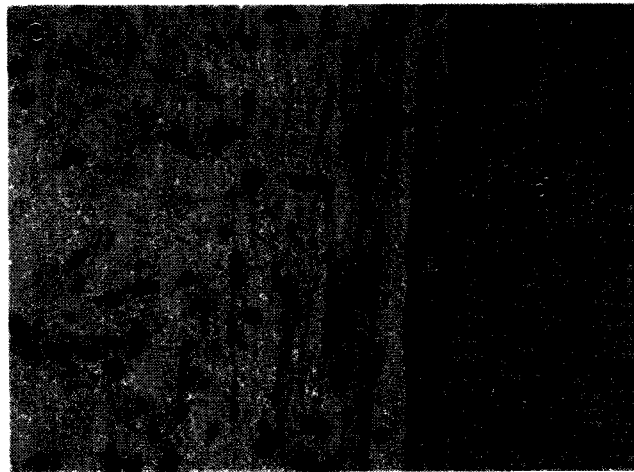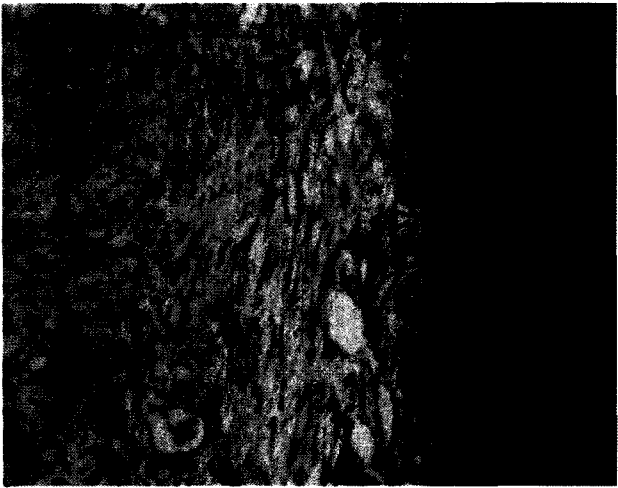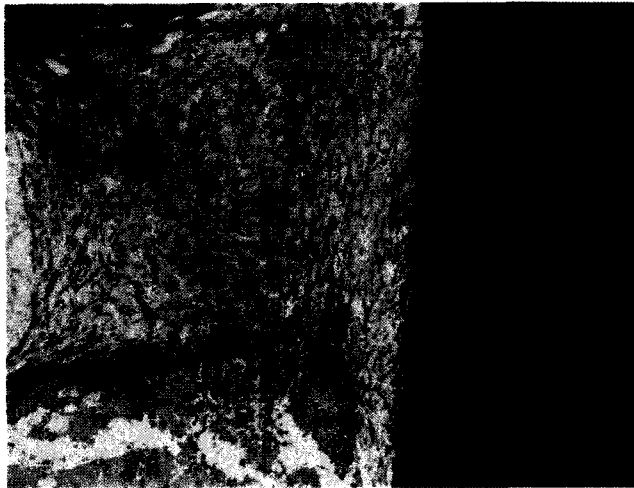
Figure 33: DPSC after 5 weeks.

(A) Properly organized tissue highly similar to dental pulp can be found. The cells are embedded in a lose network of collagen, and they line the walls of the cylinder, tightly associated with the dentin.

(B) Higher magnification of A.

(C) The cells are packed more tightly towards the dentin. The columnar, polarized cell shape of mature odontoblasts cannot be observed.

(D) Small and dense collagen deposits can be found, usually in close vicinity to microvessels (arrows).

(E) The dentin surface appears disrupted, and large cells with multiple nuclei reminiscent of osteoclasts appear (arrows), suggesting resorption of the dentin.

(F) The hydrogel has mainly been degraded, only small remnants can be found (arrows).

d: dentin.

Islands of Dsp-positive cells were found in DPSC and differentiation factor-containing hydrogels (Figure 34). However, these islands were sparse, and distributed throughout the matrix rather than lining the dentin wall, as expected. Still, expression of Dsp in these cells demonstrates that they undergo a differentiation process.
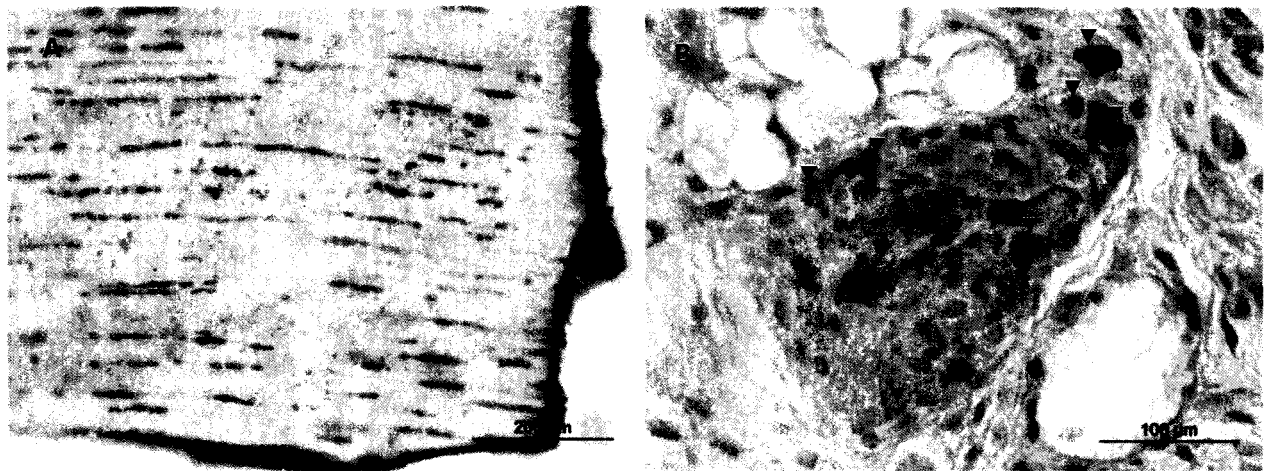
Figure 34: Localization of dentin sialoprotein.

(A) The dentin cylinder served as a positive control, as Dsp is entrapped within the dentin matrix and shows up in dark brown after immunohistochemistry.

(B) Cell clusters within the newly formed tissue showed Dsp expression (arrowheads) as an indicator or cellular differentiation towards an odontoblast-like cell type.

Overall, we can show that combining dental stem cells with this customized hydrogel results in the formation of a pulp-like tissue. However, the desired tissue formation could not be observed in all constructs but in about 50 % of the implants, whereas the rest was filled with fibrous tissue and vacuoles or showed areas with gel remnants similar to the empty cylinders. Reasons for these differences could be the site of implantation, where implants placed directly behind the ears seemed less exposed to movement of the skin, and could not be reached by the animals, which tended to scratch at the implantation sites. In future work, the implants should be placed as far up and towards the midsection as possible to avoid these effects.

In constructs with proper tissue formation, the hydrogel carrier is degraded and replaced by a collagenous extracellular matrix. VEGF aids in quick organization of a microvascular network to provide oxygen and nutrients to the cells. Pre-treatment of the dentin did not noticeably affect cellular organization and differentiation; however, intimate association of the implanted cells with the dentin walls can be seen. Some areas show signs of dentin resorption, and cells similar to osteoclasts appear at the cell-dentin interface. This unwanted effect could possibly be overcome by pretreatment of the dentin wall. A directional deposition of collagen and pre-dentin deposition towards the existing dentin walls cannot be observed.

4. Troubelshooting

4.1. Cell Seeding

Seeding the hydrogel into the small space of the cylinders proved to be difficult at first, since bubbles within the cylinder had to be avoided. Using small pipette tips (10 µL), starting at the bottom of the cylinder, slowly lifting the pipette as the gels were injected provided good results. Repeated centrifugation of the hydrogel/cell stock at 1000 rpm for 30 sec between seeding into individual cylinders removed bubbles from the stock, which are created during mixing and pipetting.

4.2. Transplantation

In general, the animals tolerated the surgical procedure well. One animal was lost 5 days after surgery due to a post-surgical infection. One problem we encountered was penetration of some of the implants through the skin and partial exposure of the implant after a few days *in situ*, which happened in four cases. Other implants were lost, as the mice tended to scratch the incision site and remove the implants. For a total of 10 implants, the surgeries had to be repeated. We tried to place the implants as far up and centered on the dorsum as possible to keep them out of reach for the animals, and less implants were lost after that.

4.3. Sectioning

Sectioning of the dentin cylinders proved difficult, as it is for most demineralized tissues. Alignment of the cylinders perpendicular to the direction of the blade during cutting made

sectioning easier. Not more than two cylinders could be placed into one block to obtain sufficient quality of the sections. Keeping the blocks at -20°C before sectioning, and cooling the blade with cooling spray (Freeze it, Fisher Sci, Pittsburgh, PA) between sections helped to improve the quality of the sections.

4.4. Immunohistochemistry

As typical for immunohistochemistry, the optimal protocol had to be developed for both antibodies. Different dilutions of primary antibody were tested (1:100, 1:250, 1:500) as well as different incubation times (30 min, 45 min) and temperatures (RT, 37°) with primary and secondary antibody. A dilution of 1:100 for both primary antibodies and incubation periods of 45 min at 37° C provided best results.

CHAPTER VII: CONCLUSIONS AND FUTURE PERSPECTIVE

The described system of dental stem cells encapsulated in a multidomain hydrogel scaffold laden with bioactive factors for cell differentiation and new blood vessel formation offers great promise for future tissue engineering strategies to regenerate dental pulp.

Multipotent dental stem cells are available from disposable sources, such as baby teeth or extracted wisdom teeth, and they maintain their differentiation potential after cryopreservation. They have been the focus of commercial stem cell banks as an autologous cell source, which can be derived non-invasively and might be useful for a variety of applications. Preservation of these cells might become a routine procedure in the near future.

The peptide-based hydrogel complements these cells for the envisioned treatment strategy, as it is compatible with the cells, can be injected into small spaces, and allows for custom-made matrices and incorporation of various growth and differentiation factors. In this case, β-glycerophosphate was added to aid in cell differentiation and mineralization, and vascular endothelial growth factor stimulated new blood vessel formation.

Implantation of this system *in vivo* resulted in the formation of a vascularized connective tissue highly similar to dental pulp. Whereas this marks our work as a success, it is only the first step in developing bioactive delivery systems designed to serve a specific purpose. Further modifications can result in even more sophisticated systems, carrying various growth factors to take advantage of potentially synergistic effects. Particularly the possibility of growth factor incorporation via heparin should be exploited further. Bioactive peptide sequences for mineral nucleation could be inserted, bilayered scaffolds with different properties for soft hard tissue

formation are imaginable, or the establishment of growth factor gradients within the gels, to name only a few ideas.

Several challenges in engineering dental pulp remain. In order to regenerate the soft tissue within the root canal, a long and narrow space, proper nutrition of the cells is paramount. In our model, addition of VEGF allowed for sufficient nutrition at a length of 4 mm. Although this result is promising, it has to be demonstrated that longer distances up to 10 mm can be bridged. If connection to the vasculature at the apex of the tooth can be achieved, engineering of the dental pulp instead of placing root canal fillers might move closer into the realm of possible treatment options.

In order to apply the described system as a pulp capping agent in deep cavities to encourage reparative dentin formation, the problem of directional dentin deposition has to be resolved. Currently we do not know how to direct dentin formation in a synthetic system. However, in a clinical setting, the inflammatory response at the site of injury triggers recruitment of progenitor cells, their differentiation and subsequent dentin bridging, which separates the soft tissue from the site of injury. It is worthwhile to explore whether dental stem cells delivered in a clinical setting can aid in this process and accelerate and optimize healing.

Whereas these challenges remain, we believe that the first steps we have undertaken have the potential to significantly impact further developments in oral healthcare, and might also have broader applications to the engineering of other body tissues.

CHAPTER VIII: APPENDICES

APPENDIX A

Table 3: List of amino acids in the order of appearance in the text

Amino Acid	1-letter code	3-letter code	Side chain polarity	Side chain charge (pH 7)
Glutamic acid	E	Glu	polar	negative
Glutamine	Q	Gln	polar	neutral
Leucine	L	Leu	nonpolar	neutral
Arginine	R	Arg	polar	positive
Glycine	G	Gly	nonpolar	neutral
Aspartic acid	D	Asp	polar	negative
Serine	S	Ser	polar	neutral
Phenylalanine	P	Phe	nonpolar	neutral
Histidine	H	His	polar	neutral
Asparagine	N	Asp	polar	neutral
Lysine	K	Lys	polar	positive
Valine	V	Val	nonpolar	neutral

APPENDIX B

Self-Assembling Peptide Amphiphile Nanofibers as a Scaffold for Dental Stem Cells

Kerstin M. Galler[1,2,3], Adriana Cavender[1], Virany Yuwono[2], He Dong[2], Songtao Shi[4], Gottfried Schmalz[3], Jeffrey D. Hartgerink[2*] and Rena N. D'Souza[1*]

[1] Dept of Biomedical Sciences, TAMUHSC - Baylor College of Dentistry, 3302 Gaston Ave., Dallas, TX, 75246.

[2] Depts of Chemistry and Bioengineering, Rice University, 6100 Main, Houston, TX 77005-1827.

[3] Depts of Operative Dentistry and Periodontology, University of Regensburg, Franz-Josef-Strauss Allee 11, Regensburg, Germany, 93053

[4] Center for Craniofacial Molecular Biology, School of Dentistry, University of Southern California, 2250 Alcazar Street, CSA 104, Los Angeles, CA, 9003.

* Equally corresponding authors:

Rena N. D'Souza, DDS, MS, PhD
Professor and Chair,
Department of Biomedical Sciences
Baylor College of Dentistry
3302 Gaston Avenue
Dallas, Texas 75246
Office: (214) 828-8260
Labs: (214) 828-8484;
        (713) 677-7556
Fax: (214) 874-4538
e-mail: rdsouza@bcd.tamhsc.edu

Jeffrey D. Hartgerink, PhD
Assistant Professor
Departments of Chemistry
and Bioengineering
Rice University
Houston, TX 77251-1892
Office: 713-348-4142

e-mail: jdh@rice.edu

ABSTRACT

Dental caries remains one of the most prevalent infectious diseases in the world. So far, available treatment methods rely on the replacement of decayed soft and mineralized tissue with inert biomaterials alone. As an approach to develop novel regenerative strategies and engineer dental tissues, two dental stem cell lines were combined with peptide-amphiphile (PA) hydrogel scaffolds. PAs self-assemble into three-dimensional networks of nanofibers, and living cells can be encapsulated. Cell-matrix interactions were tailored by incorporation of the cell adhesion sequence RGD and an enzyme-cleavable site. SHED (stem cells from human exfoliated deciduous teeth) and DPSC (dental pulp stem cells) were cultured in PA hydrogels for four weeks using different osteogenic supplements. Both cell lines proliferate and differentiate within the hydrogels. Histologic analysis shows degradation of the gels and extracellular matrix production. However, distinct differences between the two cell lines can be observed. SHED show a spindle-shaped morphology, high proliferation rates and collagen production, resulting in soft tissue formation. In contrast, DPSC reduce proliferation, but exhibit an osteoblast-like phenotype, express osteoblast marker genes, and deposit mineral. Since the hydrogels are easy to handle and can be introduced into small defects, this novel system might be suitable for engineering both soft and mineralized matrices for dental tissue regeneration.

INTRODUCTION

In every respect, the field of tooth bioengineering encompasses broad strategies and multidisciplinary approaches directed at restoring one of the most complex organ systems in vertebrates. Although rather small, a tooth is a composite of three calcified matrices, each of which possesses unique biochemical, biomechanical and structural properties. The anatomic tooth crown contains the hard tissues enamel and dentin, as well as soft tissue in its core, the dental pulp. The root anchors the tooth to the surrounding alveolar bone via the tendon-like periodontal ligament, which inserts into the cementum, a thin layer of yet another species of mineralized tissue covering the root surface. Enamel is a very hard and brittle substance mainly made of inorganic hydroxyapatite; cementum is similar to bone, but lacks vascularization. Dentin, a mineralized connective tissue surrounding and embedding the dental pulp, exhibits a unique tubular structure. Dentin-producing odontoblasts lining the pulp chamber send cellular processes into these tubules, connect both tissues to form the dentin-pulp complex, and thus make dentin a live tissue. Exposure of dentin after attrition, trauma or carious invasion by bacteria triggers inflammation and pain, which upon resolution leads to the recruitment and differentiation of progenitor cells and the rapid deposition of a reparative dentin matrix. This active defense mechanism of the dental pulp to separate itself from the site of injury and maintain its vitality illustrates its strong intrinsic regenerative potential. In recent years the healing capacity of dental pulp was underscored by the identification and characterization of populations of postnatal stem cells capable of differentiating into odontoblasts.

Dental tissues harboring stem cells are easily accessible and most often discarded as a byproduct of routine surgical treatment. Stem cell characteristics can be detected in cells isolated from the pulp of deciduous (1) as well as permanent teeth (2, 3), periodontal ligament (4, 5) or periapical follicle (5). Using stem cell markers such as STRO-1 or CD 146, mesenchymal stem cells, which represent less than 4 % of the total cell population, can be tagged and sorted by fluorescence-activated cell-sorting analysis (1). Tooth-derived stem cells are capable of differentiating into adipocytes, neurons and odontoblast-like cells (1, 6).

They form mineralized nodules *in vitro* (5) and create bone or dentin-pulp like complexes after transplantation into immunocompromised mice (1, 3).

As new sources of stem cells are explored and optimal permissive conditions for their differentiation are investigated, there is a strong need for advanced biomimetic scaffolding materials, which are versatile enough to be targeted for tooth-specific applications. These scaffolds have to provide a suitable three-dimensional network to accommodate cells and guide their growth, organization and subsequent differentiation. *In vivo*, these features are carried out by the extracellular matrix (ECM). Fibrillar proteins account for most of the ECM network, they self-assemble and form a well-organized structure. It surrounds cells, offers physical support and specific ligands for cell adhesion and migration. ECM also regulates cell proliferation and dynamic characteristics through various growth factors and signaling molecules. Recently, a novel class of hydrogel scaffolds has been developed, which offers several properties of natural ECM (7-13). These peptide amphiphile (PA) molecules consist of a peptide segment coupled to a fatty acid chain; they assemble into three-dimensional nanofiber networks to form self-supporting gels. The process is driven by formation of a hydrophobic core composed of closely packed alkyl tails, whereby fibrous strands can build because of hydrogen bond formation between the amino acids of adjacent PA molecules. Long cylindrical structures that are nanometers in diameter and microns in length create a gel by trapping water. Whereas the PAs remain amorphous aggregates at neutral pH due to the repulsive negative charge, addition of polyvalent ions eliminates the charge and allows self-assembly into cylindrical micelles, which undergo physical cross-linking to provide the gelled macrostructure. Self-assembly can be triggered upon mixture of PA solutions with cell culture media or other physiological fluids that contain polyvalent metal ions. When cells are suspended in the fluid, these can be encapsulated in the nanofibrillar matrix. It has been shown that cells can move, proliferate and differentiate within the hydrogel (10, 12-15). Several modifications of PAs have been described in the literature, allowing for mineral deposition (16), optimized cell adhesion (11, 17), selective cell differentiation into neurons (14) or ectopic bone formation (15).

A modification of a PA system that has previously been described was used in this study (10). The structure of these molecules can be divided into four regions of function: the peptide sequence contains an enzyme-cleavable site composed of GTAGLIGQ; a glutamic acid to assist in calcium binding; and RGDS, a cell-adhesion sequence that was first described in 1987 (18), which is present in natural ECM and has been integrated into various bioengineering scaffolds. The GTAGLIGQ is expected to be cleaved between glycine and leucine residues by matrix metalloproteinase 2 (MMP-2). Members of the MMP family are able to hydrolyze most of the proteins found in ECM; and MMP-2 is the major matrix metalloproteinase expressed by human pulp cells to remodel their environment (19). Incorporation of this specific cleavage site is expected to result in cell-mediated proteolytic degradation of the network, enabling cell migration and remodeling of the matrix with natural ECM. The fourth region of functionality is added after peptide synthesis by N-acylation with palmitic acid, which provides the driving force for self-assembly. These modifications of PA hydrogels are first steps to optimize tissue engineering scaffolds for a specific cell type.

In this study, we tested the use of the PA hydrogel scaffold with the following two well-characterized postnatal stem cell lines: SHED cells, which were isolated from human deciduous incisors (1), and DPSC from impacted wisdom teeth (2, 3). Our goal was to explore the compatibility of PA nanofibers with these two cell lines and to assess their potential as a suitable scaffold for cell proliferation and differentiation. Combinations of dexamethasone with inorganic phosphate (β-glycerophosphate or potassium phosphate) have previously been used as osteogenic supplements, and induced calcium accumulation in SHED and DPSC cells (1, 3, 20, 21). Cell differentiation was monitored by alkaline phosphatase assay, histologic analysis and quantitative real-time PCR analysis, which included marker genes for extracellular matrix synthesis and for differentiated osteoblasts and odontoblasts (collagen type I and III, alkaline phosphatase, bone sialoprotein, osteocalcin, and Runx2 and dentin sialophosphoprotein).

The results of our study show compatibility of both dental stem cell lines with the PA nanofibers. Cells spread, proliferate and differentiate within the hydrogels. However, we provide evidence that there are distinct differences between the two cell lines and their reaction to specific osteogenic supplements. SHED appear more adept for soft tissue regeneration, which is enhanced by β-glycerophosphate, while DPSC have a greater potential for terminal differentiation and subsequent mineralization, especially in combination with potassium phosphate. The results of this study provide the bases for further optimization of PA nanofibers as a scaffold for dental stem cells and for future tissue engineering strategies to regenerate dental tissues *in vivo*.

MATERIALS AND METHODS

Preparation of Peptide Amphiphiles

Peptide amphiphile molecules were synthesized as previously described as a thirteen amino-acid peptide (GTAGLIGQERGDS) by standard solid phase chemistry on an Advanced Chemtech Apex 396 peptide synthesizer (10). Preparation of the peptide portion was followed by acylation of the N - terminus. 150 mg of crude peptide was dissolved in 50 mL DI at pH 7.0. For purification purposes, peptides were precipitated at pH 3, centrifuged (4000 rad/min, 5 min), the supernatant was removed and peptides were freeze-dried for 24 hours. PA stock solution of 2 % by weight was prepared in DI water by adjusting the pH with NaOH to 7.0. PAs were characterized by matrix-assisted laser desorption ionization time-of flight (MALDI-TOF) mass spectrometry and were found to have the expected molecular weight. Stock solutions were kept under UV-light overnight for sterilization purposes.

Cell Culture of Dental Stem Cells

Two mesenchymal human stem cell lines were used in this study: DPSC derived from adult third molars (3), and SHED cells from exfoliated deciduous teeth (1). Cells were cultured with alpha MEM supplemented with 15% fetal bovine serum, 50 µg/mL L-ascorbic acid 2-phosphate, 100 U/mL penicillin and 100 µg/mL streptomycin, and incubated at 37°C with 5% CO_2. Subconfluent cells of passage 5 were detached using trypsin EDTA (Invitrogen, Carlsbad, CA), and 1.0 x 10^5 cells were seeded per gel. Therefore, 50 µl of PA stock solution (2% by weight) were placed in wells of a 96-well plate. Self-assembly into nanofiber networks was triggered by addition of 50 µl of cell suspension (2 x 10^6 cells/mL) containing 0.1 M $CaCl_2$ (pH 7.4). The solution was gently and briefly mixed, and gel formation was observed after 2-3 seconds. For each assay to be performed and for each time point and culture condition, triplicates were seeded. After 30 min, 200 µl of media were added to each well. The medium was changed after 24 hrs and osteogenic supplements were added according to previous reports (3, 20-22). Three different conditions were established: one group of gels was cultured with medium as described above (0 - control), for the second group, 10mM β-glycerophosphate and 10nM dexamethasone (SIGMA-Aldrich, St. Louis, MO) were added (βGP + dex); for the third group 10mM potassium phosphate (KH_2PO_4) (SIGMA-Aldrich, St. Louis, MO) and 10nM dexamethasone were added to the media (KPh + dex), all of the above being final concentrations. Gels were cultured for up to 4 weeks, media was changed every other day, and samples for different assays were collected at several time points.

Measurement of DNA content

After 3, 7, 14 and 28 days, cells samples were harvested after enzymatic digestion as described above, and cell pellets were frozen down at -80°C for further analysis. After completion of sample collection, these were thawed, and assays and measurements were performed on all samples at the same time. The number of cells in all samples was

determined by fluorometric quantification of DNA content using CyQuant cell proliferation assay kit (Invitrogen, Molecular Probes, Carlsbad, CA) and a FLUOstar Optima fluorescence plate reader (BMG Laboratories, Durham, NC). Actual cell numbers were calculated based on a standard curve created from suspensions of known cell densities.

Alkaline Phosphatase Activity

Samples for the detection of alkaline phosphatase (ALP) activity were prepared as described for the DNA assay. Cell pellets were resuspended in 60 µl of PBS. After addition of 60 µl of alkaline buffer and 100 µl alkaline substrate solution (SIGMA-Aldrich, St. Louis, MO), samples were incubated at 37°C for 30 min and the liberated p-nitrophenol was measured spectrophotometrically at 410 nm. Samples were compared to a dilution series of p-nitrophenol standard (SIGMA-Aldrich, St. Louis, MO) and ALP activity was normalized to the corresponding cell numbers obtained from the proliferation assay.

Quantitative Real-time PCR

To assess the effect of osteogenic induction on the expression of genes involved in differentiation, matrix formation and mineralization, real-time PCR was performed on samples after 28 days of culture. RNA was extracted using RNA Stat 60 (Tel-Test Inc. Friendswood, TX) from 6 gels per group at a time to get sufficient amounts for reverse transcription, which was performed according to standard protocols for cDNA synthesis using an oligo-dT primer. 100 ng of RNA were used for one reaction of reverse transcription, which provided cDNA for 10 real-time PCR reactions. Primer sets for marker genes of osteoblast and odontoblast differentiation were designed from mRNA sequences published in GenBank (identification number given in parentheses) using primer 3 software and synthesized as follows: collagen α(I)I (Col I) (NM_000088), collagen III (Col III) (NM_000090), alkaline phosphatase (ALP) (NM_000478), bone sialoprotein (Bsp) (NM_000582),

osteocalcin (Oc) (X_53698), Runx2 (NM_004348), dentin sialophosphoprotein (Dspp) (NM_014208), matrix metalloproteinase-2 (MMP-2) (NM_004530), and glyceraldehyde 3 phosphate dehydrogenase (GAPDH) (M_33197) as an internal control. Primer efficiency was determined prior to quantification. Conditions for real-time PCR were as follows: After a denaturation step at 95°C for 15 minutes, 60 cycles were run with 95°C (15 sec), 58°C (30 sec), 72°C (30 sec), with a final dissociation step to generate the dissociation profile of the PCR products. Experiments were run in triplicates (ABI Prism 7900HT), gene expression was quantified using SYBR green (QuantiTect SYBR green PCR kit, Qiagen Inc. Valencia, CA) and normalized to GAPDH activity in respective samples. Calculations of fold-change in gene expression between controls and treated samples were performed according to the Pfaffl-method for relative quantification in real-time PCR as described in http://pathmicro.med.sc.edu/pcr/realtime-home.htm.

Histologic analysis

For histological analysis, gels after 28 days in culture were fixed in 4% paraformaldehyde for 3 hrs, dehydrated through ethanol series, embedded in paraffin and sectioned at 5 μm thickness. Sections were stained with hematoxylin and eosin (H&E), Masson's trichrome for collagen detection and von Kossa stain for calcium deposition using standard methods.

Cryo-transmission electron microscopy (cryoTEM)

To further investigate the mineralization properties, cryoTEM analysis was performed for all groups and samples. Three samples per cell line and condition were cultured as described above. As a cell-free control, additional gels were incubated with osteogenic supplements for 4 weeks. A small quantity of the sample solution (2-3 μl) was applied to a TEM copper grid with holey carbon film purchased from Quantifoil (400 mesh Cu grid, 1.2 μm hole diameter), and blotted with filter paper using a Vitrobot type FP 5350/60 under 100%

relative humidity for two seconds to create a thin layer of sample on the surface of the grid. The grid was plunged into liquid ethane and quickly transferred to liquid nitrogen. The sample was then analyzed using JEOL 2010 TEM at an accelerating voltage of 200 kV under low-dose imaging conditions.

RESULTS

Cell proliferation

When embedded in 3D peptide-amphiphile hydrogels, SHED cell proliferation was markedly higher as compared to DPSC. Addition of βGP + dex resulted in slightly increased proliferation rates in both cell lines, whereas KPh + dex showed attenuated cell growth. The DNA assay yielded corroborative data. After 28 days, cell numbers of SHED were close to 4 x 10^5 cells when cultured with βGP + dex, DPSC did not exceed 1.5 x 10^5 cells per gel. Growth curves under different culture conditions as well as actual cell numbers for different time points for both cell lines are shown in Figure 2.

Differentiation of dental stem cells with different culture conditions

Quantitative measurements of ALP activity showed differences between the two cell lines as well as between groups treated with different osteogenic media. The general trend shows a dramatic increase in both cell lines over time. SHED responded to treatment with βGP + dex with a considerably higher enzyme activity compared to controls, whereas KPh + dex seemed to have to opposite effect. DPSC showed a different profile, where KPh+ dex evoked slightly higher ALP levels than βGP + dex.

Analysis of marker genes for osteoblast and odontoblast differentiation (Fig. 3) revealed increased expression levels for all the genes investigated after 28 days in culture, with one exception, DPSC ceased to express dentin-specific Dspp after treatment with KPH + dex. In

SHED, higher expression levels of genes coding for extracellular matrix components (Col I, Col III) could be observed, especially with βGP + dex, and levels of MMP-2 were noticeably elevated. SHED treated with KPh + dex show an increase in osteoblast marker genes, such as bone sialoprotein, osteocalcin and Runx2. The prominent finding for DPSC is that when cultured with KPh + dex, the genes involved in the mineralization process, namely alkaline phosphatase, bone sialoprotein and osteocalcin, show a substantial increase, which is higher than in SHED.

Histologic analysis revealed degradation of the PA gel (Fig. 4A) and replacement with extracellular matrix as observed by Masson's trichrome (Fig. 4B, C). Whereas SHED formed clusters of cells (Fig 4 A, B), DPSC were more sparsely distributed within the gel (Fig. 4C), they showed a round, osteoblast-like morphology, and mineral deposition with both osteogenic supplements, but to a higher degree with KPh + dex (Fig. 4D). SHED treated with βGP + dex did not produce mineral deposits, but few deposits were visible for cells treated with KPh + dex after von Kossa stain (data not shown).

Vitreous ice cryoTEM was performed on the PA scaffold surrounding the cultured cells. Mineralization of the artificial matrix was observed mirroring the mineralization observed by histology. cryoTEM images revealed little mineral deposition for SHED cultured with βGP + dex (Fig. 5B), but a slightly higher mineralization rate with KPh + dex (Fig. 5C). Mineralization potential in DPSC is much higher, βGP + dex induces deposition mainly of larger crystals (Fig. 5E), whereas potassium phosphate appears to be most conducive for the formation of multiple mineral deposits (Fig. 5F). Control gels with cells cultured with regular media (Fig. 5A, D) or gels incubated with osteogenic supplements for an equivalent period of time without cells (images not shown) did not show mineral deposits.

DISCUSSION

In this study, we present an *in vitro* system in which we combined nanofibrous peptide-amphiphile hydrogels with two adult tooth-derived mesenchymal stem cell lines. Our data

provides evidence that these cells are able to 1) proliferate within the gel, 2) remodel it by enzymatic degradation and deposition of a collagenous matrix, 3) change their morphology and gene expression profile as a sign of differentiation, and 4) deposit calcium and form a mineralized matrix. All these characteristics vary between the two cell lines as well as between groups treated with different osteogenic supplements. SHED maintain a high proliferation rate and a spindle-shaped, fibroblast-like morphology. They produce large amounts of collagen, which goes hand in hand with a higher MMP-2 activity as an indication of matrix degradation and remodeling; and they form coherent soft tissues during a four-week culture period. β-glycerophosphate with dexamethasone enhances proliferation and induces upregulation of early differentiation markers such as collagen and alkaline phosphatase. In contrast, potassium phosphate and dexamethasone slightly decrease proliferation and affect the expression of markers of terminal differentiation of cells involved in biomineralization. These include Runx2, Bsp and Oc. DPSC growth is significantly slower in the three-dimensional environment compared to SHED. Histological images and the change in gene expression after 4 weeks suggest that these cells can be driven further towards terminal differentiation, but adopt an osteoblast-like phenotype displaying a round morphology, significant upregulation of osteoblast markers, downregulation of Dspp, and calcium deposition, especially if cultured with potassium phosphate. cryoTEM analysis shows that mineral deposition occurs on the synthetic peptide-amphiphile matrix in a cell-mediated fashion. The extent of mineralization observed by TEM on the PA matrix mirrors the extent of mineralization observed by histology in deposited natural ECM. Importantly, this mineralization does not occur in the absence of cells.

Our data are in accordance with the established model for terminal differentiation where cells exit the cycle and cease to proliferate. They are also consistent with previous findings, where SHED cells were described to be distinct from DPSC regarding their higher proliferation rates and differences in differentiation potential in vitro, which led to the conclusion that they might represent a more immature population of stem cells (1). Furthermore, our observations reflect the behavior of these cells in vivo and the differences regarding their mineralization potential in deciduous and permanent teeth. Clinical studies

have shown that pulp capping after exposure of the soft tissue in primary teeth shows high failure rates (23). In permanent teeth, reparative dentin formation after application of calcium hydroxide has been reported in numerous studies (24). However, formation of dentin with its unique tubular structure can only be observed if the odontoblast layer remains intact, destruction of these cells leads, in many cases, to deposition of an osteoid matrix by replacement cells. Whereas bone and dentin are similar in their matrix protein composition, and osteoblasts and odontoblasts are closely related lineages, their organ structure, cell phenotype and gene expression profile are distinct. However, the detailed mechanisms underlying the initiation and maintenance of an osteoblast- versus an odontoblast-like phenotype remain to be elucidated. The conditions used in this study seem to favor a differentiation pathway towards the osteoblast lineage. Although both stem cell lines have been shown to differentiate into odontoblasts *in vivo*, the optimum permissive conditions for odontoblast differentiation *in vitro* have yet to be clarified. Growth and differentiation factors such as dexamethasone, TGFβ-1, different BMPs, Dmp-1 or a mixture of dentin non-collagenous proteins have yielded differentiation of cells into odontoblasts *in vitro* (25-28). In this study, the cell culture medium was supplemented with dexamethasone to induce cell differentiation, and inorganic phosphate to enhance the mineralization process.

Our data leads to the conclusion that PA molecules provide a nanostructured, cell-responsive matrix that is specifically conducive to dental stem cells. The hydrogels are easy to handle, and due to their mechanical properties they could be inserted into small defects, such as cavities of periodontal pockets, without difficulties. The two cell lines seeded in PA hydrogels show differences in morphology, proliferation and differentiation behavior. SHED seem to be a suitable tool for soft tissue regeneration, such as dental pulp, whereas DPSC might be useful for engineering mineralized tissues like bone or dentin, which can be enhanced by the choice of osteogenic supplement. This research may provide us with an applicable system for new treatment strategies to regenerate both soft and mineralized dental tissues.

FIGURES

Figure 1
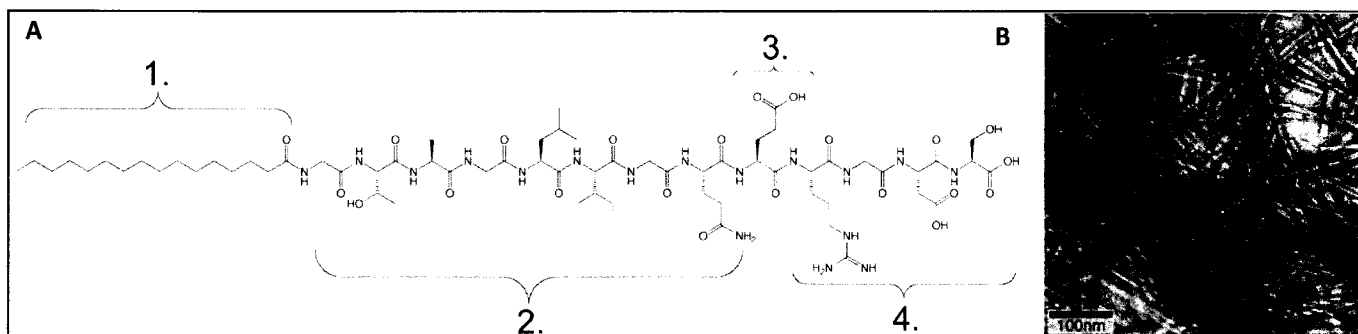
(A) Chemical structure of the peptide amphiphile, highlighting the four regions of function: 1) alkyl tail, 2) enzyme-cleavable site, 3) glutamic acid for calcium binding, 4) cell adhesion motif RGD. (B) cryoTEM image of the self-assembled nanofiber network.

Figure 2
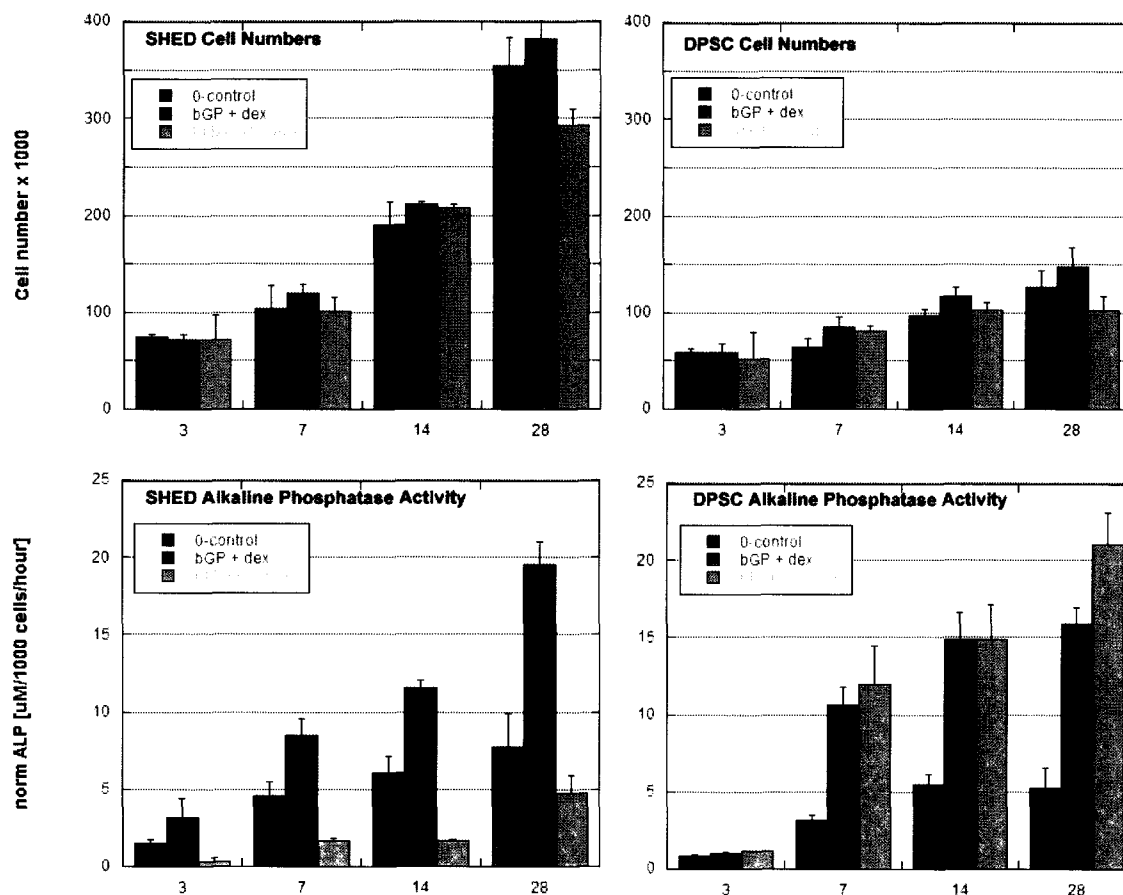
(A) Quantitative cell proliferation assay revealed higher proliferation rates for SHED as compared to DPSC, a slight increase for cells treated with β-glycerophosphate + dexamethasone, the opposite effect with potassium phosphate + dexamethasone. (B) Alkaline phosphatase activity in SHED is increased with β-glycerophosphate + dexamethasone, but reduced with potassium phosphate + dexamethasone compared to the control, again DPSC shows the contrary.

Columns show mean values of triplicates, and error bars indicate standard deviation.

FIGURE 3
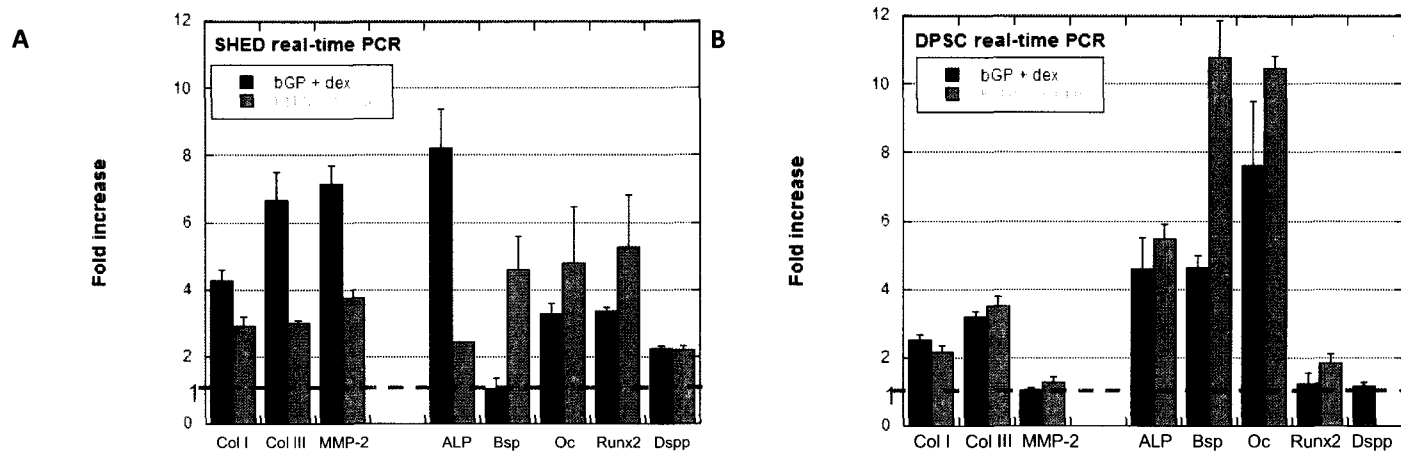
Gene expression profile of SHED and DPSC after 4 weeks of osteogenic induction. Data obtained from controls were set to 1 as indicated by the dotted line. The graph shows the fold-increase of gene expression compared to control cells cultured in media without osteogenic supplements. Columns display the mean values and error bars the standard deviation of three measurements. **(A)** SHED cultured with βGP + dex mainly increased the expression of genes involved in matrix deposition (Col I and III) and scaffold degradation and remodeling (MMP-2). Levels of ALP as an early marker of mineralization were elevated. Genes involved in the actual mineralization process, such as Runx2, Bsp and Oc were higher in cells cultured with potassium phosphate + dex. **(B)** DPSC cells show increase of collagen expression to a lesser extent than SHED. When cultured with potassium phosphate + dex, mineralization markers ALP, Bsp, and Oc are markedly upregulated and about two-fold higher than in SHED cultured under the same conditions. Dspp, a dentin-specific marker gene, ceases to be expressed.

FIGURE 4
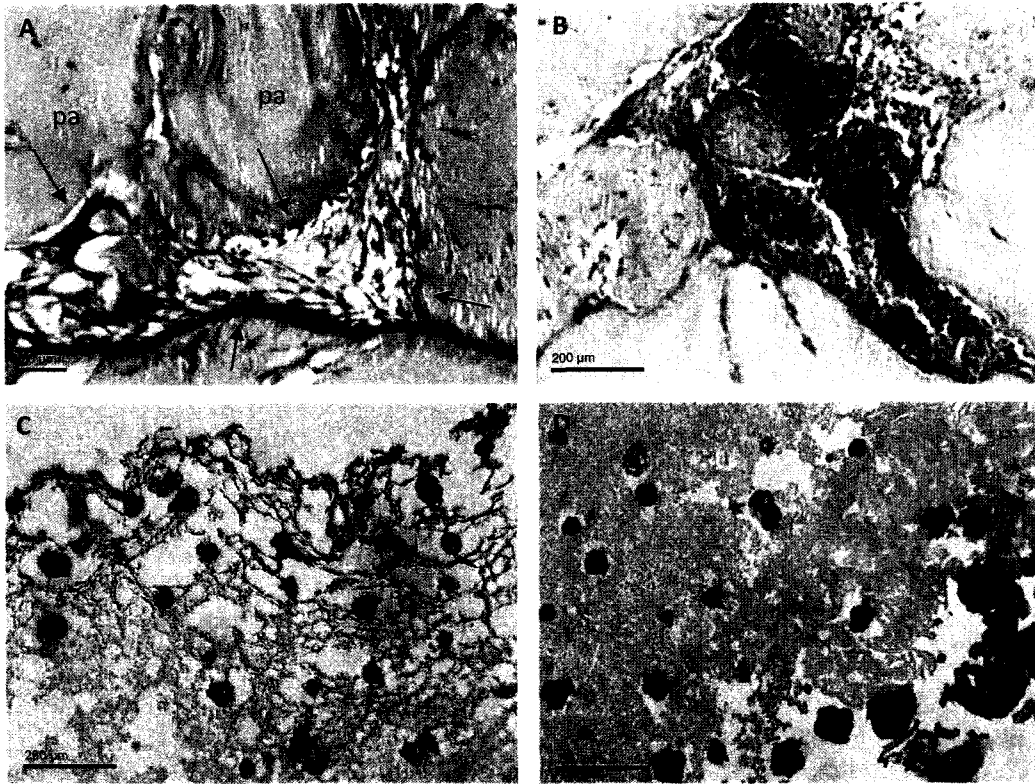
(A) SHED cultured with βGP + dex form cell clusters and degrade the gel (arrows, pa = peptide amphiphile gel (H&E). **(B)** SHEDs show a fibroblast-like cell morphology and deposit a collagenous matrix (Masson's trichrome). **(C)** DPSC cultured with potassium phosphate + dex adopt an osteoblast-like phenotype, produce collagen localized around cells (Masson's trichrome) and **(D)** deposit mineral (von Kossa stain).

FIGURE 5
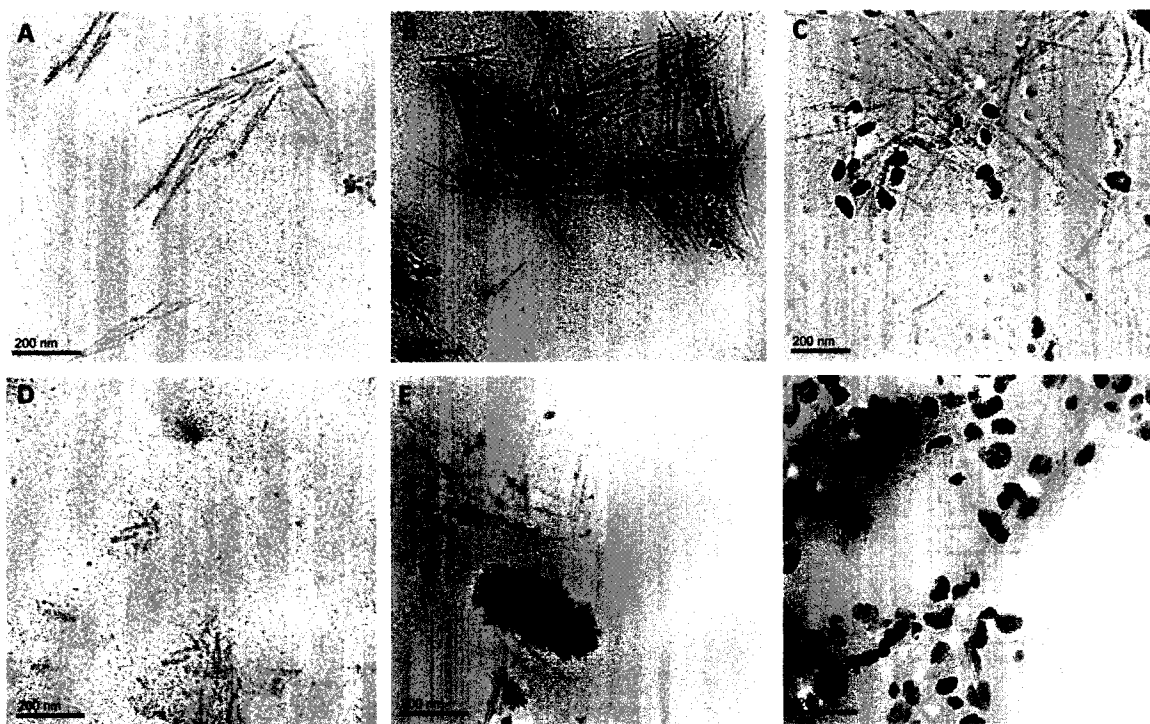
cryoTEM images show mineral deposition only for cells treated with osteogenic supplements after four weeks in culture. Whereas SHED cells produce few deposits, DPSC exhibit a much higher tendency for mineralization. Treatment with potassium phosphate + dex enhances mineral deposition significantly. **(A)** SHED control, **(B)** SHED cultured with βGP and dex, **(C)** SHED cultured with KPh + dex, **(D)** DPSC control, **(E)** DPSC cultured with βGP + dex, **(F)** DPSC cultured with KPh + dex.

REFERENCES

1. Miura, M., Gronthos, S., Zhao, M., Lu, B., Fisher, L.W., Robey, P.G., and Shi, S. SHED: Stem cells from human exfoliated deciduous teeth. PNAS 100, 5808, 2003.

2. Gronthos, S., Brahim, J., Li, W., Fisher, L.W., Cherman, N., Boyde, A., DenBesten, P., Robey PG, and Shi S. Stem cell properties of human dental pulp stem cells. J Dent Res 81, 531, 2002.

3. Gronthos, S., Mankani, M., Brahim, J., Robey, P.G., and Shi, S. Postnatal human dental pulp stem cells (DPSCs) in vitro and in vivo. Proc Natl Acad Sci USA 97, 13625, 2000.

4. Seo, B.M., Miura, M., Gronthos, S., Bartold, P.M., Batouli, S., Brahim, J., Young, M., Robey, P.G., Wang, C.Y., and Shi, S. Investigation of multipotent postnatal stem cells from human periodontal ligament. Lancet 364, 149, 2004.

5. Jo, Y.Y., Lee, H.J., Kook, S.Y., Choung, H.W., Park, J.Y., Chung, J.H., Choung, Y.H., Kim, E.S., Yang, H.C., and Choung, P.H. Isolation and characterization of postnatal stem cells from human dental tissues. Tissue Eng 13, 767, 2007.

6. Morsczeck, C., Schmalz, G., Reichert, T.E., Völlner, F., Galler, K., and Driemel, O. Dental stem cells for regenerative medicine. Clin Oral Invest. In press.

7. Hartgerink, J.D., Beniash, E., and Stupp, I.S. Self-assembly and mineralization of peptide amphiphile nanofibers. Science 294, 1684, 2001.

8. Hartgerink, J.D., Beniash, E., and Stupp, I.S. Peptide-amphiphile nanofibers: A versatile scaffold for the preparation of self-assembling materials. Proc Natl Acad Sci USA 99, 5133, 2002.

9. Beniash, E., Hartgerink, J.D., Storrie, H., Stendahl, L.C., and Stupp, S.I. Self-assembling peptide amphiphile nanofiber matrices for cell entrapment. Acta Biomater 1, 387, 2005.

10. Jun, H.W., Yuwono, V., Paramonov, S.E., and Hartgerink, J. Enzyme-mediated degradation of peptide-amphiphile nanofiber networks. Adv. Mater 17, 2612, 2005.

11. Harrington, D.A., Cheng, E.Y., Guler, M.O., Lee, L.K., Donovan, J.L., Claussen, R.C., and Stupp, S.I. Branched peptide-amphiphiles as self-assembling coatings for tissue engineering scaffolds. J Biomed Mater Res A 78, 157, 2006.

12. Rajangam, K., Behanna, H.A., Hui, M.J., Han, X., Hulvat, J.F., Lomasney, J.W., and Stupp, S.I. Heparin binding nanostructures to promote growth of blood vessels. Nano Lett 6, 2086, 2006.

13. Paramonov, S.E., Jun, H.E., and Hartgerink, J.D. Self-assembly of peptide-amphiphile nanofibers: The roles of hydrogen bonding and amphiphilic packing. J Am Chem Soc 128, 7291, 2006.

14. Silva, G.A., Czeisler, C., Niece, K.L., Beniash, E., Harrington, D.A., Kessler, J.A., and Stupp, S.I. Selective differentiation of neural progenitor cells by high-epitope density nanofibers. Science 303, 1352, 2004.

15. Hosseinkhani, H., Hosseinkhani, M., Tian, F., Kobayashi, H., and Tabata, Y. Osteogenic differentiation of mesenchymal stem cells in self-assembled peptide-amphiphile nanofibers. Biomaterials 27, 4079, 2006.

16. Hartgerink, J.D. Covalent capture: a natural complement to self-assembly. Curr Opin Chem Biol 8, 604, 2004.

17. Guler, M.O., Hsu, L., Soukasene, S., Harrington, D.A., Hulvat, J.F., and Stupp, S.I. Presentation of RGDS epitopes on self-assembled nanofibers of branched peptide amphiphiles. Biomacromolecules 7, 1855, 2006.

18. Ruoslahti, E. and Pierschbacher, M.D. New perspectives in cell adhesion: RGD and integrins. Science 23, 491, 1987.

19. Huang, F.M., Yang, S.F., Hsieh, Y.S., Liu, C.M., Yang, L.C., and Chang, Y.C. Examination of the signal transduction pathways involved in matrix metalloproteinases-2 in human pulp cells. Oral Surg Oral Med Oral Pathol Oral Radiol Endod 97, 398, 2004.

20. Gronthos, S., Graves, S.E., Ohta, S., and Simmons, P.J. The STRO-1+ fraction of adult human bone marrow contains the osteogenic precursors. Blood 84, 4164, 1994.

21. Zhang, W., Walboomers, X.F., van Kuppevelt, T.H., Daamen, W.F., Bian, Z., and Jansen, J.A. The performance of human dental pulp stem cells on different three-dimensional scaffold materials. Biomaterials 27, 5658, 2006.

22. Garreta, E., Genove, E., Borros, S., and Semino, C.E. Osteogenic differentiation of mouse embryonic stem cells and mouse embryonic fibroblasts in a three-dimensional self-assembling peptide scaffold. Tissue Eng 12, 2215, 2006.

23. Ranley, D.M. and Garcia-Godoy, F. Current and potential pulp therapies for primary and young permanent teeth. J Dent Res 28, 153, 2000.

24. Olsson, H., Petersson, K., and Rohlin, M. Formation of hard tissue barrier after pulp cappings in humans. A systematic review. Int Endod J 39, 429, 2006.

25. Alliot-Licht, B., Bluteau, G., Magne, D., Lopez-Cazaux, S., Lieubeau, B., Daculsi, G., and Guicheux, J. Dexamethasone stimulates differentiation of odontoblast-like cells in human dental pulp cultures. Cell Tissue Res 321, 391, 2005.

26. Deng, M., Shi, J., Smith, A.J., and Jin, Y. Effects of transforming growth factor beta1 (TGFbeta-1) and dentin non-collagenous proteins (DNCP) on human embryonic ectomesenchymal cells in a three-dimensional culture system. Arch Oral Biol 50, 937, 2005.

27. Almushayt, A., Narayanan, K., Zaki, A.E., and George, A. Dentin matrix protein 1 induces cytodifferentiation of dental pulp stem cells into odontoblasts. Gene Ther 13, 611, 2006.

28. Nakashima, M. Tissue engineering in endodontics. Aust Endod J 31, 111, 2005.

APPENDIX C

Table 4: Primers for real-time PCR

Primer	Abbreviation	Sequence (5`-3`)	GenBank Identification
glyceraldehyde 3 phosphate dehydrogenase Sense Antisense	**GAPDH**	GAG TCA ACG GAT TTG GTC GT GAC AAG CTT CCC GTT CTG AG	M_33197
collagen α(I)I Sense Antisense	**Col I**	AAA AGG AAG CTT GGT CCA CT GTGTGG AGA AAG GAG CAG AA	NM_000088
collagen III Sense Antisense	**Col III**	GGG AAC AAC TTG ATG GTG CT CCT CCT TCA ACA GCT TCC TG	NM_000090
Alkaline Phosphatase Sense Antisense	**ALP**	CCA CGT CTT CAC ATT TGG TG AGA CTG CGC CTG GTA GTT GT	NM_000478
Bone Sialoprotein Sense Antisense	**Bsp**	GTG GAT GAA AAC GAA CAA GG CCC CTT CTT CTC CAT TGT CT	NM_000582
Osteocalcin Sense Antisense	**Oc**	ACT GTG ACG AGT TGG CTG AC CAA GGG CAA GAG GAA AGA AG	X_53698
Runx2 Sense Antisense	**Runx2**	GAA CTG GGC CCT TTT TCA GA GCG GAA GCA TTC TGG AAG GA	NM_004348
Dentin Sialophosphoprotein Sense Antisense	**Dspp**	TTA AAT GCC AGT GGA ACC AT ATT CCC TTC TCC CTT GTG AC	NM_014208
Matrix Metalloproteinase-2 Sense Antisense	**MMP-2**	TGA GAT CTG CAA ACA GGA CA CCT CGT ATA CCG CAT CAA TC	NM_004530

Table 5: Statistical Analysis of Cell Proliferation

Legend:
- *   p ≤ 0.05
- **   p ≤ 0.01
- ***   p ≤ 0.001
- ns   = non significant

One way ANOVA Summary Cell Proliferation D3

	Collagen I	PuraMatrix	$E_2(SL)_6E_2$	$E_2(SL)_6E_2GRGDS$	$K_2(SL)_6K_2$	$K_2(SL)_6K_2GRGDS$	$K(SL)_3RG(SL)_3K$
Collagen I	-	-					
PuraMatrix	*	-					
$E_2(SL)_6E_2$	***	ns	-				
$E_2(SL)_6E_2GRGDS$	**	ns	ns	-			
$K_2(SL)_6K_2$	***	***	ns	***	-		
$K_2(SL)_6K_2GRGDS$	***	*	ns	*	ns	-	
$K(SL)_3RG(SL)_3K$	***	**	ns	**	ns	ns	-
$K(SL)_3RG(SL)_3K\ GRGDS$	***	ns	ns	ns	*	ns	ns

One way ANOVA Summary Cell Proliferation D7

	Collagen I	PuraMatrix	$E_2(SL)_6E_2$	$E_2(SL)_6E_2GRGDS$	$K_2(SL)_6K_2$	$K_2(SL)_6K_2GRGDS$	$K(SL)_3RG(SL)_3K$
Collagen I	-	-					
PuraMatrix	*	-					
$E_2(SL)_6E_2$	***	*	-				
$E_2(SL)_6E_2GRGDS$	ns	*	***	-			
$K_2(SL)_6K_2$	***	**	ns	***	-		
$K_2(SL)_6K_2GRGDS$	***	ns	ns	***	*	-	
$K(SL)_3RG(SL)_3K$	***	ns	ns	***	ns	ns	-
$K(SL)_3RG(SL)_3K\ GRGDS$	ns	ns	ns	ns	*	*	*

One way ANOVA Summary Cell Proliferation D14

	Collagen I	PuraMatrix	$E_2(SL)_6E_2$	$E_2(SL)_6E_2GRGDS$	$K_2(SL)_6K_2$	$K_2(SL)_6K_2GRGDS$	$K(SL)_3RG(SL)_3K$
Collagen I	-	-					
PuraMatrix	ns	-					
$E_2(SL)_6E_2$	***	***	-				
$E_2(SL)_6E_2GRGDS$	**	ns	*	-			
$K_2(SL)_6K_2$	***	***	***	ns	-		
$K_2(SL)_6K_2GRGDS$	***	***	ns	ns	*	-	
$K(SL)_3RG(SL)_3K$	*	ns	*	ns	***	ns	-
$K(SL)_3RG(SL)_3K\ GRGDS$	ns	ns	***	ns	***	**	ns

APPENDIX E

Table 6: Rheometry Data Stress Sweep

Peptide	G′ [Pa]	G″ [Pa]
$K_2(SL)_6K_2$	558.05	81.26
$K_2(SL)_6K_2$_w/o sucrose, no PBS	28.7	7.9
$K_2(SL)_6K_2$_sucrose, no PBS	112.63	15.4
$K_2(SL)_6K_2$_βGP	513.27	63.38
$K_2(SL)_6K_2$_βGP + PBS	422.27	49.14
$K_2(SL)_6K_2$GRGDS	153.84	12.64
$K(SL)_3RG(SL)_3K$	184.57	25.05
$K(SL)_3RG(SL)_3KGRGDS$	182.932	20.22
$K_2(SL)_3RG(SL)_3K_2$	42.69	6.91
$K(SL)_3VLSLRG(SL)_3K$	67.93	9.96
$K_2(SL)_6K_2$ 2w% + hep 5mg/mL	4823.12	490.162
$K_2(SL)_6K_2$ 1w% + hep 2.5mg/mL	35.663	11.774
$K_2(SL)_6K_2$ 1w% + hep 1.25mg/mL	35.45	11.54
$K(SL)_3RG(SL)_3KGRGDS$ 1w% + hep 1mg/mL + PBS	505.43	59.38
$K(SL)_3RG(SL)_3KGRGDS$ 1w% + hep 1mg/mL + βGP	498.12	57.16
$E_2(SL)_6E_2$	473.5	43.127
$E_2(SL)_6E_2$GRGDS	141.57	16.19
$E_2(SL)_6E_2$GRGDS_no Ca2+	3.35	1.82
Col I (1.0 mg/mL)	30.72	7.45
Col I (2.0 mg/mL)	98.20	19.11
Col I (2.5 mg/mL)	102.10	19.40
Col I (3.0 mg/mL)	149.29	27.51
Col I (3.2 mg/mL)	154.4	37.07
Col I (3.3 mg/mL)	231.6	39.31
PuraMatrix	4501.86	584.8

Ang. Frequency: 0.5 rad/s

Osc. Stress: 0.01 – 1000 Pa

REFERENCES

[1]   Tooth anatomy.
      https://www.nlm.nih.gov/medlineplus/ency/article/001055.htm

[2]   Cohen S, Hargreaves KM, eds. Pathways of the pulp. 9th ed. St Louis: Mosby, Inc., 2006:460.

[3]   Tooth decay.
      http//www.dentalgentlecare.comdecay_process.htm

[4]   Vaidyanathan TK, Vaidyanathan J. Recent advances in the theory and mechanism of adhesive resin bonding to dentin: a critical review. J Biomed Mater Res B Appl Biomater. 2009. 88:558-78.

[5]   Salehrabi R, Rotstein I. Endodontic treatment outcomes in a large patient population in the USA: an epidemiological study. J Endod. 2004. 30:846-50.

[6]   Cvek M, Mejàre I, Andreasen JO. Conservative endodontic treatment of teeth fractured in the middle or apical part of the root. Dent Traumatol. 2004. 20:261-9.

[7]   Jacobs SG. The treatment of traumatized permanent anterior teeth: case report & literature review. Part I--Management of intruded incisors. Aust Orthod J. 1995. 13:213-8.

[8]   Petersen PE. The World Oral Health Report 2003: continuous improvement of oral health in the 21st century--the approach of the WHO Global Oral Health Programme. Community Dent Oral Epidemiol. 2003. 31:3-23.

[9]   Petersen PE. World Health Organization global policy for improvement of oral health--World Health Assembly 2007. Int Dent J. 2008. 58:115-21.

[10] Thesleff I. Developmental biology and building a tooth. Quintessence Int. 2003. 34:613-20.

[11] Skalak R and Fox CF. Tissue Engineering. Preface P.xx. New York, Alan R. Riss (1988).

[12] Mooney DJ, Mikos AG. Growing new organs. Sci Am. 1999. 280:60-5.

[13] Fortier LA. Stem cells: classifications, controversies, and clinical applications. Vet. Surg. 2005. 34:415-23.

[14]   Carey BW, Markoulaki S, Hanna J, Saha K, Gao Q, Mitalipova M, Jaenisch R. Reprogramming of murine and human somatic cells using a single polycistronic vector. Proc Natl Acad Sci U S A. 2009. 106:157-62.

[15]   Kaji K, Norrby K, Paca A, Mileikovsky M, Mohseni P, Woltjen K. Virus-free induction of pluripotency and subsequent excision of reprogramming factors. Nature. 2009. 458:771-5.

[16]   Weisser M, Ledderose G, Jochem Kolb H. Lon-term follow-up of allogeneic HSCT for CML reveals significant improvement in the outcome over the last decade. Ann Hematol. 2007. 86:127-32.

[17]   Vassalli G, Vanderheyden M, Renders F, Eeckhout E, Bartunek J. Bone marrow stem cell therapy for cardiac repair: challenges and prospectives. Minerva Cardioangiol. 2007. 55:659-67.

[18]   Kim BG, Hwang DH, Lee SI, Kim EJ, Kim SU. Stem cell-based cell therapy for spinal cord injury. Cell Transplant. 2007. 16:355-64.

[19]   Cui L, Liu B, Liu G, Zhang W, Cen L, Sun J, Yin S, Liu W, Cao Y. Repair of cranial bone defects with adipose derived stem cells and coral scaffold in a canine model. Bioomaterials. 2007. 28:5477-86.

[20]   De Bari C, Dell'accio F. Mesenchymal stem cells in rheumatology: a regenerative approach to joint repair. Clin Sci (Lond). 2007. 113:339-48.

[21]   Garcia M, Escamez MJ, Carretero M, Mirones I, Martinez-Santamaria L, Navarro M, Jorcano JL, Meana A, Del Rio M, Larcher F. Modeling normal and pathological processes through skin tissue engineering. Mol Carcinog. 2007. 46:741-5.

[22]   Ogawa R, Oki K, Hyakusoku H. Vascular tissue engineering and vascularized 3D tissue regeneration. Regen Med. 2007. 2:831-7.

[23]   Poulsom R, Alison MR, Forbes SJ, Wright NA. Adult stem cell plasticity. J Pathol. 2002. 197:441-56.

[24]   Ruch JV. Patterned distribution of differentiating dental cells: facts and hypotheses. Journale de Biologie Buccale. 1990. 18:91-98.

[25]   Gronthos S, Mankani M, Brahim J, Robey PG, Shi S. Postnatal human dental pulp stem cells (DPSCs) in vitro and in vivo. Proc Natl Acad Sci USA. 2000. 97:13625-30.

[26]   Gronthos S, Brahim J, Li W, Fisher LW, Cherman N, Boyde A, DenBesten P, Robey PG, Shi S. Stem cell properties of human dental pulp stem cells. J Dent Res. 2002. 81:531-5.

[27]   Miura M, Gronthos S, Zhao M, Lu B, Fisher LW, Gehron Robey P, Shi S. SHED: Stem cells from human exfoliated deciduous teeth. PNAS. 2003. 100:5808-5812.

[28]   Shi S, Gronthos S. Perivascular niche of postnatal mesenchymal stem cells in human bone marrow and dental pulp. J Bone Miner Res. 2003. 18:696-704.

[29]   Papaccio G, Graziano A, d'Aquino R, Graziano MF, Pirozzi G, Menditti D, De Rosa A, Carinci F, Laino G. Long-term cryopreservation of dental pulp stem cells (SBP-DPSCs) and their differentiated osteoblasts: a cell source for tissue repair. J Cell Physiol. 2006. 208:319-325.

[30]   Zhang W, Walboomers XF, Shi S, Fan M, Jansen JA. Multilineage differentiation potential of stem cells derived from human dental pulp after cryopreservation. Tissue Eng. 2006. 12:2813-23.

[31]   Mano JF, Silva GA, Azevedo HS, Malafaya PB, Sousa RA, Silva SS, Boesel LF, Oliveira JM, Santos TC, Marques AP, Neves NM, Reis RL. Natural origin biodegradable systems in tissue engineering and regenerative medicine: present status and some moving trends. J R Soc Interface. 2007. 4: 999-1030.

[32]   Chan G, Mooney DJ. New materials for tissue engineering: towards greater control over the biological response. Trends Biotechnol. 2008. 26: 382-92.

[33]   Langer R, Tirrell DA. Designing materials for biology and medicine. Nature. 2004. 428: 487-92.

[34]   Nicodemus GD, Bryant SJ. Cell encapsulation in biodegradable hydrogels for tissue engineering applications. Tissue Eng Part B Rev. 2008. 14:149-65.

[35]   Ahmed TA, Dare EV, Hincke M. Fibrin: a versatile scaffold for tissue engineering applications. Tissue Eng Part B Rev. 2008. 14:199-215.

[36]   Zhang S, Holmes TC, DiPersio CM, Hynes RO, Su X, Rich A. Self-complementary oligopeptide matrices support mammalian cell attachment. Biomaterials. 1995;16:1385-93.

[37]   Hartgerink JD, Beniash E, Stupp IS. Peptide-amphiphile nanofibers: A versatile scaffold for the preparation of self-assembling materials. Proc Natl Acad Sci U.S.A. 2002. 99:5133-8.

[38]   Beniash E, Hartgerink JD, Storrie H, Stendahl LC, Stupp SI. Self-assembling peptide amphiphile nanofiber matrices for cell entrapment. Acta Biomater. 2005. 1:387-97.

[39]   Jun HW, Yuwono V, Paramonov SE, Hartgerink J. Enzyme-mediated degradation of peptide-amphiphile nanofiber networks. Adv. Mater. 2005. 17:2612-2617.

[40]   Rajangam K, Behanna HA, Hui MJ, Han X, Hulvat JF, Lomasney JW, Stupp SI. Heparin binding nanostructures to promote growth of blood vessels. Nano Lett. 2006. 6:2086-90.

[41]   Horii A, Wang X, Gelain F, Zhang S. Biological designer self-assembling peptide nanofiber scaffolds significantly enhance osteoblast proliferation, differentiation and 3-D migration. PLoS ONE. 2007.2:e190.

[42]   Silva GA, Czeisler C, Niece KL, Beniash E, Harrington DA, Kessler JA, Stupp SI. Selective differentiation of neural progenitor cells by high-epitope density nanofibers. Science. 2004. 303:1352-5.

[43]   Hosseinkhani H, Hosseinkhani M, Tian F, Kobayashi H, Tabata Y. Osteogenic differentiation of mesenchymal stem cells in self-assembled peptide-amphiphile nanofibers. Biomaterials. 2006. 27:4079-86.

[44]   Segers VFM, Lee RT. Local delivery of proteins and the use of self-assembling peptides. Drug Discovery. 2007. 12:561-8.

[45]   Holmes TC, de Lacalle S, Su X, Liu G, Rich A, Zhang S. Extensive neurite outgrowth and active synapse formation on self-assembling peptide scaffolds. Proc. Natl. Acad. Sci. U. S. A. 2000. 97:6728–6733.

[46]   Davis ME, Motion JP, Narmoneva DA, Takahashi T, Hakuno D, Kamm RD, Zhang S, Lee RT. Injectable self-assembling peptide nanofibers create intramyocardial microenvironments for endothelial cells. Circulation. 2005. 111:442–450.

[47]   Hsieh PC, Davis ME, Gannon J, MacGillivray C, Lee RT. Controlled delivery of PDGF-BB for myocardial protection using injectable self-assembling peptide nanofibers. J. Clin. Invest. 2006. 116:237–248.

[48]   Dong H, Paramonov SE, Aulisa L, Bakota EL, Hartgerink JD. Self-assembly of multidomain peptides: balancing molecular frustration controls conformation and nanostructure. J Am Chem Soc. 2007. 129:12468-72.

[49]   Bègue-Kirn C, Smith AJ, Ruch JV, Wozney JM, Purchio A, Hartmann D, Lesot H. Effects of dentin proteins, transforming growth factor beta 1 (TGF beta 1) and bone morphogenetic protein 2 (BMP2) on the differentiation of odontoblast in vitro. Int J Dev Biol. 1992. 36:491-503.

[50]   Tziafas D. Basic mechanisms of cytodifferentiation and dentinogenesis during dental pulp repair. Int J Dev Biol. 1995. 39:281-90.

[51]   Tziafas D, Alvanou A, Panagiotakopoulos N, Smith AJ, Lesot H, Komnenou A, Ruch JV. Induction of odontoblast-like cell differentiation in dog dental pulps after in vivo implantation of dentine matrix components. Arch Oral Biol. 1995. 40:883-93.

[52]   D'Souza RN, Happonen RP, Ritter NM, Butler WT. Temporal and spatial patterns of transforming growth factor-beta 1 expression in developing rat molars. Arch Oral Biol. 1990. 35:957-65.

[53]   D'Souza RN, Flanders K, Butler WT. Colocalization of TGF-beta 1 and extracellular matrix proteins during rat tooth development. Proc Finn Dent Soc. 1992: 88:419-26.

[54]   Roberts-Clark DJ, Smith AJ. Angiogenic growth factors in human dentine matrix. Arch Oral Biol. 2000. 45:1013-6.

[55]   Smith AJ, Matthews JB, Hall RC. Transforming growth factor-beta1 (TGF-beta1) in dentine matrix. Ligand activation and receptor expression. Eur J Oral Sci. 1998. 106 Suppl 1:179-84.

[56]   Smith AJ, Murray PE, Sloan AJ, Matthews JB, Zhao S. Trans-dentinal stimulation of tertiary dentinogenesis. Adv Dent Res. 2001. 15:51-4.

[57]   Nakashima M, Nagasawa H, Yamada Y, Reddi AH. Regulatory role of transforming growth factor-beta, bone morphogenetic protein-2, and protein-4 on gene expression of extracellular matrix proteins and differentiation of dental pulp cells. Dev Biol. 1994. 162: 18-28.

[58]   Iohara K, Nakashima M, Ito M, Ishikawa M, Nakasima A, Akamine A. Dentin regeneration by dental pulp stem cell therapy with recombinant human bone morphogenetic protein 2. J Dent Res. 2004. 83:590-5.

[59]   Six N, Decup F, Lasfargues JJ, Salih E, Goldberg M. Osteogenic proteins (bone sialoprotein and bone morphogenetic protein-7) and dental pulp mineralization. J Mater Sci Mater Med. 2002. 13:225-32.

[60]   Almushayt A, Narayanan K, Zaki AE, George A. Dentin matrix protein 1 induces cytodifferentiation of dental pulp stem cells into odontoblasts. Gene Ther. 2006. 13:611-20.

[61]   Alliot-Licht B, Bluteau G, Magne D, Lopez-Cazaux S, Lieubeau B, Daculsi G, Guicheux J. Dexamethasone stimulates differentiation of odontoblast-like cells in human dental pulp cultures. Cell Tissue Res. 2005. 321:391-400.

[62]   Couble ML, Farges JC, Bleicher F, Perrat Mabillon B, Boudeulle M, Magloire H. Odontoblast differentiation of human dental pulp cells in explant cultures. Calcif Tissue Int. 2000. 66:129-38.

[63]   Mooney DJ, Powell C, Piana J, Rutherford B. Engineering dental pulp-like tissue in vitro. Biotechnol Prog. 1996. 12:865-8.

[64]   Bohl KS, Shon J, Rutherford B, Mooney DJ. Role of synthetic extracellular matrix in development of engineered dental pulp. J Biomater Sci Polym Ed. 1998. 9:749-64.

[65]   Cordeiro MM, Dong Z, Kaneko T, Zhang Z, Miyazawa M, Shi S, Smith AJ, Nör JE. Dental pulp tissue engineering with stem cells from exfoliated deciduous teeth. J Endod. 2008. 34:962-9.

[66]   Jun HW, Yuwono V, Paramonov SE, Hartgerink J. Enzyme-mediated degradation of peptide-amphiphile nanofiber networks. Adv. Mater. 2005. 17:2612-2617.

[67]   Wei X, Ling J, Wu L, Liu L, Xiao Y. Expression of minerlizaiton markers in dental pulp cells. J Endod. 2007. 33:703-8.

[68]   Kitagawa M, Ueda H, Iizuka S, Sakamoto K, Oka H, Kudo Y, Ogawa I, Miyauchi M, Tahara H, Takata T. Immortalization and characterization of human dental pulp cells with odontoblastic differentiation. Arch Oral Biol. 2007. 52:727-31.

[69]   Huang GT, Sonoyama W, Chen J, Park SH. In vitro characterization of human dental pulp cells: various isolation methods and culturing environments. Cell Tissue Res. 2006. 324:225-36.

[70]   Huang FM, Yang SF, Hsieh YS, Liu CM, Yang LC, Chang YC. Examination of the signal transduction pathways involved in matrix metalloproteinases-2 in human pulp cells. Oral Surg Oral Med Oral Pathol Oral Radiol Endod. 2004. 97:398-403.

[71]   Aulisa L, Dong H, Hartgerink JD. Self-assembly of multidomain peptides: Sequence variation allows control over crosslinking and viscoelasticity. Accepted at Biomacromolecules.

[72]   Ruoslahti E. RGD and other recognition sequences for integrins. Annu Rev Cell Dev Biol. 1996. 12:697-715.

[73]   Ochsenhirt SE, Kokkoli E, McCarthy JB, Tirrell M. Effect of RGD secondary structure and the synergy site PHSRN on cell adhesion, spreading and specific integrin engagement. Biomaterials. 2006. 27:3863-74.

[74]   Turk BE, Huang LL, Piro ET, Cantley LC. Determination of protease cleavage site motifs using mixture-based oriented peptide libraries. Nat Biotechnol. 2001. 19:661-7.

[75]   Hirano Y, Okuno M, Hayashi T, Goto K, Nakajima A. Cell-attachment activities of surface immobilized oligopeptides RGD, RGDS, RGDV, RGDT, and YIGSR toward five cell lines. J Biomater Sci Polym Ed. 1993. 4:235-43.

[76]   Galler KM, Schweikl H, Thonemann B, D'Souza RN, Schmalz G. Human pulp-derived cells immortalized with Simian Virus 40 T-antigen. Eur J Oral Sci. 2006. 114:138-46.

[77]   Greenfield N, Fasman GD. Computed circular dichroism spectra for the evaluation of protein conformation. Biochemistry. 1969. 8: 4108-16.

[78]   Dikovsky D, Bianco-Peled H, Seliktar D. Defining the role of matrix compliance and proteolysis in three-dimensional cell spreading and remodeling. Biophys J. 2008. 94:2914-25.

[79]   Lutolf MP, Weber FE, Schmoekel HG, Schense JC, Kohler T, Müller R, Hubbell JA. Repair of bone defects using synthetic mimetics of collagenous extracellular matrices. Nat Biotechnol. 2003. 21:513-8.

[80]   Seliktar D, Zisch AH, Lutolf MP, Wrana JL, Hubbell JA. MMP-2 sensitive, VEGF-bearing bioactive hydrogels for promotion of vascular healing. J Biomed Mater Res A. 2004. 68:704-16.

[81]   Lee SH, Moon JJ, Miller JS, West JL. Poly(ethylene glycol) hydrogels conjugated with a collagenase-sensitive fluorogenic substrate to visualize collagenase activity during three-dimensional cell migration. Biomaterials. 2007. 28:3163-70.

[82]   Jun, H.W., Yuwono, V., Paramonov, S.E., and Hartgerink, J. Enzyme-mediated degradation of peptide-amphiphile nanofiber networks. Adv. Mater. 2005. 17:2612.

[83]   Chau Y, Luo Y, Cheung AC, Nagai Y, Zhang S, Kobler JB, Zeitels SM, Langer R. Incorporation of a matrix metalloproteinase-sensitive substrate into self-assembling peptides - a model for biofunctional scaffolds. Biomaterials. 2008. 29:1713-9.

[84]   Galler KM, Cavender A, Yuwono V, Dong H, Shi S, Schmalz G, Hartgerink JD, D'Souza RN. Self-assembling peptide amphiphile nanofibers as a scaffold for dental stem cells. Tissue Eng Part A. 2008.14:2051-8.

[85]   Primer 3
         http://biotools.umassmed.edu/bioapps/primer3_www.cgi

[86]   Real-time PCR Tutorial
         http://pathmicro.med.sc.edu/pcr/realtime-home.htm

[87]   Hessle L, Johnson KA, Anderson HC, Narisawa S, Sali A, Goding JW, Terkeltaub R, Millan JL. Tissue-nonspecific alkaline phosphatase and plasma cell membrane glycoprotein-1 are central antagonistic regulators of bone mineralization. Proc Natl Acad Sci U S A. 2002. 99:9445-9.

[88]   Wei X, Ling J, Wu L, Liu L, Xiao Y. Expression of mineralization markers in dental pulp cells. J Endod. 2007. 33:703-8.

[89]   Kitagawa M, Ueda H, Iizuka S, Sakamoto K, Oka H, Kudo Y, Ogawa I, Miyauchi M, Tahara H, Takata T. Immortalization and characterization of human dental pulp cells with odontoblastic differentiation. Arch Oral Biol. 2007. 52:727-31.

[90]   Linde A. The extracellular matrix of the dental pulp and dentin. J Dent Res. 1985. 64:523-9.

[91]   Fisher LW, Fedarko NS. Six genes expressed in bones and teeth encode the current members of the SIBLING family of proteins. Connect Tissue Res. 2003. 44 Suppl 1:33-40.

[92]   Camilleri S, McDonald F. Runx2 and dental development. Eur J Oral Sci. 2006. 114:361-73. Review.

[93]   Rickard DJ, Sullivan TA, Shenker BJ, Leboy PS, Kazhdan I. Induction of rapid osteoblast differentiation in rat bone marrow stromal cell cultures by dexamethasone and BMP-2. Dev Biol. 1994. 161:218-28.

[94]   Atmani H, Audrain C, Mercier L, Chappard D, Basle MF. Phenotypic effects of continuous or discontinuous treatment with dexamethasone and/or calcitriol on osteoblasts differentiated from rat bone marrow stromal cells. J Cell Biochem. 2000. 85:640-50.

[95]   Igarashi M, Kamiya N, Hasegawa M, Kasuya T, Takahashi T, Takagi M. Inductive effects of dexamethasone on the gene expression of Cbfa1, osterix and bone matrix proteins during differentiation of cultured primary rat osteoblasts. J Mol Histol. 2004. 35:3-10.

[96]   Mikami Y, Omoteyama K, Kato S, Tagaki M. Inductive effects of dexamthasone on the mineralization and the osteoblastic gene expressions in mature osteoblast-like ROS17/2.8 cells. Biochem Biophys Res Commun. 2007. 362:368-73.

[97]   Ferrara N, Gerber HP, LeCouter J. The biology of VEGF and its receptors. Nat Med. 2003. 9:669-76.

[98]   Ferrara N. Role of vascular endothelial growth factor in physiologic and pathologic angiogenesis: therapeutic implications. Semin Oncol. 2002. 29:10-4. Review.

[99]   Jain RK. Tumor angiogenesis and accessibility: role of vascular endothelial growth factor. Semin Oncol. 2002. 29:3-9. Review.

[100] Klagsbrun M. Mediators of angiogenesis: the biological significance of basic fibroblast growth factor (bFGF)-heparin and heparin sulfate interactions. Semin Cancer Biol. 1992. 3:81-7.

[101] Rajangam K, Behanna HA, Hui MJ, Han X, Hulvat JF, Lomasney JW, Stupp SI. Heparin binding nanostructures to promote growth of blood vessels. Nano Lett. 2006. 6:2086-90.

[102] Pike DB, Cai S, Pomraning KR, Firpo MA, Fisher RJ, Shu XZ, Prestwich GD, Peattie RA. Heparin-regulated release of growth factors in vitro and angiogenic response in vivo to implanted hyaluronan hydrogels containing VEGF and bFGF. Biomaterials. 2006. 27:5242-51.

[103] Cardin AD, Weintraub HJ. Molecular modeling of protein-glycosaminoglycan interactions. Arteriosclerosis. 1989. 9:21-32.

[104] Rajangam K, Arnold MS, Rocco MA, Stupp SI. Peptide amphiphile nanostructure-heparin interactions and their relationship to bioactivity. Biomaterials. 2008. 29:3298-305.

[105] Rowlands AS, George PA, Cooper-White JJ. Directing osteogenic and myogenic differentiation of MSCs: interplay of stiffness and adhesive ligand presentation. Am J Physiol Cell Physiol. 2008. 295:1037-44.

[106] Buxton PG, Bitar M, Gellynck K, Parkar M, Brown RA, Young AM, Knowles JC, Nazhat SN. Dense collagen matrix accelerates osteogenic differentiation and rescues the apoptotic response to MMP inhibition. Bone. 2008. 43:377-85.

[107] He H, Yu J, Liu Y, Lu S, Liu H, Shi J, Jin Y. Effects of FGF2 and TGFbeta1 on the differentiation of human dental pulp stem cells in vitro. Cell Biol Int. 2008. 32:827-34.

[108] George A, Sabsay B, Simonian PA, Veis A. Characterization of a novel dentin matrix acidic phosphoprotein. Implications for induction of biomineralization. J Biol Chem. 1993. 268:12624-30.

[109] Tye CE, Rattray KR, Warner KJ, Gordon JA, Sodek J, Hunter GK, Goldberg HA. Delineation of the hydroxyapatite-nucleating domains of bone sialoprotein. J Biol Chem. 2003. 278:7949-55.

[110] Krebsbach PH, Kuznetsov SA, Satomura K, Emmons RV, Rowe DW, Robey PG. Bone formation in vivo: comparison of osteogenesis by transplanted mouse and human marrow stromal fibroblasts. Transplantation. 1997. 63:1059-69.

[111] Wolff LF. Guided tissue regeneration in periodontal therapy. Northwest Dent. 2000. 79:23-8,40.

[112] Kim KH, Ramaswamy N. Electrochemical surface modification of titanium in dentistry. Dent Mater J. 2009. 28:20-36.

[113] Galler K, Hiller KA, Ettl T, Schmalz G. Selective influence of dentin thickness upon cytotoxicity of dentin contacting materials. J Endod. 2005. 31:396-9.

[114] Liu J, Jin T, Ritchie HH, Smith AJ, Clarkson BH. In vitro differentiation and mineralization of human dental pulp cells induced by dentin extract. In Vitro Cell Dev Biol Anim. 2005. 41:232-8.

[115] Breschi L, Mazzoni A, Ruggeri A, Cadenaro M, Di Lenarda R, De Stefano Dorigo E. Dental adhesion review: aging and stability of the bonded interface. Dent Mater. 2008. 24:90-101.

[116] Shibata Y, Fujita S, Takahashi H, Yamaguchi A, Koji T. Assessment of decalcifying protocols for detection of specific RNA by non-radioactive in situ hybridization in calcified tissues. Histochem Cell Biol. 2000. 113:153-9.